

MEASUREMENTS OF THE VELOCITY FIELD
IN THE FRASER RIVER PLUME

by

RUTH ELEANOR CORDES
B.Sc. Dalhousie University, 1973

A THESIS SUBMITTED IN PARTIAL FULFILLMENT OF
THE REQUIREMENTS FOR THE DEGREE OF
MASTER OF SCIENCE

in

THE FACULTY OF GRADUATE STUDIES
IN THE DEPARTMENT OF PHYSICS
AND THE INSTITUTE OF OCEANOGRAPHY

We accept this thesis as conforming
to the required standard

THE UNIVERSITY OF BRITISH COLUMBIA

May, 1977

© Ruth Eleanor Cordes, 1977

In presenting this thesis in partial fulfilment of the requirements for an advanced degree at the University of British Columbia, I agree that the Library shall make it freely available for reference and study. I further agree that permission for extensive copying of this thesis for scholarly purposes may be granted by the Head of my Department or by his representatives. It is understood that copying or publication of this thesis for financial gain shall not be allowed without my written permission.

Department of Physics (Oceanography)

The University of British Columbia
2075 Wesbrook Place
Vancouver, Canada
V6T 1W5

Date July 28/77

ABSTRACT

A program of Lagrangian velocity measurements was carried out in the Fraser River plume, at the mouth of the main (south) arm of that river. The data were collected over three days of equatorial tides and three days of tropic tides during the early part of freshet (May 28-31 and June 4-6, 1974). Mini-Fix positioning was used to hand-record positions of the drogues. The data were keypunched and checked for errors, and smoothed positions and velocities were interpolated between the observed points.

The experimental data give a more detailed description of the spatial and temporal variations of flow in the plume than was previously available. Tides were found to be the dominant factor controlling the flow. The velocity fields measured on similar stages of the tide were compared and contrasted, noting the effects of winds and Coriolis force. Composite velocity fields were prepared by averaging the data from similar tidal phases. Plots of velocity components as a function of distance were prepared to correspond to most of the composite velocity fields; these provided an alternate way of looking at the results. Examination of the horizontal divergence yielded estimates of the entrainment velocity consistent with those of other investigators.

TABLE OF CONTENTS

	<u>Page</u>
ABSTRACT	i
LIST OF FIGURES	iii
ACKNOWLEDGEMENT	vii
CHAPTER 1	
INTRODUCTION	1
CHAPTER 2	
THE EXPERIMENT	12
CHAPTER 3	
THE DATA ANALYSIS AND METHOD OF PRESENTATION	25
CHAPTER 4	
RESULTS	36
CHAPTER 5	
SUMMARY AND CONCLUSIONS	127
LIST OF REFERENCES	136

LIST OF FIGURES

		<u>Page</u>
Figure 1.1	Map of the Strait of Georgia	2
1.2	Discharge from the Fraser River, 1974	4
1.3	Map of the area near the mouth of the Fraser River	5
1.4	Graphs of tide height at Tsawwassen	7
2.1	Map of the southern Strait with the Mini-Fix grid	13
2.2	Schematic diagram of a drogue	17
2.3	Sample log sheet - observer's copy	19
2.4	Sample log sheet - control copy	21
2.5	Sample hand plot of float paths	22
4.1	Tide height and wind velocity for Week 1	38
4.2	Path lines, Set 2	40
4.3	Path lines, Set 6	41
4.4	Velocity fields, Sets 2 and 6, near lower low tide	42
4.5	Composite velocity field, Sets 2 and 6, time sampling	45
4.6	Composite velocity field, Sets 2 and 6, distance sampling	47
4.7	Path lines, Set 4	49
4.8	Path lines, Set 4	50
4.9	Velocity field, Set 4, on small flood tide	51
4.10	Velocity field, Set 4, near lower high tide	53
4.11	Velocity field, Set 4, on small ebb tide	54
4.12	Path lines, Set 7	55
4.13	Path lines, Set 7	57
4.14	Velocity field, Set 7, on small flood tide	58
4.15	Velocity field, Set 7, near lower high tide	59

LIST OF FIGURES (continued)

		<u>Page</u>
Figure 4.16	Velocity field, Set 7, small flood and high tide, distance sampled	61
4.17	Velocity field, Set 7, small flood and high tide, time sampled	62
4.18	Velocity field, Set 7, small ebb tide	63
4.19	Path lines, Set 1	65
4.20	Velocity field, Set 1, small ebb tide	66
4.21	Composite velocity field, Sets 4 and 7, small flood tide	67
4.22	Composite velocity field, Sets 1, 4 and 7, small ebb tide	69
4.23	Path lines, Set 5	70
4.24	Velocity fields, Set 5, before and after higher high tide	71
4.25	Path lines, Set 8	73
4.26	Velocity field, Set 8, before higher high tide	74
4.27	Velocity field, Set 8, after higher high tide	76
4.28	Path lines, Set 3	77
4.29	Velocity field, Set 3, after higher high tide	79
4.30	Composite velocity field, Sets 5 and 8, before higher high tide	80
4.31	Composite velocity field, Sets 5 and 8, after higher high tide	81
4.32	Tide height and wind velocity for Week 2	82
4.33	Path lines, Set 12	84
4.34	Velocity fields, Set 12, start of large ebb	85
4.35	Path lines, Set 16	87

LIST OF FIGURES (continued)

		<u>Page</u>
Figure 4.36	Velocity fields, Set 16, start of large ebb	88
4.37	Composite velocity field, Sets 12 and 16, start of large ebb	89
4.38	Path lines, Sets 16 and 17	90
4.39	Velocity field, Sets 16 and 17, end of large ebb	92
4.40	Path lines, Sets 13 and 9	94
4.41	Velocity fields, Sets 13 and 9, end of large ebb	95
4.42	Composite velocity field, Sets 9, 13, 16 and 17, end of large ebb	97
4.43	Path lines, Sets 10 and 14	98
4.44	Velocity fields, Sets 10 and 14, start of large flood	99
4.45	Path lines and velocity field, Set 18, start of large flood	100
4.46	Composite velocity field, Sets 10, 14 and 18, start of large flood	102
4.47	Path lines, Sets 11 and 15	103
4.48	Velocity fields, Sets 11 and 15, end of large flood	105
4.49	Velocity versus distance plots, Sets 2 and 6	108
4.50	Velocity versus distance plots, Sets 4 and 7	110
4.51	Velocity versus distance plots, Sets 1, 4 and 7	111
4.52	Velocity versus distance plots, Sets 12 and 16	113
4.53	Velocity versus distance plots, Sets 9, 13, 16 and 17	115
4.54	Velocity versus distance plots, Sets 10, 14 and 18	116
4.55	Current meter data from 1967	120
4.56	Sample calculation of Keulegan's constant	125

LIST OF FIGURES (continued)

		<u>Page</u>
Figure 5.1	Composite velocity fields for small floods and ebbs, Week 1	128
5.2	Composite velocity fields for large floods and ebbs, Week 1	130
5.3	Composite velocity fields for large ebbs and floods, Week 2	132

ACKNOWLEDGEMENT

The study of the Fraser River plume was directed by Dr. S. Pond of the Institute of Oceanography, U.B.C., and Dr. P. B. Crean of the Marine Sciences Directorate of the Department of the Environment, but it could not have been carried out without the assistance of the many graduate students and staff members of IOUBC and staff members of MSD who volunteered to act as observers. They all deserve many thanks for their contributions to the success of the project. Thanks are also extended to MSD for providing the *Richardson*, the two Arctic launches, and crews for these three vessels, as well as for chartering the *Swift Invader* for our use. The loan of the *Caligus* and crew from the Nanaimo laboratory of the Fisheries Research Board was arranged through the generous cooperation of Dr. J. Sibert. We also wish to thank the Canadian Hydrographic Service, MSD, which provided, installed and maintained the Mini-Fix system.

Funding for the experiment was provided by a contract from the Department of the Environment. I was supported by a postgraduate scholarship from the National Research Council and from a DoE grant.

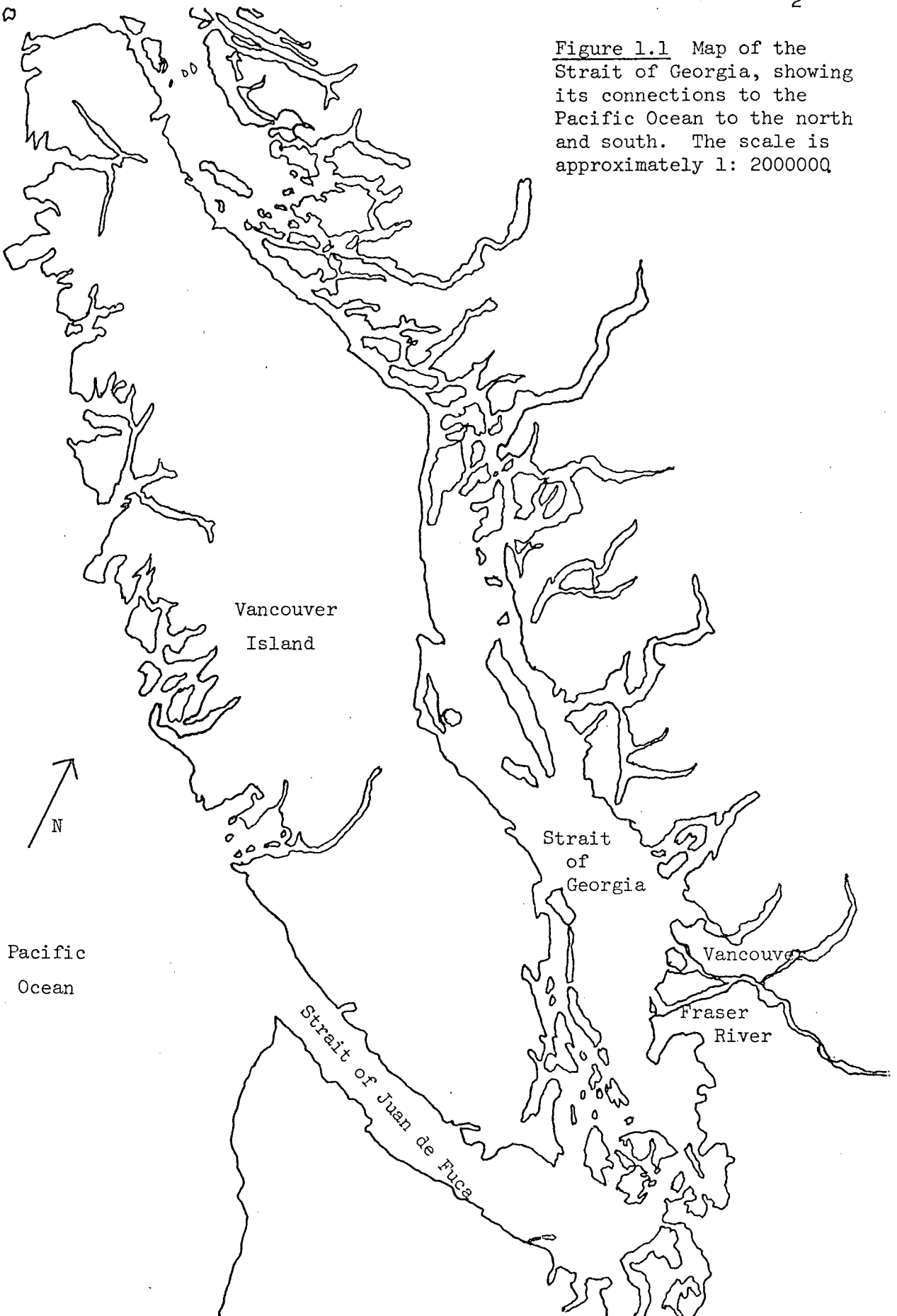
This acknowledgement would not be complete without special mention of those, who, as well as working hard on the experiment, helped me struggle through the task of thesis writing. I am very grateful to J. R. Buckley who provided me with a great deal of assistance in carrying out the data analysis. Finally, I wish to thank my supervisor, Dr. S. Pond, whose patience, encouragement and guidance were of great value to me during the preparation of this thesis.

CHAPTER 1
INTRODUCTION

The Strait of Georgia, shown in Figure 1.1, is a large waterway between Vancouver Island and the mainland of British Columbia. It is connected with the Pacific Ocean to the south by passages through the Gulf Islands and San Juan Islands to the Strait of Juan de Fuca, and to the north by channels among the northern islands. It trends northwest-southeast, with a length of about 220 km, and an average width of 33 km (Waldichuk, 1957). The water in the Strait is a mixture of salt water from the Pacific and fresh water supplied by runoff and precipitation. The less dense fresh water forms a distinct surface layer over the whole Strait in summer and its stability is increased by heating due to solar radiation. Turbulent mixing caused by strong tidal currents in the narrow entrance passages combines the fresh water with the deeper salt water. This water is carried into the Strait, forming the denser lower layer. In winter, the reduced supply of fresh water, cooling of the surface waters, and mixing by strong winds break down the surface layer and create a much more homogeneous water column in the Strait (Tully and Dodimead, 1957).

Most of the fresh water comes from the Fraser River, the drainage basin of which covers a large portion of the interior of southern British Columbia. Tully and Dodimead (1957) calculate that it supplies 80 to 85% of the fresh water flowing into the Strait, the rest flowing from small rivers into the fjord-like inlets which open into the Strait. Outflow from the Fraser River varies greatly throughout the year, since

Figure 1.1 Map of the Strait of Georgia, showing its connections to the Pacific Ocean to the north and south. The scale is approximately 1: 200000Q



a large portion of the precipitation in its drainage basin falls as snow in the winter. The river carries its largest volume of water during the late spring and early summer freshet, when melting snow raises the river level, occasionally causing flooding. There may also be a secondary maximum in the discharge in autumn if heavy rains occur before the temperatures drop enough to turn the precipitation over most of the drainage basin to snow. The Fraser River discharge as measured at Hope for the year 1974 is shown in Figure 1.2. The tributaries which enter the Fraser below Hope increase the volume by about 35% (Waldichuk, 1957).

Silt carried by the river has built up a large delta and extensive shallow banks. The flat, arable land of the delta and the gentle slopes nearby have become the site of British Columbia's most densely populated area, Vancouver and its suburbs. Figure 1.3 shows the area of the river mouth, where the river divides into smaller channels as it flows through the delta. The South Arm carries the largest portion of the outflow. The river's channel across the banks has been found to shift over the years. To mark its location and make navigation safer for large ships using the river the Steveston Jetty was built in the early 1950s. It constrains the river water from spreading to the north until it reaches the edge of the banks. The momentum of the fresh water causes it to remain as a jet or plume when it flows into the Strait, although there is some spreading to the south. The silty fresh water of the plume forms an easily recognized surface layer, overriding the denser, clearer Strait water. At some phases of the tide, the salt water

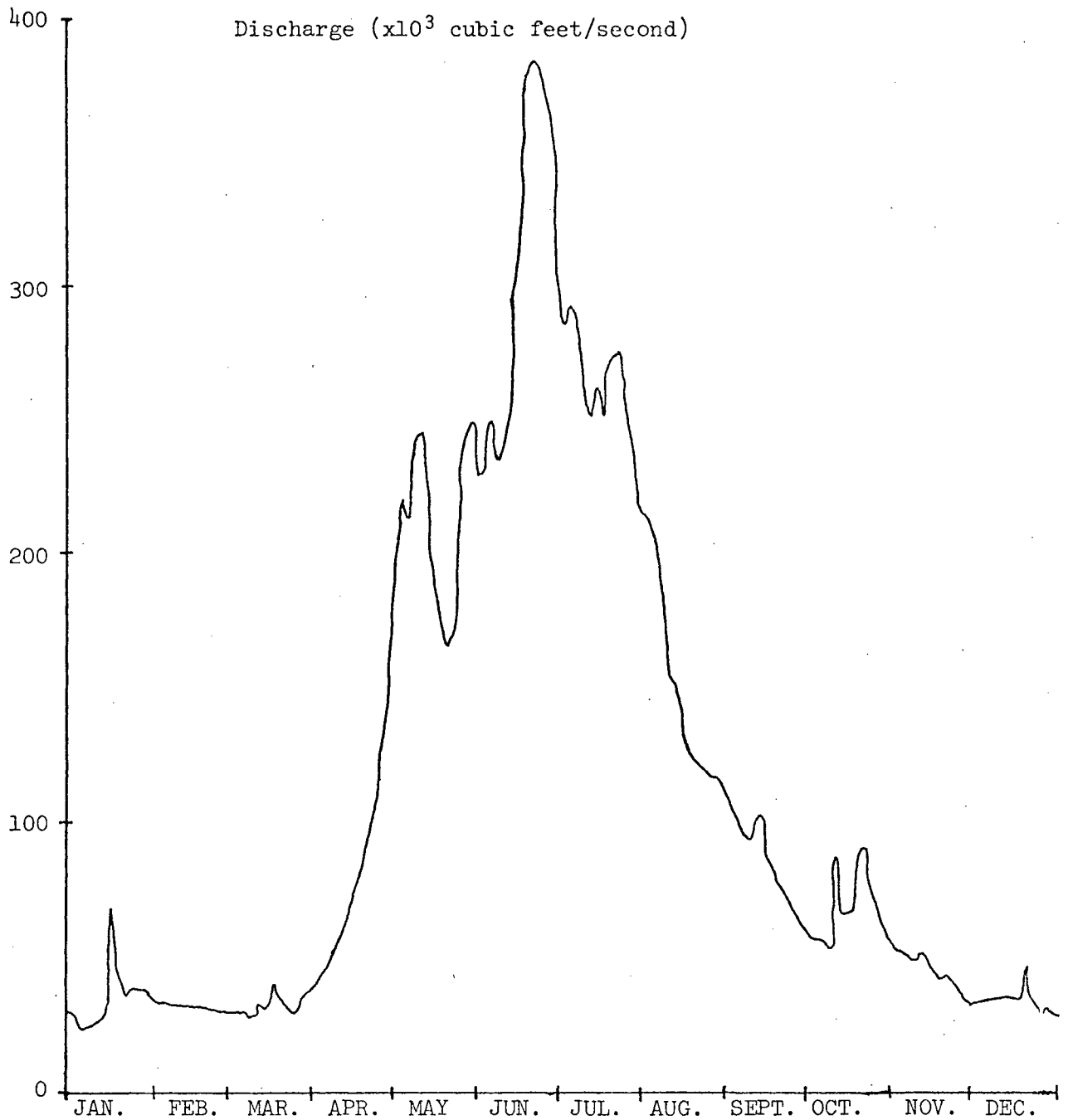


Figure 1.2 Fraser River discharge for 1974, measured at Hope. During the experiment (May 28 - June 6), discharge was about 60% of the maximum attained on June 21.

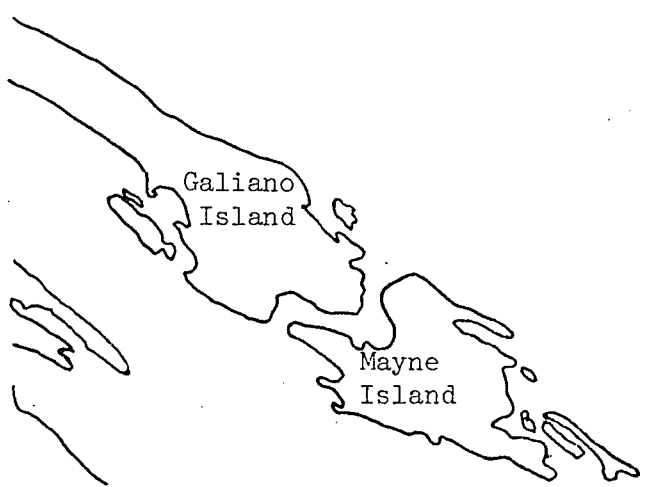
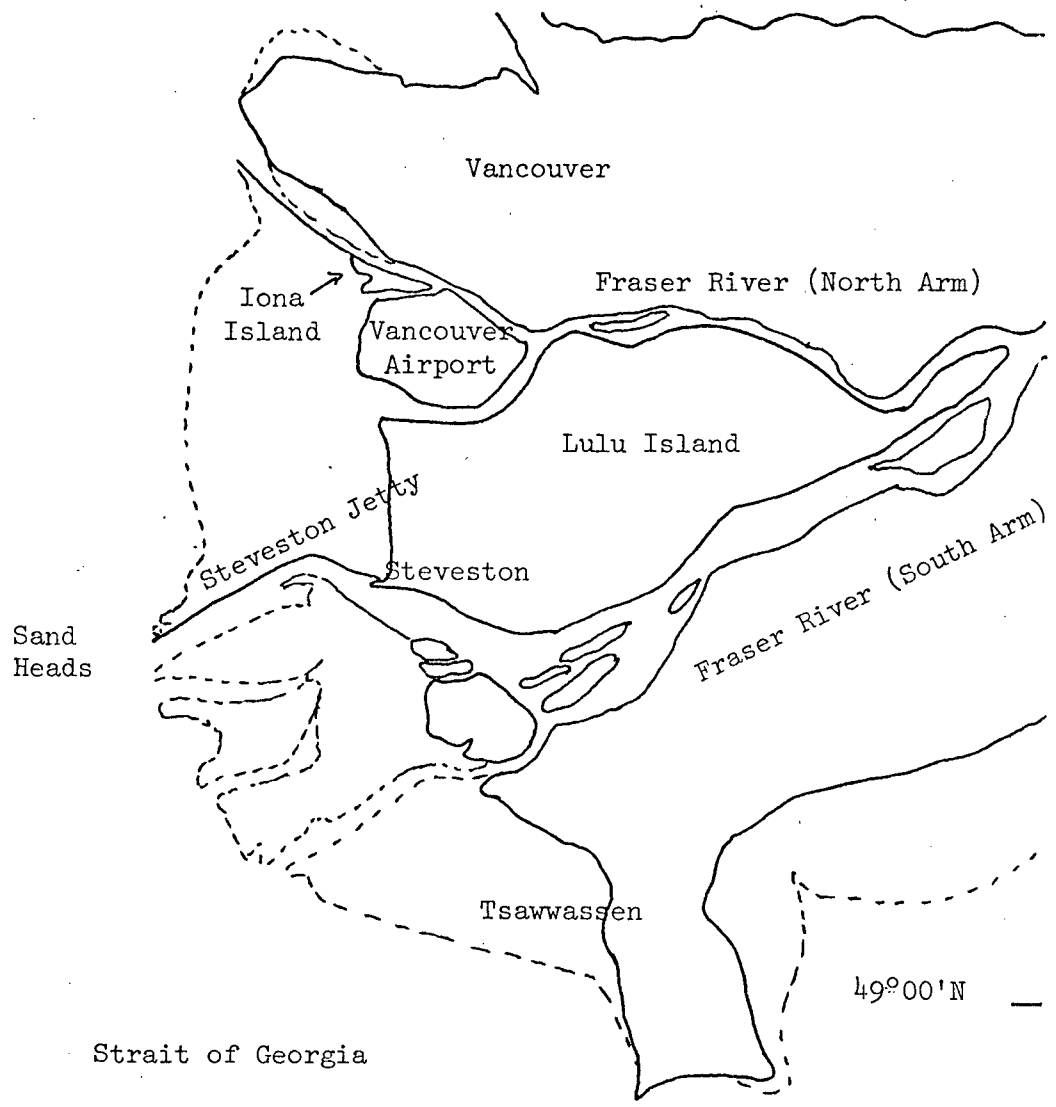


Figure 1.3 Map of the area near the mouth of the Fraser River. The dotted lines indicate the extent of the shallow banks of the delta. The scale is 1:250000.

intrudes into the river under the fresh water, forming a so-called salt wedge. As the plume spreads over the salt water in the Strait, the surface layer becomes thinner. Entrainment and/or mixing of salt water occurs, making the surface layer less and less well defined. Once the fresh water of the river plume has entered the Strait it is subject to all the forces affecting the circulation there. Of primary importance are the tide and the wind.

Tides in the Strait of Georgia are of the semidiurnal mixed variety and are strongly declinational. They pass through tropic and equatorial sequences (Tully and Dodimead, 1957). Figure 1.4 shows typical tide curves of the two types. The tidal range is greater during the tropic tides, when there is one large and one small tide each day. The largest tidal ranges occur near the solstices, while the smallest ranges are observed at the times of the equinoxes. The tides in the Strait are driven by those in the Pacific, with water flooding and ebbing through the channels at both the north and south ends. Tidal fluctuations at the mouth of the Fraser are driven from the southern channels, so the water moves northwest on the flood tide and southeast on the ebb. It has been observed that the currents associated with the flooding tide are stronger on the east side of the Strait, while those of the ebb dominate on the west side. The net effect is a counter-clockwise gyre in the residual current. This hypothesis is supported by Tully and Dodimead, (1957) who noted that the stability of the surface layer decreased with distance north from the river mouth along the east side of the Strait, and continued to diminish to the south along the west side. The Coriolis

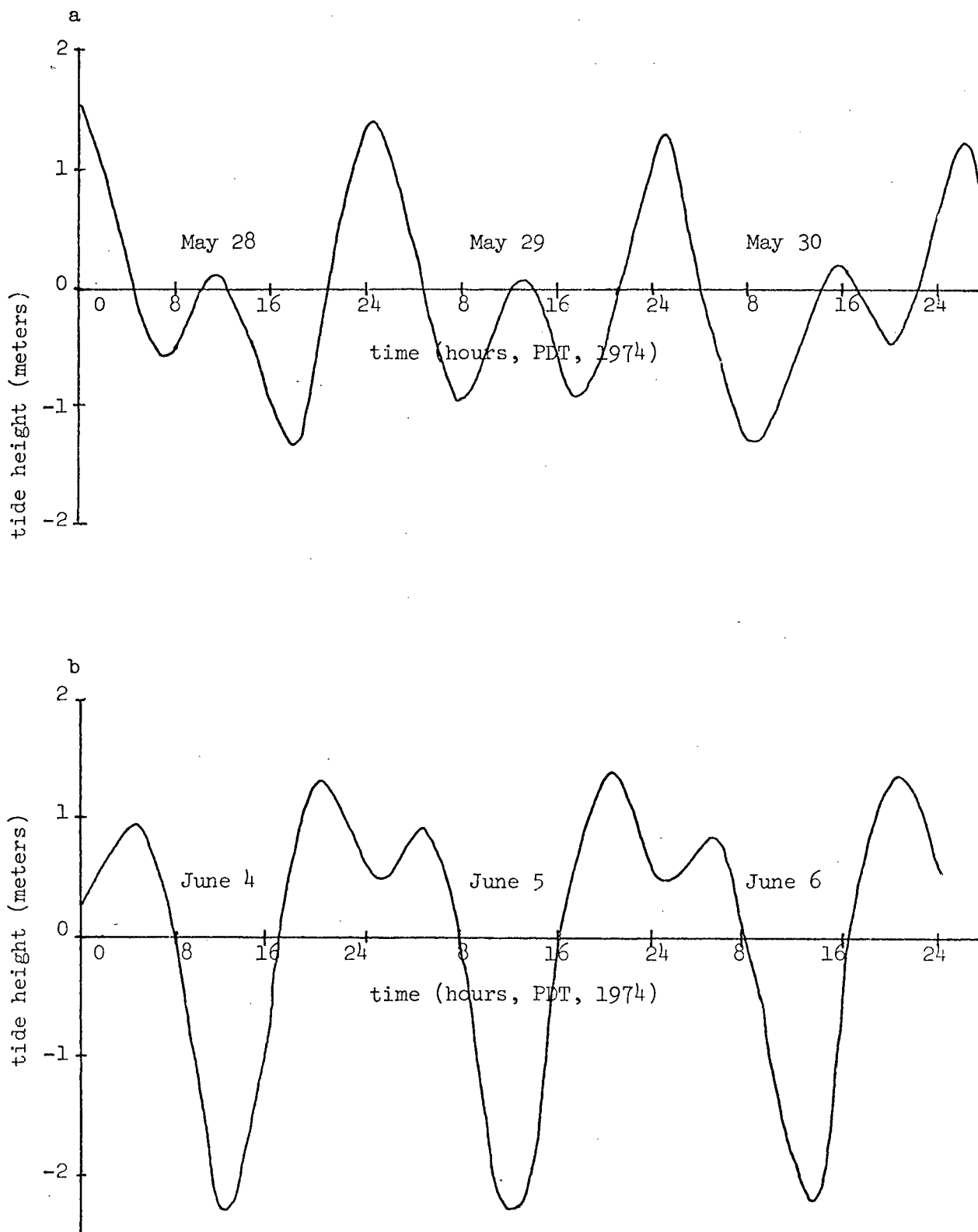


Figure 1.4 Tide height at Tsawwassen, during a. a period of equatorial tides and b. a period of tropic tides.

force, which causes moving water to veer to the right of its original path in the northern hemisphere may be responsible for this inequality in the flow.

Wind stress acts on the surface of the water and imparts momentum to it. The effect of this force decreases with depth. When there is a surface layer of less dense water defined by a fairly sharp interface, the wind stress influence will be confined almost completely to the upper layer and can have quite a pronounced effect if this layer is shallow. The prevailing winds over the Strait of Georgia are from the northwest and southeast - along the axis of the Strait - but there are often local variations. A counterclockwise gyre is often observed in the southern Strait. Since the wind stress on the water surface is proportional to the square of the wind velocity, strong winds have a much larger effect on the velocity of the surface water than weaker winds do. Ekman (1905) developed a theoretical model of a steady wind acting on a homogeneous rotating ocean. In his Ekman spiral, the surface water moves 45° to the right of the wind direction, and the velocity of deeper water decreases in magnitude and continues to rotate in direction. In a situation like the Strait of Georgia the limited fetch of the wind, its variability, and the presence of a well defined surface layer probably prevent the classical spiral from occurring; instead, one might expect the wind-driven water to move in a direction close to that of the wind, and much of the wind influence to be confined to the surface layer. Wind mixing helps to make the layer homogeneous, so the interface becomes sharper and the layer more stable.

As the main source of fresh water for the surface layer of the Strait of Georgia, the Fraser River affects the biological productivity of the whole Strait. With increased use of the river and the Strait for both industrial and recreational purposes, better knowledge of the circulation can help in making decisions about such things as effluent disposal. For example, pollutants in the river entering the Strait on a strong ebb tide might be mostly flushed from the Strait, while those entering on the flood could be pushed to the north and remain in the Strait much longer. In an attempt to understand the circulation and properties of the Strait, many sets of measurements have been made.

The earliest oceanographic work in the Strait of Georgia was done by members of the Nanaimo Laboratory of the Fisheries Research Board of Canada, who began by studying aspects of its biological oceanography (e.g., Fraser and Cameron, 1916). To better understand the distribution of flora and fauna, they began to measure the physical properties of the water and observed some of the effects on productivity of the nutrient-rich mixed surface layer generated by the Fraser. The first study of the surface circulation was made in 1926-31, with the release of a series of lines of drift bottles. These data were examined by Waldichuk (1958), and show the basic gyral circulation, but also indicate that large variations may occur because of the influence of wind and tide. Tully and Dodimead (1957) analyzed data collected by Carter and Tully in 1931-32. They occupied a series of bottle stations covering the Strait and its approaches during different seasons of the year, collecting data at each over a full tidal cycle in order to assess both daily and seasonal variations.

Hutchinson and Lucas (1931) summarized their work on the physical oceanography of the Strait, and related plankton productivity to the physical properties. They were particularly concerned with the Fraser River as a source of fresh water and nutrients which the plume entrains from below.

More recently, studies have been directed toward an understanding of the processes governing the circulation. Newer instruments (e.g. recording current meters) and use of computers for data reduction have increased the scope of possible projects, but the complexities of the Strait still make it difficult to obtain detail in sampling. One problem which generated a great deal of study was the selection of a site for a sewerage outfall to serve the greater Vancouver area. Before choosing the Iona Island site near the North Arm of the Fraser River, extensive oceanographic work, supplemented by aerial photography, was carried out in the waters near Vancouver. The photographs have been analyzed in an attempt to study the motion of the Fraser River plume (Tabata, 1972). When the sewage disposal facility at Iona Island was to be expanded, further study was done, involving drogue tracking, current profiling with a meter, and tracking of suspended dye tracers (Tabata *et al.*, 1971).

In 1966 and 1967 drogue tracking was done in the Fraser River plume, chiefly off the (main) South Arm (Giovando and Tabata, 1970). Since only one vessel was available it was impossible to obtain a synoptic picture of the plume. They were able to gain some knowledge of the water movement at various stages of the tide, and to estimate the

effects of the wind on the surface flow. Some current meter data was also taken in the Fraser plume area in 1967 and subsequent years (e.g. Tabata *et al.*, 1970).

In order to obtain more detailed information about the movement of the Fraser River plume, an experiment was carried out in 1974 by members of the Institute of Oceanography, University of British Columbia, (IOUBC), and the Marine Sciences Directorate (now Ocean and Aquatic Affairs), Department of the Environment. The river has its greatest influence on the Strait during freshet in late spring and early summer, which is also the time much of the biological growth occurs. The experiment was thus scheduled for two 3-day periods during the beginning of freshet, including one period of equatorial tides (May 28-31) and one of tropic tides (June 4-6)(Fig. 1.4). The tides were of near maximum range since the time selected was near the summer solstice. Surface drogues were used to make quantitative measurements of the flow in the plume, in order to determine the effects of the tides, winds and other forces on the flow. As well as the drogue-following work, some water property data were collected with an Inter-Ocean CSTD, and aerial photographs of the plume were taken.

The remaining chapters of this thesis describe the collection, analysis, and interpretation of these data. It is hoped that the existence of such detailed data on an important aspect of the Strait's circulation will aid in planning future use of the waters. It should also be of assistance to those who are attempting to simulate aspects of the circulation by means of numerical modelling.

CHAPTER 2

THE EXPERIMENT

In studying the water movement in the Fraser River plume, we chose to use the Lagrangian method of tracking free-floating drogues. A collection of drogues which had been used by the IOUBC group working on surface circulation was available so the first major decision to be made was how to track their positions. The earlier experiments (Buckley and Pond, 1976) had used radar for this purpose, and each float had a radar reflector attached to it. By frequently photographing the radar screen and a watch, quite a large number of drogues (20 to 40) could be tracked at once. This procedure gives a fairly detailed description of the flow, but since the radar set used cannot detect the drogues beyond a range of three nautical miles, it is only feasible for work in relatively small enclosed areas. Because of the diverging flow in the Fraser plume area a larger range was necessary. We had to look for a system which was readily available and would give the desired coverage. The system chosen was "Mini-Fix", which was generously loaned to us and installed by the Canadian Hydrographic Service (CHS) of the Marine Sciences Directorate in Victoria.

The Mini-Fix system consists of three synchronized transmitters which produce two intersecting interference patterns. As illustrated in Figure 2.1, these form a hyperbolic grid which the receivers use as a coordinate system when indicating their positions. The receivers must be set at a known position, but as they are moved they count nodal lines to keep track of their current location. Position is displayed as 'lanes'

Bowen Island
Slave One

13

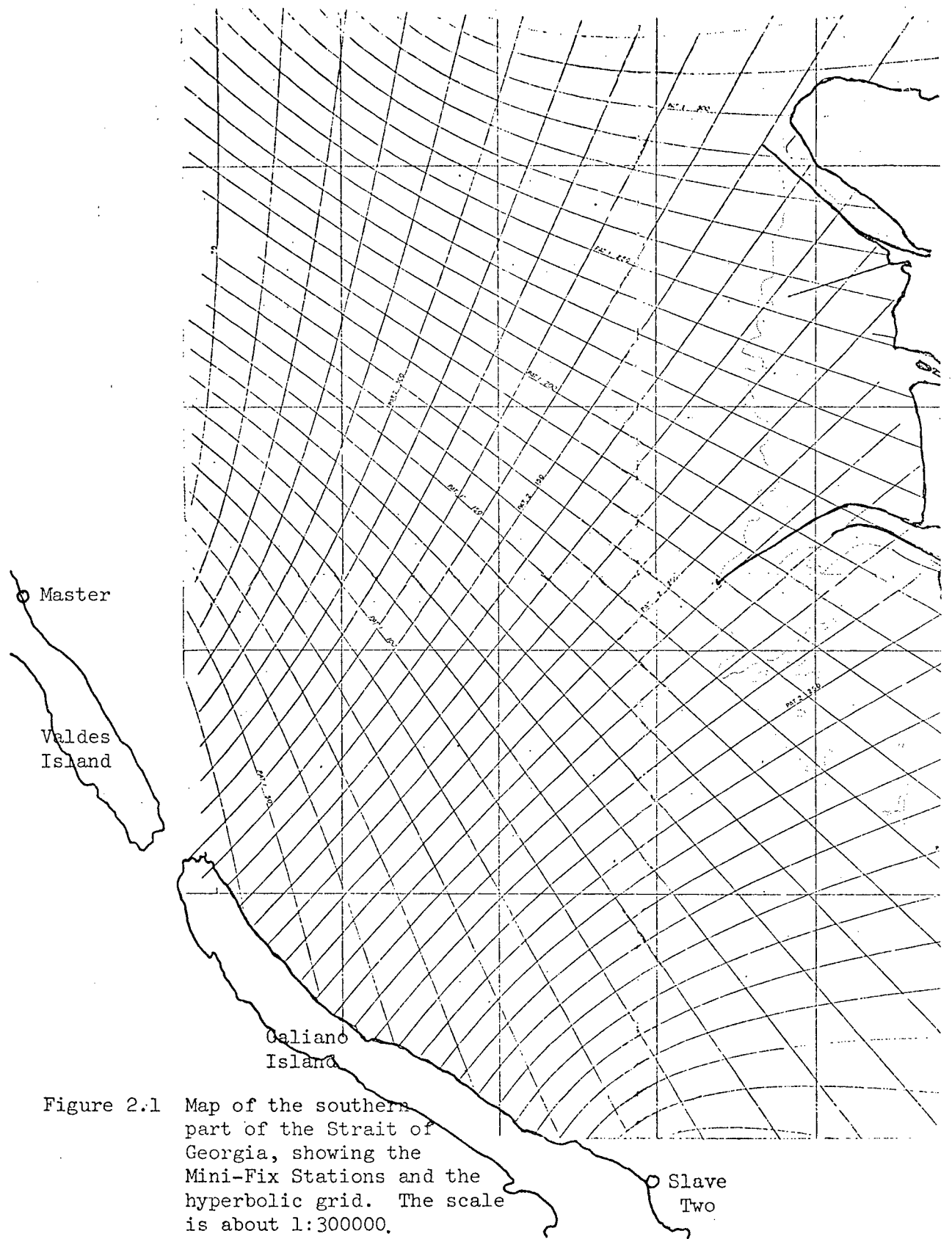


Figure 2.1 Map of the southern part of the Strait of Georgia, showing the Mini-Fix Stations and the hyperbolic grid. The scale is about 1:300000.

and hundredths for each of the coordinates, "Pattern 1" and "Pattern 2". The precision of positioning is ± 5 ft. Based on the observed drift of a fixed receiver at Steveston, the variation over several days is ± 50 ft. and is mainly diurnal. Correction for this drift can be made by monitoring the position displayed by a fixed receiver, but was unnecessary in this experiment since the results are based on differences between positions observed within a short time of each other.

Each of the vessels used in the operation was equipped with a receiver, from which position coordinates were recorded when a fix was taken on a drogue. Occasionally a receiver would temporarily lose lock and after regaining stability would show the wrong lane number. This lane skipping could be missed if the observers were busy with other tasks. To watch for possible occurrences the vessels checked their positions whenever it was convenient against known references such as the navigation buoys or with each other. If a lane skip had occurred it was noted so that the data could be corrected and the receiver was reset to show the proper position.

It is a credit to the members of the CHS electronics group who installed and maintained the system that it functioned so well. It had not previously been used at night and they were afraid that increased sky wave transmission might cause problems then. While there was more noise than during the day, with rapid oscillations of two to five hundredths of a lane occurring at times, lane skips occurred no more frequently. Another cause for concern was the proximity of the Vancouver International Airport to the Fraser plume area. Planes have

been known to cause lane skips, but we had little trouble from that source. In all, less than ten instances of lane skipping were detected during the whole experiment.

Five boats were used to do the float tracking. The Canadian Hydrographic Service kindly lent us the *Richardson*, a 65 ft. survey vessel, and two Artic launches, as well as supplying crews to operate them. The loan of the *Caligus* and crew from the Fisheries Research Board Biological Station in Nanaimo was arranged by Dr. J. Sibert. An aluminum-hulled jet boat, *Swift Invader*, of Vancouver was chartered by the Marine Sciences Directorate, Victoria. It and *Caligus* each had two crews and worked two shifts. During the first week of the experiment we attempted to work around the clock in two 12-hour shifts. *Caligus*, *Swift Invader*, and the two launches worked the day shift, while *Richardson* was anchored near Sand Heads at the end of the Steveston Jetty and was used as the control centre. At night *Richardson* worked with *Caligus* and *Swift Invader*. To obtain better coverage of the large tides which occurred during the days of the second week, the night shift was dropped in favour of morning and afternoon shifts for vessels with two crews and staggered shifts for the others. Float tracking was done from about 6 a.m. to 9 p.m. each day.

An experiment such as this could not be expected to proceed without some problems. One of the launches ran aground when returning from Victoria after the weekend and was out of service for most of the second week. *Swift Invader* developed engine trouble and *Richardson* had electrical problems, but these did not take too long to repair. On one

occasion during each week operations had to be stopped because of high winds. However, a much more extensive data set than any obtained previously was collected.

The drogues used in the experiment were of the window-blind variety, in which the drag element is a heavy plastic "sail" which can be rolled up like a window blind for easier handling and compact storage. Figure 2.2 is a schematic diagram of a drogue showing its structure and dimensions. Vachon (1974) tested drogues of various shapes and found the window-blind drogue to have the highest drag coefficient of the group. It remains essentially perpendicular to the direction of flow, oscillating only in situations with high relative velocity. He noted that in a vertical velocity shear the bottom of the drogue must be sufficiently weighted to keep it from rising up and effectively reducing the drag area. The shear in the surface layer forming the Fraser River plume was apparently quite pronounced, since the drogues sometimes had tilts of 15 degrees or so from the vertical despite the weighting of each sail with an iron reinforcing rod.

When there is a velocity shear the drogue moves at an "average" velocity and is tilted at a small angle to the vertical. Buckley (1977) who used the same drogues in an earlier experiment has derived equations for the behaviour of a sail in a vertical shear by balancing the forces and torques acting on it. Solving these equations for simple velocity profiles with all the shear in the top two meters shows that, for small tilt angles, the drogue speed is no more than 10% greater than the calculated average speed for the profile. In a linear velocity profile in

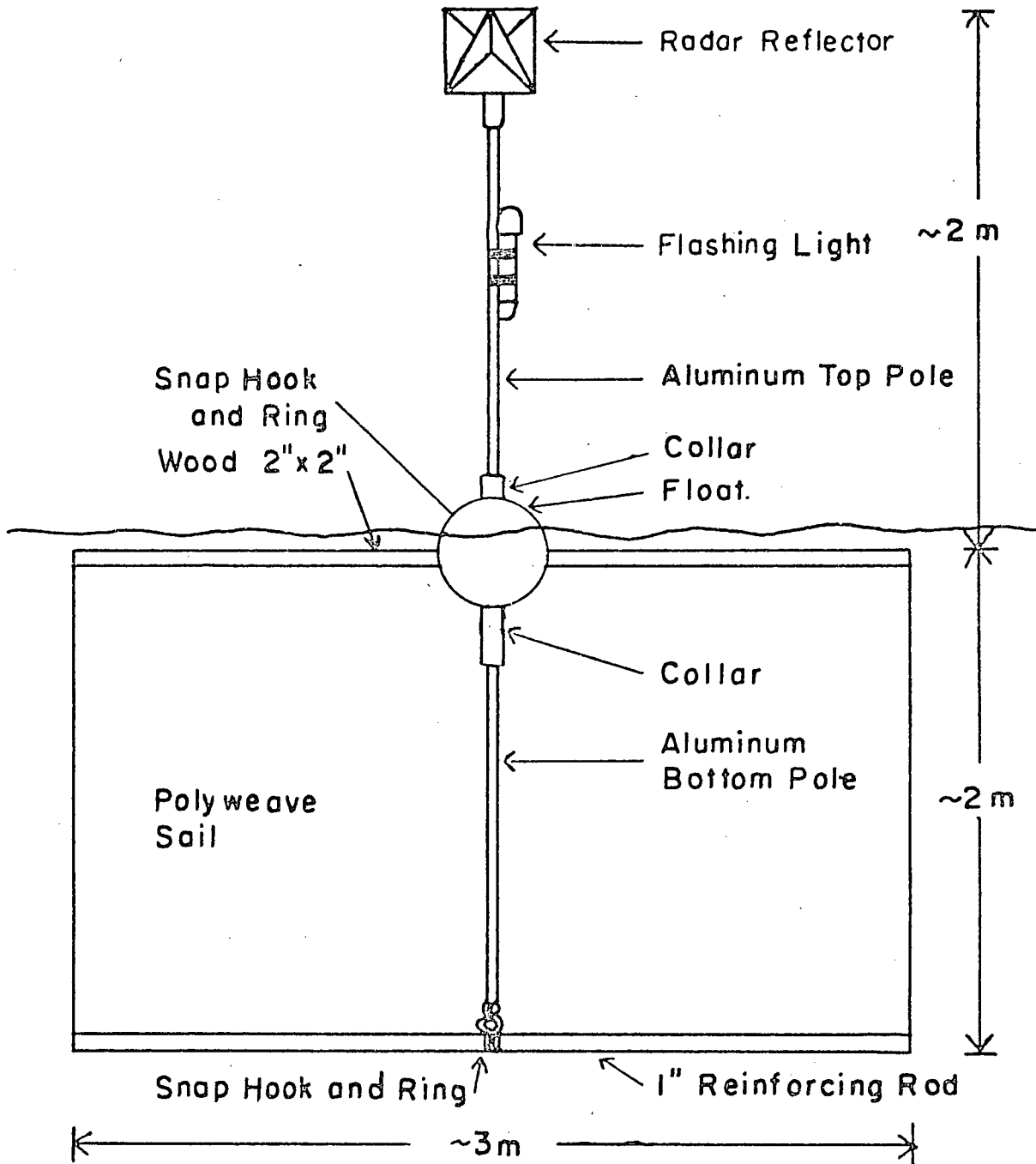


Figure 2.2 Design of the surface drogues used in this experiment (after Buckley and Pond, 1976.)

which the speed decreases from 70 cm/s at the surface to zero at a depth of two meters, a drogue would be tilted at an angle of 16° . Its speed would be 4% larger than the average water speed. Shear effects thus seem to be small enough to be neglected.

The procedure for taking a position fix on a float was determined by the nature of the Mini-Fix system. Each boat was equipped with a receiver which indicated its position. When the boat came up beside a float, attempting to be a standard distance away from it, the position was recorded on specially prepared log sheets like the one shown in Figure 2.3. An Accutron watch was used for timing. Since the hundredths of lanes and seconds were changing quickly, they were recorded first, with hours, minutes and lanes being filled afterward. Occasionally, a lane number changed between recording of the hundredths and the whole number. If the observer did not notice this change and correct for it, the recorded position was in error by one lane. This and other errors such as times out by five minutes and lane skips made it necessary to check the data carefully during processing. The data analysis, however, was much simpler than that for a radar positioning experiment, since the data were already in digital form, ready for key-punching. The long and tedious job of digitizing positions and times from pictures of the radar screen was eliminated.

Each boat was in charge of tracking three to six floats at a time. Ideal coverage involved taking a fix on each one at least once every 20 minutes; if possible, two fixes were taken a few minutes apart to give a measure of its velocity. To aid in relocating the floats

INSTITUTE of OCEANOGRAPHY
UNIVERSITY of BRITISH COLUMBIA

①

Swift Invader

DATE 28 05 28 May

OPERATOR Pond & Large
Boat # 3

TIME	FLOAT NO.	PAT. 1	PAT. 2	IOCB NO.	COMMENTS
131825	18	16847	21090	3	float aft
131855	18	16812	21091	3	
133200	19	16170	21419	3	
133515	19	16050	21442		
133820	18	15740	21146	3	Temp?
134815	18	15355	21210	3	
135145	19	15319	21524	3	
135950	20	15233	22036	3	
140440	20	15115	22100	3	
140740	19	14857	21801	3	
141345	19	14672	21822	3	
141655	18	14192	21352	3	
142355	18	13921	21361	3	
142745	19	14252	22072	3	
143150	19	14150	22145	3	
143420	20	14362	22642	3	
1441020	20	14227	22772	3	steeps back to 1
144310	19	13955	22342	3	vertical
144755	18	13159	21441	3	vertical
145315	18	12915	21459	3	
150145	18	13212	22630	3	vertical
150405	18	13723	22742	3	vertical
150725	20	13625	22333	3	"
151615	20	13410	22577	3	
151948	19	12955	22049	3	"
152250	18	13230	22116	3	
152710	18	12730	22028	3	"
153520	18	12022	21426	3	"
154015	18	11936	21505	3	"
154720	19	12412	22599	3	"
155145	19	12345	22592	3	"

Figure 2.3 Copy of a log sheet recorded on the first day of the experiment by observers on the *Swift Invader*. Time is recorded in hours, minutes and seconds. The position coordinates are in "lanes" and hundredths. IOCB stands for "in", "out", "check", "boat". The data were keypunched directly from log sheets like this one.

the observers made plots of their positions on chart overlays printed with the Mini-Fix grid. In the diverging flow, floats occasionally were lost for an hour or more, but only one escaped completely. It was lost one night in high winds and rough water, but was found washed ashore on Mayne Island.

To coordinate the efforts of the individual boats, a control centre was established on the *Richardson*. From time to time, the observers radioed in their recorded float positions which were copied onto log sheets, as in Figure 2.4. Master plots of all the float tracks were kept, and the people looking after control used them in deciding when floats should be put in, taken out, or have their custody transferred to a different vessel. Figure 2.5 is typical of these plots.

The usual plan of action was to have a line of about five floats laid across the river near Sand Heads perpendicular to the Steveston Jetty. As this line moved outward and spread apart in the diverging flow, gaps might be filled in with more floats. When these floats were some distance out a second line would be laid behind them and tracked similarly. When the first line of floats was taken from the water, the boats would go back to the river mouth to put in a third line behind the second. Of course, things did not always run so smoothly as this description may imply. There were times when the coverage was not as complete as we had hoped and gaps often occurred near shift change times.

In an attempt to learn about the thickness of the surface layer and the sharpness of the interface, some water property measurements

INSTITUTE of OCEANOGRAPHY
UNIVERSITY of BRITISH COLUMBIA

DATE 28 05

Ric
OPERATOR Buckley Davidson

TIME	FLOAT NO.	PAT. 1	PAT. 2	I C C B	NO. IN	COMMENTS
5	10	12	17	22	25	28
1 2 5 9 4 6	4 4	1 4 4 8 0	2 0 2 5 3	1 1	4	
1 3 0 5 4 6	4 4	1 4 3 6 5	2 0 2 2 2	1 1	4	
1 3 0 6 5 4	4 3	1 4 8 6 7	2 1 5 1 5	1 4	4	
1 3 3 4 5 5	4 5	1 4 1 5 6	2 0 7 0 8	1 4	4	
1 3 3 8 4 5	4 1	1 5 7 3 8	1 9 7 3 8	1 2	4	
1 3 1 8 5 5	1 8	1 6 8 1 2	2 1 0 9 1	1 3	5	
1 3 3 2 0 0	1 9	1 6 1 9 0	2 1 4 1 9	1 3	6	
1 3 3 5 1 5	1 9	1 6 0 5 0	2 1 4 4 2	1 3	6	
1 3 3 5 2 0	1 8	1 5 8 4 0	2 1 1 4 6	1 3	6	
1 3 4 2 5 5	4 5	1 3 9 9 0	2 0 7 1 6	1 4	6	
1 3 5 0 0 0	4 3	1 3 9 9 6	2 1 9 6 2	1 4	6	
1 3 4 8 1 5	1 8	1 5 3 5 5	2 1 2 1 0	1 3	6	
1 3 5 1 4 5	1 9	1 5 3 1 7	2 1 5 9 4	1 3	6	
1 3 4 2 2 5	4 1	1 5 6 8 3	1 9 7 2 7	1 2	6	
1 3 5 1 4 5	4 2	1 5 4 0 6	2 0 3 0 4	1 2	7	
1 3 5 6 2 0	4 8	1 5 3 5 9	2 0 8 7 5	1 2	8	
1 3 5 7 0 8	4 3	1 3 8 7 7	2 2 0 8 7	1 4	8	
1 4 0 1 0 0	4 4	1 3 3 8 1	1 9 7 9 0	1 1	8	
1 3 5 9 5 0	2 0	1 5 2 5 3	2 2 0 3 6	1 3	9	
1 4 0 4 4 0	2 0	1 5 1 1 5	2 2 1 0 0	1 3	9	
1 4 0 7 4 0	1 9	1 4 8 5 7	2 1 8 0 1	1 3	9	
1 4 1 3 4 5	1 9	1 4 6 7 2	2 1 8 8 2	1 3	9	
1 4 1 6 2 0	1 8	1 4 1 7 3	2 1 3 5 8	1 3	9	
1 4 0 9 4 7	4 5	1 3 4 8 1	2 0 7 7 0	1 4	9	
1 4 1 6 0 2	4 5	1 3 3 5 0	2 0 7 7 3	1 4	9	
1 3 1 6 4 3	4 4	1 4 1 5 1	2 0 1 4 7	1 1	9	
1 3 2 2 2 5	4 1	1 4 0 7 7	2 0 1 2 9	1 1	9	
1 3 3 0 0 5	4 4	1 3 8 7 2	2 0 0 4 0	1 1	9	
1 3 3 6 2 7	4 4	1 3 7 7 3	1 9 9 8 6	1 1	9	
1 3 4 5 3 5	4 4	1 3 6 1 5	1 9 9 0 2	1 1	9	
1 3 5 0 5 8	4 4	1 3 5 4 5	1 9 8 5 8	1 1	9	

Figure 2.4 Copy of a log sheet recorded on the first day of the experiment at the control centre on the *Richardson*. Included in the data are some of the fixes from the log sheet in Figure 2.3, which were radioed in by the observers on the *Swift Invader* (boat 3).

were taken. The instrument used was an Interocean CSTD (Conductivity, Salinity, Temperature, Depth recorder) belonging to Mr. A. Ages of Marine Sciences. He worked from a launch near the river mouth during the day shifts of the first week, using the CSTD as he tracked a triangle of drogues. The data were hand-recorded from the digital display. During the nights of the first week and the days of the second week, it was operated by Dr. P.B. Crean from the *Richardson*, which was equipped with a chart recorder. Due to the many problems encountered with both the CSTD and the chart recorder, the available data are limited. The instrument's range was 0 to 100 m, so the depth accuracy was poor near the surface. The depth readout did not agree with estimates of the cable out for about the top five meters, so accurate depths could not be assigned to measurements in this interesting zone. Better data would have been obtained if a CSTD with a 0 to 30 m range had been available. Problems developed with the circuitry and wires in the cable broke, disrupting the measurement of temperature and calculation of salinity. It may be possible to extract some information from the CSTD data, but because of its poor quality, it has not been used in this thesis. Unfortunately, the time spent by the observers in trying to repair the instrument reduced their availability for tracking floats.

Aerial photography of the plume was done by Dr. J. Gower, on contract to the Marine Sciences Directorate. Working from a chartered plane, he flew over the plume on several occasions during the experiment taking pairs of pictures with a normal and a 'fish-eye' lens. The pictures give some information on the extent of the plume, but little on movement within it. Sheets of cardboard which we hoped would be

visible from the air were placed in the water so their motion could be followed. Unfortunately, the contrast was poor and the cardboard does not show up in the photographs.

CHAPTER 3

THE DATA ANALYSIS AND METHOD OF PRESENTATION3.1 Error Checking and interpolation

As mentioned in Chapter 2, one of the advantages of using the Mini-Fix system for float tracking is that the data are recorded in digital form, and can be keypunched directly from the log sheets. Two copies of the data were recorded, the first by the observers on the vessels taking the fixes, and the second by those at the control centre to whom the observers radioed their data. Sample log sheets from these two copies were shown in Figure 2.3 and Figure 2.4. Each line contains the date, time, float number, and Mini-Fix position coordinates, as well as information on whether the float was being put into the water, taken out, or merely checked, a number to indicate which boat took the position fix, and a running total of how many floats were in the water. Both copies of the data were keypunched from photocopies of the original log sheets. Since the data were recorded in pencil, some of the photocopies were faint and not easily legible. Errors from this source had to be corrected as well as those due to mistakes in logging the data.

In a search for such errors, the two copies of the data were cross-checked to locate discrepancies between them. The keypunched cards for each copy of each day's and night's observations were stored in a separate file on U.B.C.'s IBM 370 computer. In each file, the lines of data were sorted in order of increasing float number and, for each group of lines having the same float number, in order of increasing time. The points making up each float track were then in sequence.

Each pair of files was compared line by line, and whenever a discrepancy was found, an error message was printed. Reference was made to the original log sheets to determine the correct values before the files were amended.

At this stage of the analysis, an attempt was made to locate errors caused by lane skipping. A study of the records of the Mini-Fix checks made by the various vessels on known positions or with other boats indicated the time intervals in which skips had occurred. In order to determine the actual time of each lane skip, the plot of the float tracks in question were examined. On a plot such as Figure 2.5, a change of one lane (100 to 150 m) is difficult to detect. Only changes of several lanes could be seen readily, so further correction of lane skips had to be made later in the analysis.

Before any useful information could be obtained from the data, the positions had to be transformed from the hyperbolic Mini-Fix coordinates to a rectangular system. The Marine Sciences Directorate in Victoria provided a computer program which would calculate them in Universal Transverse Mercator (UTM) coordinates. The origin of the UTM coordinates in the zone which includes the Strait of Georgia is at latitude 0° , longitude 123° , but it seemed appropriate to the data to translate the origin of my coordinates to Sand Heads, making the numbers a more manageable size. Over a small area the UTM coordinates are essentially rectangular, but their north-south/east-west orientation was not particularly suitable. A counterclockwise rotation of 31° was done to produce a system with axes parallel and perpendicular to the

Steveston Jetty. To make the data more easily compatible with computer programs written by J.R. Buckley, position coordinates were converted from the UTM units of meters to British nautical miles (1 British naut. mi. = 1853 m).

The observed data points were now in a workable coordinate system, but were still unevenly distributed in time and space. Most float tracks comprised about ten points, though some had as few as two or as many as twenty-eight. In order to obtain anything more than rough estimates of velocities in the plume, it was desirable to fit a smooth curve through the points making up each path line. The components of velocity at points along the curves could be found by taking the derivatives of the smoothed position components with respect to time.

The interpolation of x and y coordinates was done with a cubic spline routine described by Madderom (1974). It makes use of a method given by Reinsch (1971). The method allows the specification of an error in each ordinate, so that the fitted curve need not pass exactly through the given points. The fitted curve is controlled by a parameter which sets a limit on the normalized sum of the squares of the differences between the given values and the fitted ones. Subject to this constraint the curvature of the fitted curve is also minimized, that is, the smoothest possible curve is fitted, which satisfies the imposed least square error limit. The error specified for each position coordinate was ± 0.01 naut. mi. (18.5 m), which had to allow for inaccuracies in recording time, as well as position, since the routine

assumes the abscissae to be exact. The description of the routine suggested that the parameter controlling total normalized error should be in the range $N-(2N)^{\frac{1}{2}}$ to $N+(2N)^{\frac{1}{2}}$, where N is the number of observed points. After some experimentation, it was decided that a reasonable value for the parameter for my data was $N-(2N)^{\frac{1}{2}}$. This value, in combination with the allowed error on each point of ± 0.01 naut. mi., resulted in fairly smooth curves which still contained a reasonable amount of detail. After fitting, the curves were sampled at one minute intervals to obtain the interpolated data set.

For the two tracks which had only two data points and thus could not be handled by the cubic spline routine, a straight line was fitted through the positions. Sampling was also done at one minute intervals along these float tracks.

The data were now in a form which allowed more reliable detection of errors since the components of velocity and acceleration, the first and second derivatives of position, were available. A cubic spline routine operates by fitting a cubic polynomial between each pair of points and matching first and second derivatives at these points. The fitted curves of position vs time were thus very smooth, while the velocity curves showed more variability. The acceleration components were made up of straight line segments. While the slopes of these lines changed at the observed data points, the changes were usually not too extreme. If a sharp change did occur, it often signalled an error in the data. To make use of this indicator, graphs of the interpolated components of position, velocity and acceleration as a function of time

were made for each float track. The plotting was done on a 6-track analog brush chart recorder, using the digital to analog converter of the IOUBC PDP-12 computer system.

When a suspicious acceleration spike was found, reference was made to the original log sheets. The Pattern 1 and Pattern 2 coordinates were hand-plotted as a function of time, to see if a change of one lane or an integral number of minutes would lead to a smoother float track. Such changes were necessary because of recording errors, as well as lane skips. With corrections made, the curve fitting and plotting were redone. If, as sometimes happened, the change had made the situation worse, the data were re-examined. The point in question might be discarded if no simple correction could be found. One segment of the data which required much correction was a four-hour period on June 5 when the data collected by *Launch 1* (Set 13, Floats 7 to 10 in Figure 4.40a) contained several lane skips as well as recording errors.

Occasionally the first observed position of a float track was discarded. This was done if the position fix had just been a rough one, taken quickly as a line of floats were being put in the water, and if a more accurate fix had been taken soon afterward (usually within five minutes). Since different vessels usually took their position fixes at slightly different distances from the floats, an unusually large error might occur if two ships took fixes on the same float within a few minutes. In this case one of the fixes would be discarded.

After several passes through the data, the points in doubt had been either corrected or discarded, leaving relatively smooth float tracks. While a few of the "errors" may actually have been real fluctuations in the flow, the sampling in this experiment was sufficiently sparse that study of such phenomena was not feasible. Instead, the analysis is directed toward showing the large scale features of the flow pattern in the plume.

3.2 Supplementary data: wind and tide

It is generally accepted that surface flow in a situation like the Fraser River plume is influenced by the local winds and tides. In order to understand the observed water motion, it was thus necessary to obtain data on the winds and tides which occurred during the experiment.

Although a few measurements of wind speed were recorded by *Launch 1* and *Caligus*, a comprehensive program of wind velocity measurement was not included in the experiment. To obtain such information, the Climatological Information Section of the Vancouver Airport Weather Office, Atmospheric Environment Service was contacted. There was no single source which gave complete coverage of the area during the time periods in question, so data from several stations were used to compile a composite table of wind speed and direction as functions of time. The data were taken from the lighthouse reports from Sand Heads (eight readings daily) and Tsawwassen (three readings daily), from a recording anemometer at Tsawwassen (hourly averages of wind speed and direction were measured, but this anemometer did not function properly for part

of the time), and from the routine hourly observations at the Vancouver Airport. The resulting composites of hourly wind velocities are found in Chapter 4 (Figure 4.1 and Figure 4.32).

Information on the times and heights of tidal extremes is found in the Canadian Tide and Current Tables published by the Canadian Hydrographic Service. The smooth curves of tidal height vs time shown in Figure 1.4 were generated from the tidal constants for Tsawwassen by Mr. P. Richards, a computer analyst working for Dr. P.B. Crean of MSD.

3.3 Computer generation of a "movie" of the results

While the float tracks do contain much information about the plume's flow pattern, interpretation of a plot such as Figure 2.5 is difficult. The wind and tide conditions may change considerably during the time involved, effecting changes in the flow. To aid in understanding the observations, a "movie" showing the motions of the floats was displayed on the CRT screen which is part of the IOUBC PDP-12 system, using programs developed by Mr. J.R. Buckley.

Each frame of the movie shows dots representing several successive interpolated positions of each float, displayed against an outline map of the area. Since the points for each float represent positions at one minute intervals, the length of the "worm" thus created is proportional to its velocity. Each successive frame represents a time one minute later, so a new point is added to each float track and the oldest point is dropped. Displaying these frames in rapid succession showed changes in velocity as well as in position.

To make the movie more informative, the time corresponding to each frame was written on the screen, and wind velocity and tide height were added. The components of the wind vector were obtained by resolving the previously described composite hourly winds into north/south and east/west components and interpolating them to values at one minute intervals, using a cubic spline routine. A tide curve was displayed, on which a moving marker indicated the tide height appropriate to each frame.

The area shown in the movie was a thirty kilometer square centred just south of Sand Heads. The outline of the land areas was digitized from a map produced by the Geological Survey of Canada, which uses the UTM projection. The edge of the underwater banks was digitized from a Canadian Hydrographic Service chart of the area, in Mercator projection. The slight difference in these two projections is apparent in the river channel, where the Steveston Jetty on one side was from the UTM map and the banks on the other side were from the Mercator chart. The gap between them on the movie map is narrower than it should be.

3.4 Grouping of the data and methods of presentation

After viewing the movie several times, it became apparent that the flow in the plume was affected primarily by the tide. To facilitate study of the data with regard to tidal phase, they were re-organized to group together the tracks of floats which had been installed as a line across the river mouth and those which were added to the line as it moved out in the plume. One or more of these lines of floats

which occurred on each stage of the tide were considered to form a "set". The analysis then involved comparisons of sets which occurred on corresponding phases of the tide on different days.

To allow a more leisurely examination of the data than the movie would allow, computer programs were written to produce plots on the UBC Computing Centre's Calcomp plotter. (When I moved from Vancouver to Halifax, the programs were adapted for use on the Dalhousie University CDC 6400 system.)

First, path lines for each line of floats were plotted. (These plots are shown in the results, for example, in Figure 4.2.) It was decided that sufficient detail would be retained if only one point every five minutes were plotted along each float track, instead of using the complete interpolated data set. The points corresponding to even hours and half hours were marked with special symbols to indicate the relative speeds of the floats. The floats in each set were assigned consecutive numbers, replacing the numbers actually written on the floats, to avoid confusion on the part of the reader in cases where a float was removed from the water and re-installed in a different part of the plume. Where a float was briefly removed for repairs and returned to a nearby position, the two float tracks might be numbered 21a and 21b, as in Figure 4.12b.

While the data coverage was simply not complete enough to allow a general transformation to Eulerian velocities from Lagrangian ones, it was considered useful to display velocity fields for the various sets of data. Each velocity field covers a time period of

several hours, so the velocities displayed in different parts of the plume were not measured simultaneously. To generate a velocity field such as Figure 4.9, the area was divided into half-mile squares by a grid of lines parallel and perpendicular to the Steveston Jetty. The velocity vector plotted at the centre of each square represents the average velocity of all the drogues in the specified time interval which fell within that square. The computer printout listed the component averages, their standard deviations and the number of points used for each square. In composite velocity fields such as Figure 4.5, data collected on different days at similar stages of the tide have been averaged. All the data points from the various sets falling within each grid square were averaged in forming the composites, rather than just averaging the vectors found for each of the sets.

Some thought was given to what type of sampling of the one-minute interpolated data would give a meaningful average velocity field. One possible sampling method was taking one point every five minutes, as was done in plotting the path lines. The other method considered was to take points spaced at 0.1 mile intervals along the float tracks. The method chosen for most of the plots was the latter. The reasoning behind the choice is discussed in Chapter 4 with reference to Figures 4.5 and 4.6, and to Figures 4.16 and 4.17.

Much of the discussion and interpretation of the data in Chapter 4 is based on the plots of path lines and velocity fields presented in Figures 4.2 to 4.31 and 4.33 to 4.48. The sets are compared and contrasted with respect to the changing effects of tide and wind on the flow which they portray. For each phase of the tide for which there

is sufficient coverage, a composite velocity field has been generated. The flow patterns observed on the equatorial tides of the first week were quite different from those found on the tropic tides during the second week, so data from the two weeks have not been averaged together.

To allow examination of the data from a different viewpoint, another computer program was written to produce plots of average velocity components as a function of distance from Sand Heads. Each of the graphs displayed in Figures 4.49 to 4.54 corresponds to a composite velocity field shown earlier in Chapter 4. The data sampled at 0.1 mile intervals along each float track were used, and distance from Sand Heads was calculated as distance from there to the first point of the track plus distance along the track. Since it did not seem sensible to average the low velocities found near the edges of the plume with higher ones measured in its centre, the float tracks were subjectively divided into three groups. On each graph the three traces represent average velocity components for floats in the north, centre and south regions of the plume. The standard deviation of the data used to calculate each point was printed out, and an error bar representing a typical value of the standard deviation has been plotted beside each graph.

CHAPTER 4

RESULTS

When the Fraser River flows into the Strait of Georgia, the fresh water forms a surface layer above the denser salt water. Without the confinement of the river banks and the Steveston Jetty, the fresh water spreads out to form a plume, becoming thinner as it diverges. Friction between the two layers decreases its speed, and mixing occurs along the interface between the layers. If friction were the only force acting and if the lower layer were not being advected, the plume would be symmetric. The speed of the outflowing water at Sand Heads would be determined by the runoff into the river.

There are several external forces which affect the velocity of water in the plume, and prevent the formation of a symmetric flow pattern. The Coriolis force, which is proportional to the speed of the water, gives it an acceleration to the right of the original direction of flow. As the tide rises and falls the currents which it generates move the salt water up and down the Strait, and the frictional forces between the layers cause the plume to move also. The slope of the surface in the Strait produces a pressure gradient which acts on the plume. The water level in the river relative to that in the Strait affects the speed of the outflowing fresh water. As the tide falls, the speed of water leaving the river mouth increases until shortly before low tide, when so much water has left the river mouth that its level is lower than that in the Strait. A numerical model of the Fraser River, developed by Mr. A. Ages of the Institute of Ocean Sciences, Patricia Bay, B.C., predicts

that the maximum outflow during a tidal cycle occurs about one hour before lower low water. As the water level rises with the flooding tide, the speed of discharge decreases and fresh water accumulates near the river mouth. Shortly before high tide the speed of the water leaving the river begins to increase as the continuing discharge makes the surface level at the river mouth higher than that in the Strait. Wind stress acts on the water surface and moderate to strong winds impart enough momentum to the upper layer that the plume's velocity is noticeably affected. The configuration of the banks and the Steveston Jetty introduce variations in the flow which complicate the situation even more.

This experiment has shown that the flow in the Fraser plume is dominated by tidal effects. The first week (May 28 to 31, 1974) was a period of equatorial-type tides and most of the data was taken on the small floods and ebbs. During the tropic-type tides of June 4 to 6, observations were made of only the large ebb and flood stages of the tide. The data from the two weeks are thus quite different and will be discussed separately.

4.1 Week 1 - tracks and velocities

Graphs of the tide height and wind speed and direction for the first week are shown in Figure 4.1. The times when the various sets of data were obtained are indicated on it. Time is measured in hours from midnight (PDT) on May 28, 1974.

4.1.1. Sets 2 and 6, near lower low water

During the time near lower low water, the speed of the out-flowing water reaches a maximum. The plume is deflected less by friction

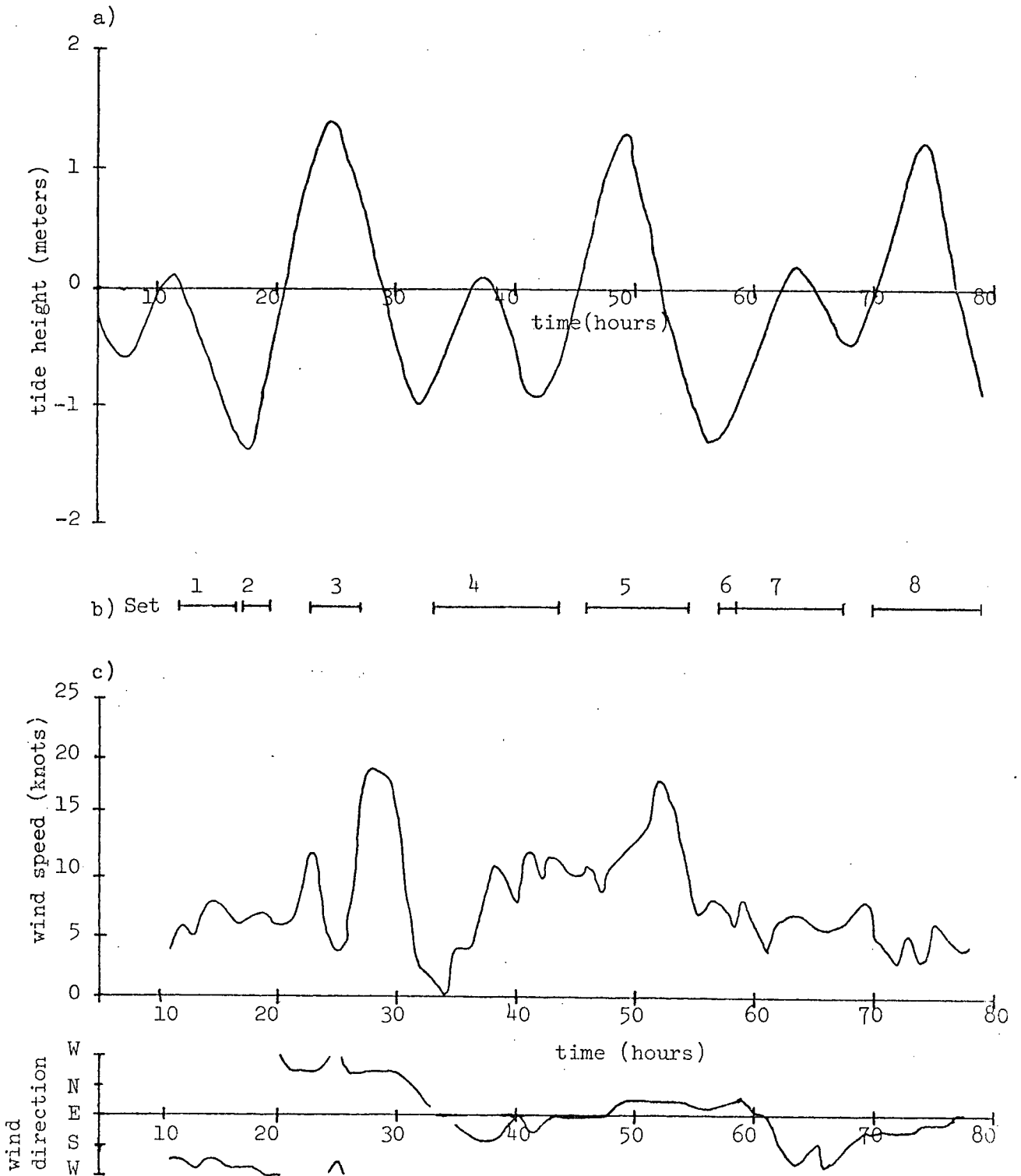


Figure 4.1 a. Tide height at Tsawwassen, b. times when the sets of data were taken and c. wind speed and direction, during the first week of the experiment. Time is measured in hours from midnight, PDT, May 28, 1974.

with the lower layer than at any other time in the tidal cycle. The resulting simplicity of the flow at this tidal stage makes it a good place to begin the examination of the data. Observations made near lower low tide are Sets 2 and 6, which were obtained on the first and third days of the week.

The floats in Set 2 were in the water from about one-half hour before lower low tide until almost two hours after it. The paths of these floats (Figure 4.2) were plotted from data interpolated to one point every five minutes. The floats are usually numbered in order of installation, but floats added to a line which is some distance from the river mouth are given numbers consecutive with those of nearby floats. Set 2 began with the installation of Float 1, about three miles from Sand Heads, and Float 4, only a mile out. Floats 2 and 3 were added near 1, while 5, 6, and later 7 were put in near 4. Almost an hour after the set began Floats 8, 9 and 10 were put in to form a third line. The floats in Set 6 (Figure 4.3) were put in near the river mouth about one-half hour after low tide on the third day of the experiment.

As described in Chapter 3, velocity fields may be generated by dividing the area into a grid of squares and averaging the velocity components of data points falling within each square. A vector representing the mean velocity may then be plotted at the centre of the square. To illustrate the variations in the flow over short time periods, each line of floats in Sets 2 and 6 was treated as a small data set to produce the superimposed velocity fields shown in Figure 4.4. The solid arrows make up the fields corresponding to Floats 1 to 3, 4 to 7, and

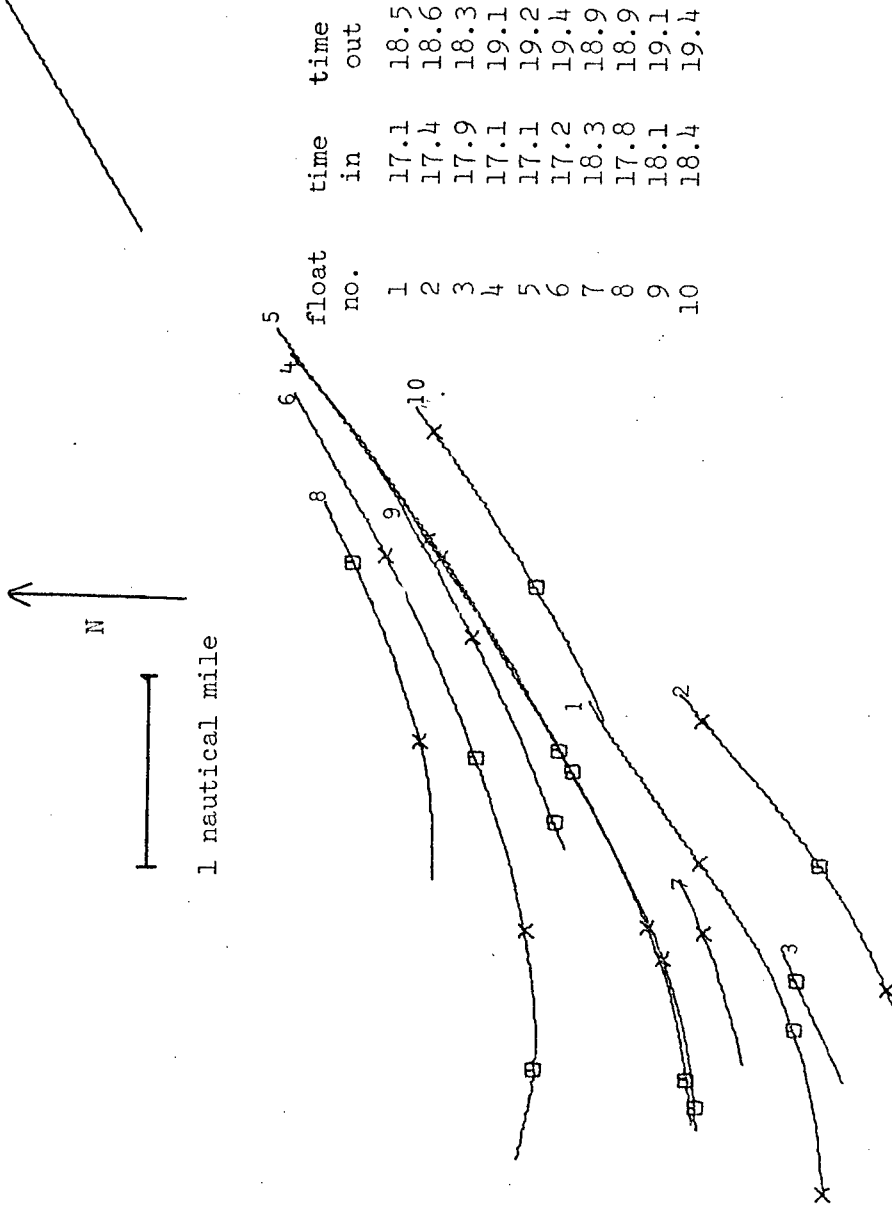


Figure 4.2 Path lines of floats in Set 2, beginning at 17.0 hours, ending at 19.4 hours, including the time near lower low tide. Winds were near west southwest 6 knots. In this and all later path line plots, the solid line at the upper right represents the Steveston Jetty; the river flows out to the south of it. The path lines are composed of interpolated points sampled every five minutes. Points on the hour are marked by a box, those on the half hour are indicated by a cross. The float number near the beginning of each path line corresponds to one in the table listing times of installation and removal.

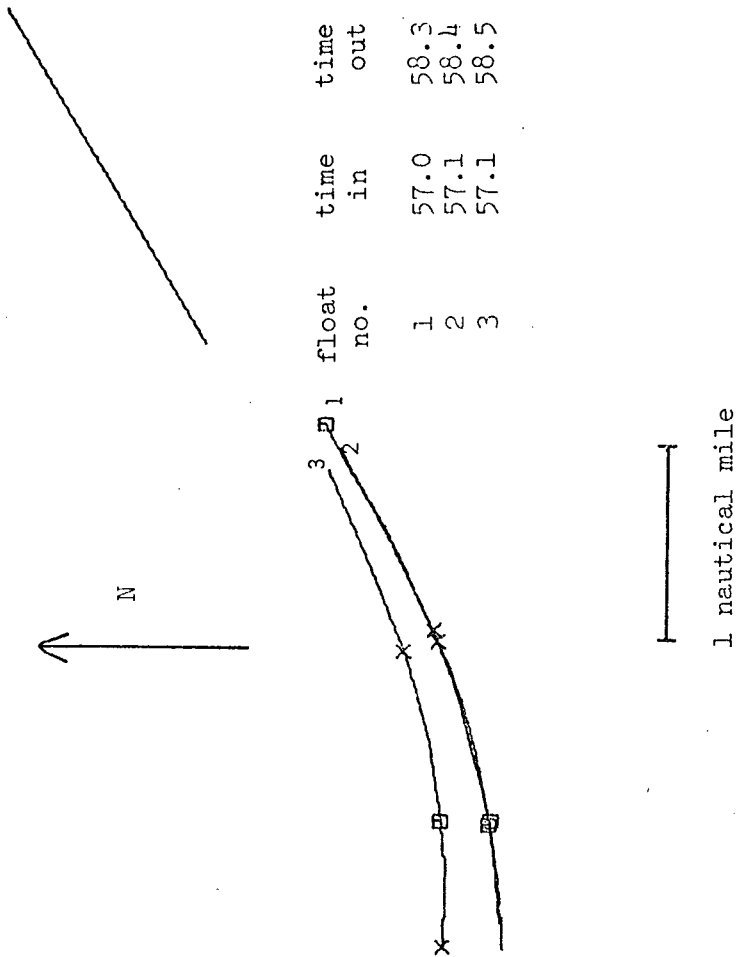


Figure 4.3 Path lines of floats in Set 6, beginning at 57.0 hours, ending at 58.5 hours, taken just after lower low tide. Winds were about northeast 7.

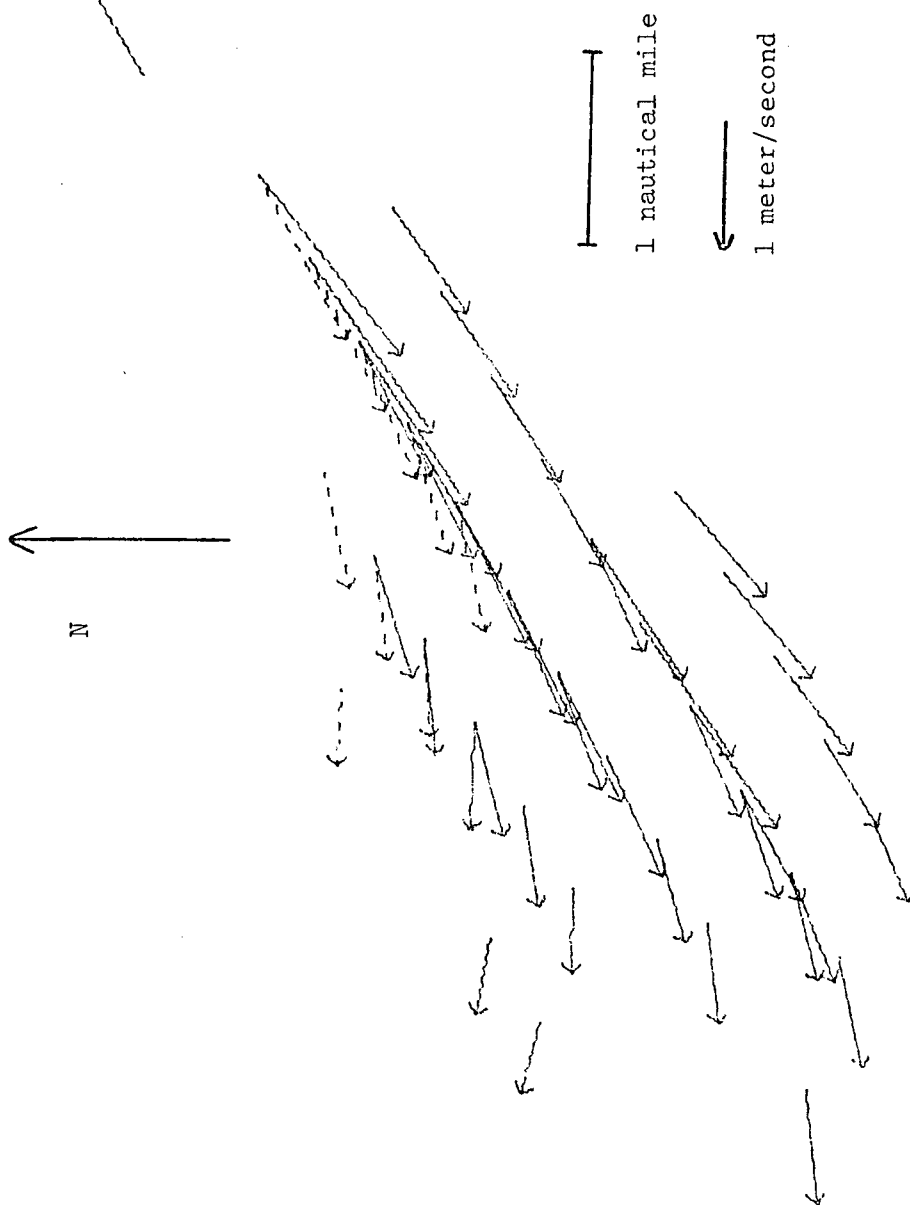


Figure 4.4 Velocity field based on the data from Set 2 (17.0 hours to 19.4 hours) and Set 6 (57.0 hours to 58.5 hours), near lower low tide. The solid arrows are the average velocity vectors obtained by treating each line of floats in Set 2 separately; the dotted arrows correspond to Set 6. The data were interpolated to one point every five minutes. As in all subsequent velocity fields, the Steveston Jetty is represented by the solid line at the upper right. Each arrow represents the average velocity of points which fall within the half-mile square surrounding the tail of the arrow.

8 to 10 of Set 2, while the dotted arrows are the velocity field for Set 6. Differences in average speed for any one square were generally 10% or less among the subsets making up Set 2, while speed variations of as much as 25% occurred between Sets 2 and 6.

From the velocity field the characteristics of the flow may be noted. The greatest speeds, of about 1.7 m/s, were found near the centre of the plume and close to Sand Heads. Farther away from the river mouth, near the edges of the plume, speeds as low as .6 m/s were measured. This reduction in speed was probably caused by the frictional drag of the salt water layer below, and of the slower moving surface water outside the plume. The small cross-stream component changed gradually from being down the Strait (southwest) to up the Strait (north-east) as the tide changed from ebb to flood over the two and one-half hour period during which the data was collected.

The Coriolis force, acting to the right of the velocity, would also be important in causing this shift. If the Coriolis force were acting alone on a current with an initial speed of 1 m/s at latitude 49°N , it would cause the water to move in a circle of radius about 9 km or 5 nautical miles. The speed would remain the same, but after an hour its cross-channel velocity component would change by about .4 m/s. Friction would reduce this effect somewhat, making the results of the calculation fairly consistent with the observed flow.

Winds during Set 2 were west-southwest to west at 6 to 7 knots, while east 15 winds were experienced during Set 6. (Since the wind data obtained from AES was in units of nautical miles per hour, this unit will be used for wind speeds throughout the thesis; 1 knot = 0.52 m/s.)

Buckley and Pond (1976) suggest that when a well defined surface layer exists, momentum transferred from the wind to the water stays in the upper layer and is distributed quite evenly throughout it. An approximate expression for the wind stress is $\tau = \rho_a C_D U^2$, where ρ_a is the air density, C_D the drag coefficient and U the wind speed. With $\rho_a = 1.2 \times 10^{-3} \text{ g cm}^{-3}$ and $C_D = 1.3 \times 10^{-3}$, the wind stress for a speed of 16 knots or 8 m/s is $\tau = 1 \text{ dyne}$. Acting on the top 3 meters this gives an acceleration of $\frac{1}{300} \text{ cm s}^{-1}$ (about one-third of the Coriolis acceleration which would act on a 1 m/s current). Over a period of an hour, the wind stress would give a velocity of 12 cm/s while a parcel of water moving at 1 m/s moved 2 nautical miles. If the wind speed were halved, the velocity change in an hour would be only 3 cm/s. This change is not large compared with the total speed or the Coriolis effect. Thus the winds during Set 2 would have had little noticeable effect on the flow, and those in Set 6, by pushing the water slightly to the right of the plume axis, would add to the turning caused by the Coriolis force and the flooding tide.

Figure 4.5 shows the velocity field obtained by averaging together all the data in Sets 2 and 6, using data sampled at five-minute intervals. This type of sampling may not be the best to use, since it might lead to biased average velocities. A quickly moving float is only represented in a particular half-mile square by one or two data points, while a float moving more slowly remains in the square longer and biases the average toward a lower value. In an attempt to reduce this problem the data were sampled at 0.1 mile intervals along each float

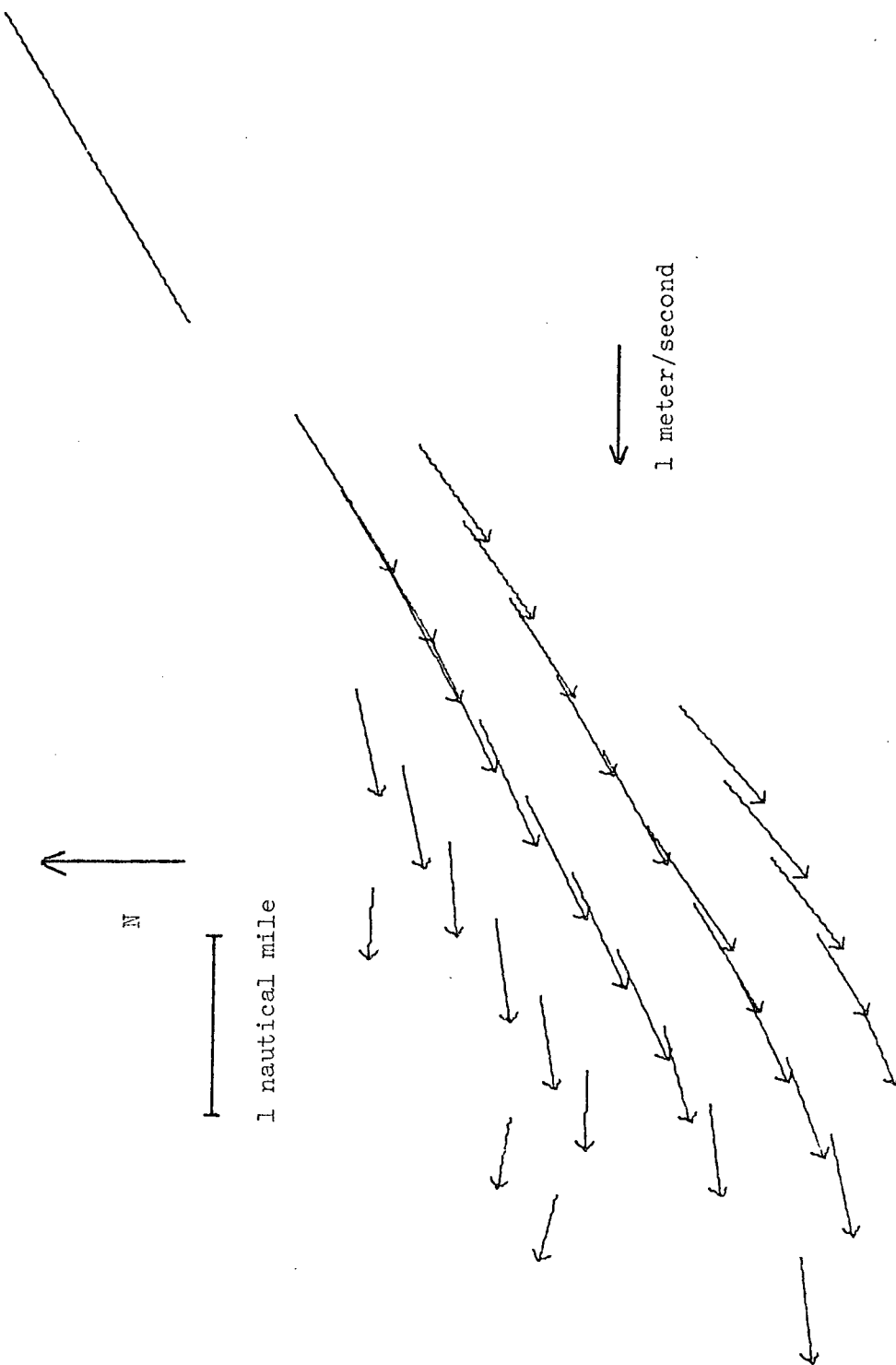


Figure 4.5 Composite velocity field averaging the data from Set 2 (17.0 hours to 19.4 hours) and Set 6 (57.0 hours to 58.5 hours), taken near lower low tide. The data were sampled at one point every five minutes.

track so that a float moving at any speed is represented by about the same number of data points in each square through which it passed. Figure 4.6 shows the velocity field averaged from the distance-sampled data for Sets 2 and 6. Although Figures 4.5 and 4.6 are very similar, the computer printouts which accompanied the plots show that the speeds in Figure 4.6 are about 1% larger than those in Figure 4.5. Since there is little variation in speed among the tracks in these sets, it hardly matters which sampling method is used over this relatively short time period. Distance sampling does give equal weight to each float track, and so is a reasonable choice in the absence of other criteria.

When averaging is extended over a longer time period, in which the flow pattern has changed significantly, the results from the two methods may differ quite markedly. Neither average would represent a flow field which was actually observed. This type of variation is noted with reference to Figures 4.16 and 4.17. A representative average over a long time period cannot be obtained if sampling has been too nonuniform in time and space. The average obtained is biased toward those situations which were observed, and cannot include those which were not. Morel and Desbois (1974) recognize this problem in their analysis of wind data obtained by tracking EOLE balloons.

4.1.2 Sets 4, 7, 1 period from lower low water through lower high water to subsequent low water

Three sets of data were taken on the small flood and ebb tides. On the second day of the experiment Set 4 began shortly after low tide, spanning the flood to lower high water, the subsequent ebb, and about

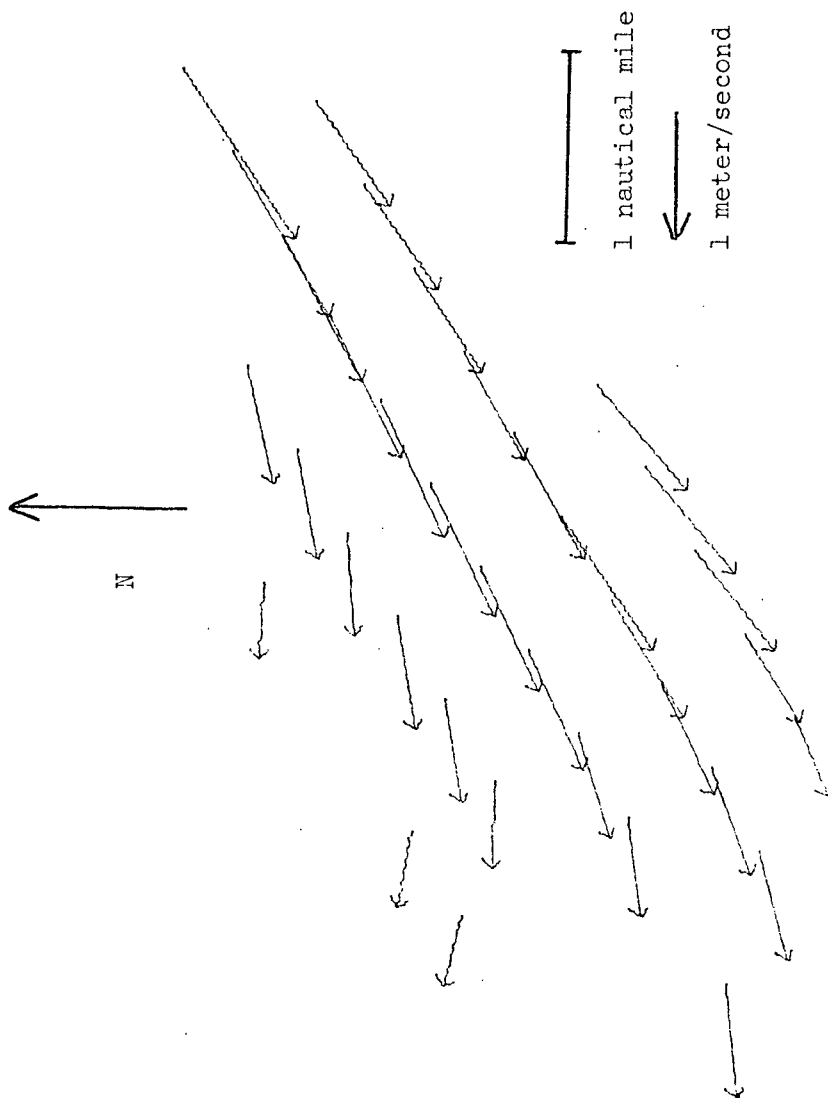


Figure 4.6 Composite velocity field for Set 2 (17.0 hours to 19.4 hours) and Set 6 (57.0 hours to 58.5 hours), taken near lower low tide. The data were sampled at 0.1 mile intervals along each float track. Unless otherwise specified, all subsequent velocity fields will be plotted from data sampled in this way.

three hours of the next flood tide. Set 7 began near lower low tide on the third day and continued through lower high tide to higher low water. Operations on the first day got underway at lower high tide and Set 1, which continues until about an hour before lower low tide, is discussed after Sets 4 and 7, since it includes only the ebb. Variations in winds and tidal ranges on the three days lead to differences among the three sets, so they will be examined separately and then compared.

The float tracks in Set 4 are shown in Figures 4.7 and 4.8. The first line of floats (1-3) was put in about one and one-half hours after low tide, followed by the second line (4-10) about an hour later. While those floats were still in the water a third line (11-14) was put in, and a fourth line (15-18) was begun partway up the river. Just at high tide four floats (19-22) were put in the water on the northern side of the plume, and over one and one-half hours later a line (23-30) was put in across the main part of the river. Two or three lines were in the water at most times so information is available about more than one area of the plume at any one time.

Figure 4.9 is the velocity field for the time from the beginning of the set to about one hour after lower high tide. The winds during the period were quite light at first, but eventually swung from east 4 to south-southeast 11. The flow speeds decreased from 1.1 m/s near the river mouth to .3 m/s at the western edge of the observed area as the flooding tide held back the river water. The velocity was initially directed slightly to the south of a line

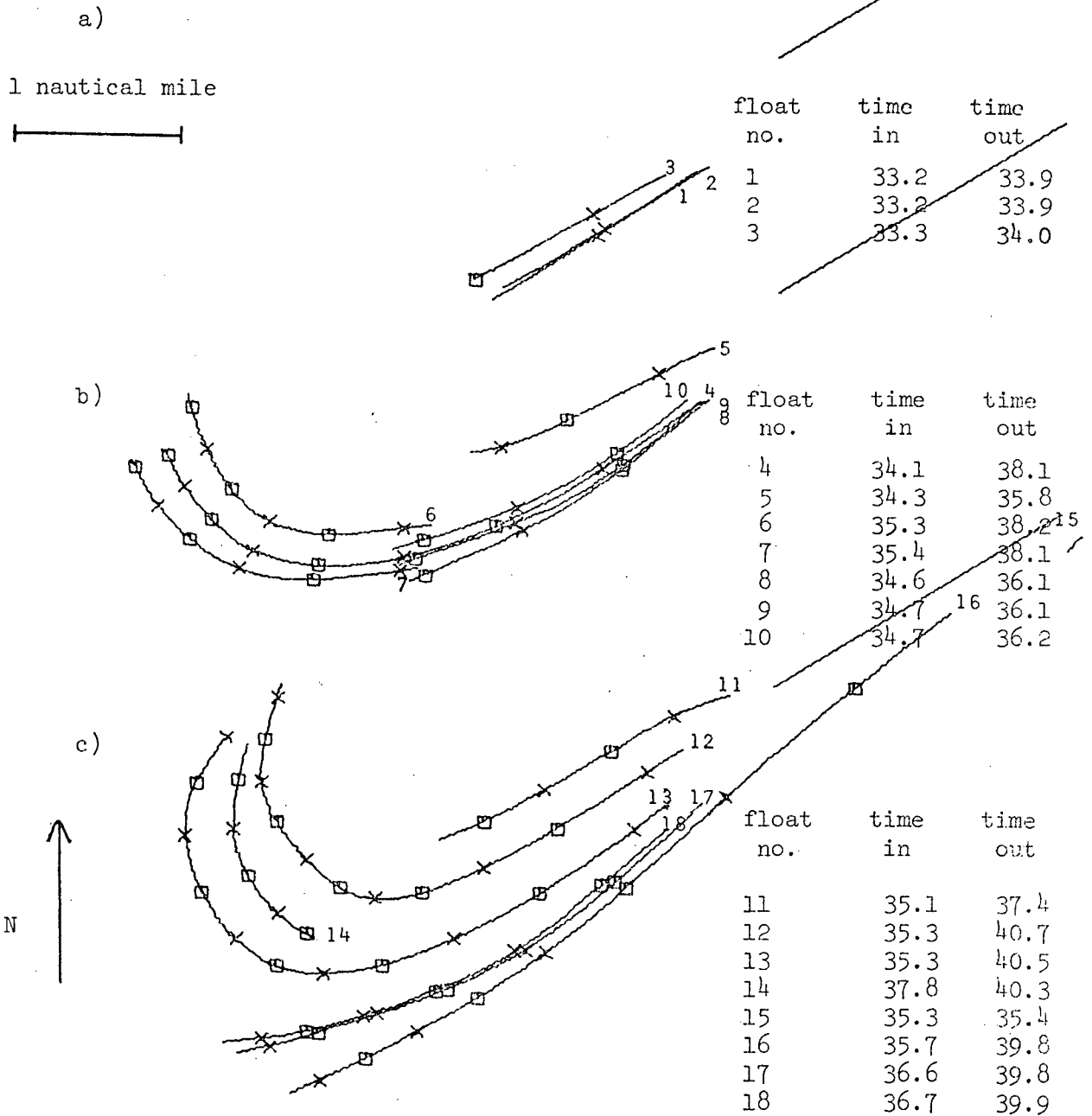


Figure 4.7 Path lines of floats in Set 4, on the rise to and ebb from lower high tide. a, 33.1 hours to 34.0 hours, when winds were near east 2 knots. b, 34.1 hours to 38.2 hours, when winds were east 2 to southeast 11. c, 35.1 hours to 40.7 hours, when winds were southeast 4 to southeast 11.

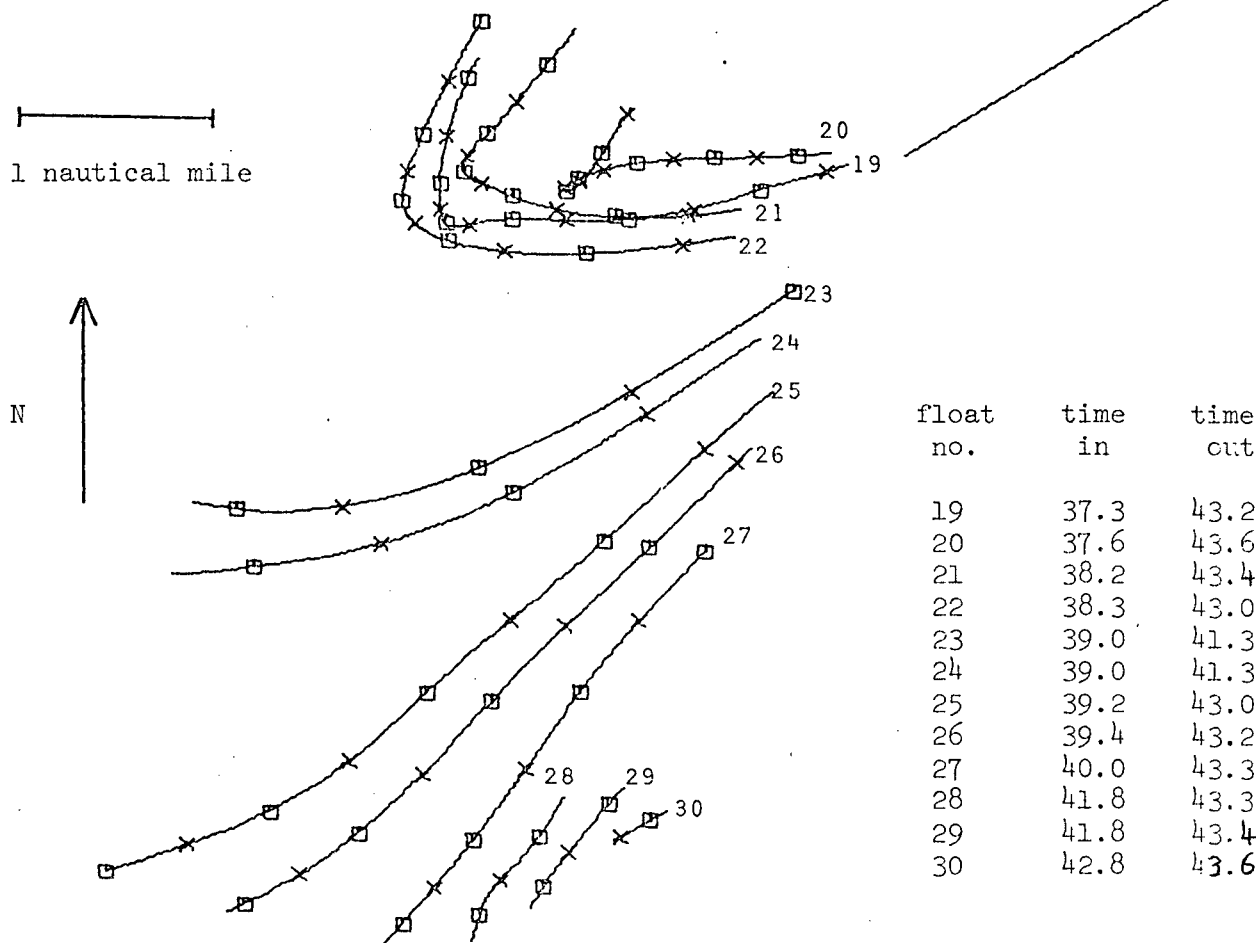


Figure 4.8 Path lines of floats in Set 4, from 37.3 hours to 43.6 hours, on the ebb to and rise from higher low tide. Winds were southeast 8 to east 12.

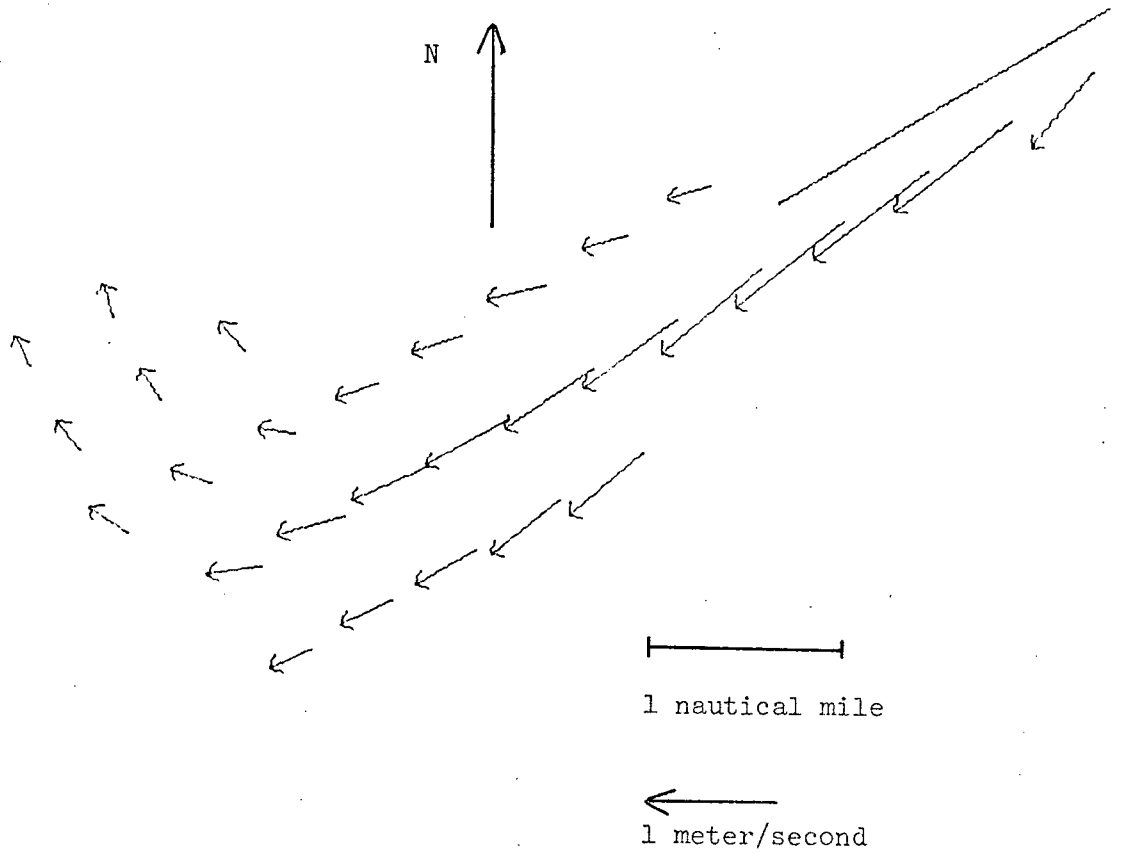


Figure 4.9 Velocity field for Set 4 (33.1 hours to 38.9 hours) on the rise to lower high tide.

parallel to the jetty, but the Coriolis force and the flooding tide turned the flow toward the right, and when the wind speed increased, the turning became much more pronounced.

The velocity field shown in Figure 4.10 is an average of the data from lower high water to about two hours before low tide. The north side of the plume showed progressively more clockwise curling and slowing, while in the central and southern parts speeds increased as the tide began to ebb and the flow tended slightly to the south. Slower moving floats at the end of the flood tide gave rise to the smaller speeds farther out in the plume. Even the faster moving central part of the plume was kept from turning much to the south as the wind remained near southeast 10.

The velocity field for the ebbing tide (Figure 4.11) shows the remaining part of the flood time plume still curling to the north, while the drag of the ebb tide had overcome the wind and Coriolis forces and turned the main part of the plume slightly to the south. Speeds near the river mouth were about 1 m/s. The ebb was quite a small one and the last few floats remained in the water after the beginning of the next flood, so the speeds seen at the end of the period were as low as .2 m/s.

Set 7 began with a very large line of floats (Figure 4.12a) being put in across the river. These floats were further supplemented by those shown in Figure 4.12b. The float tracks numbered 21a and 21b indicate that the float was removed from the water for repairs and replaced soon after. The floats were in the water from about five hours

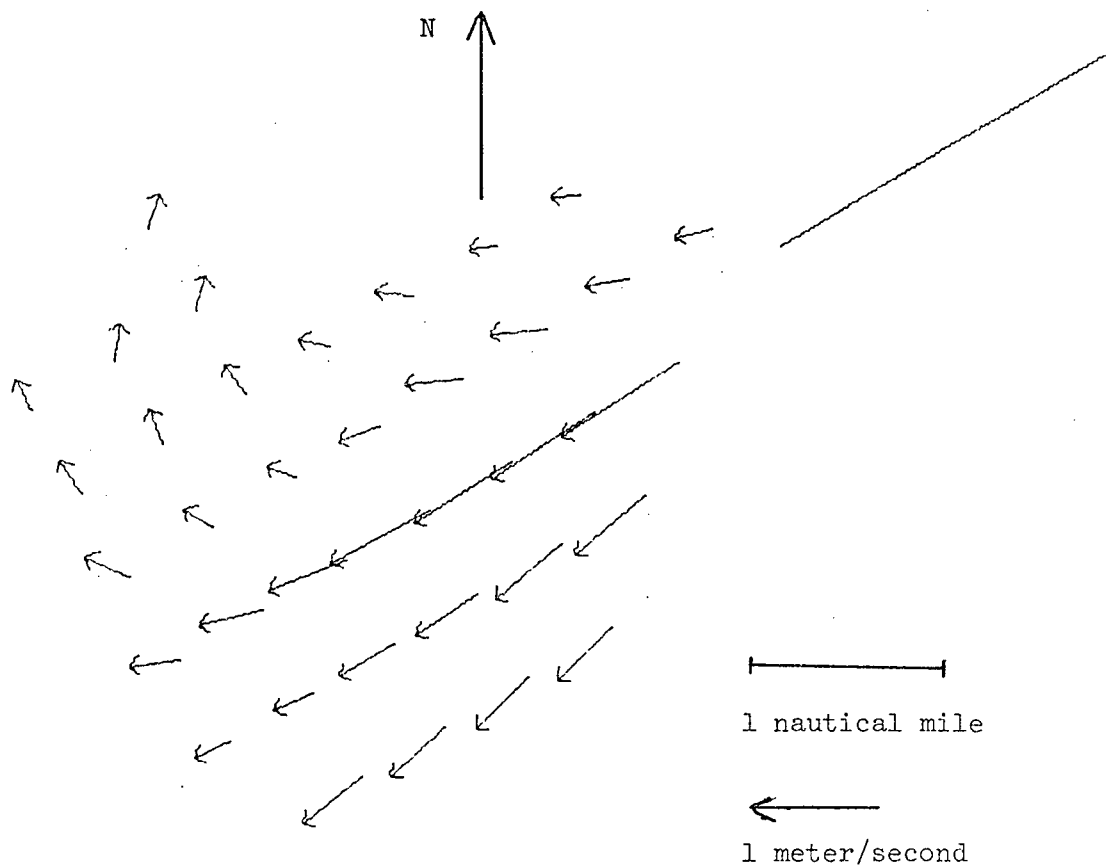


Figure 4.10 Velocity field for Set 4 (37.0 hours to 40.7 hours), near lower high tide.

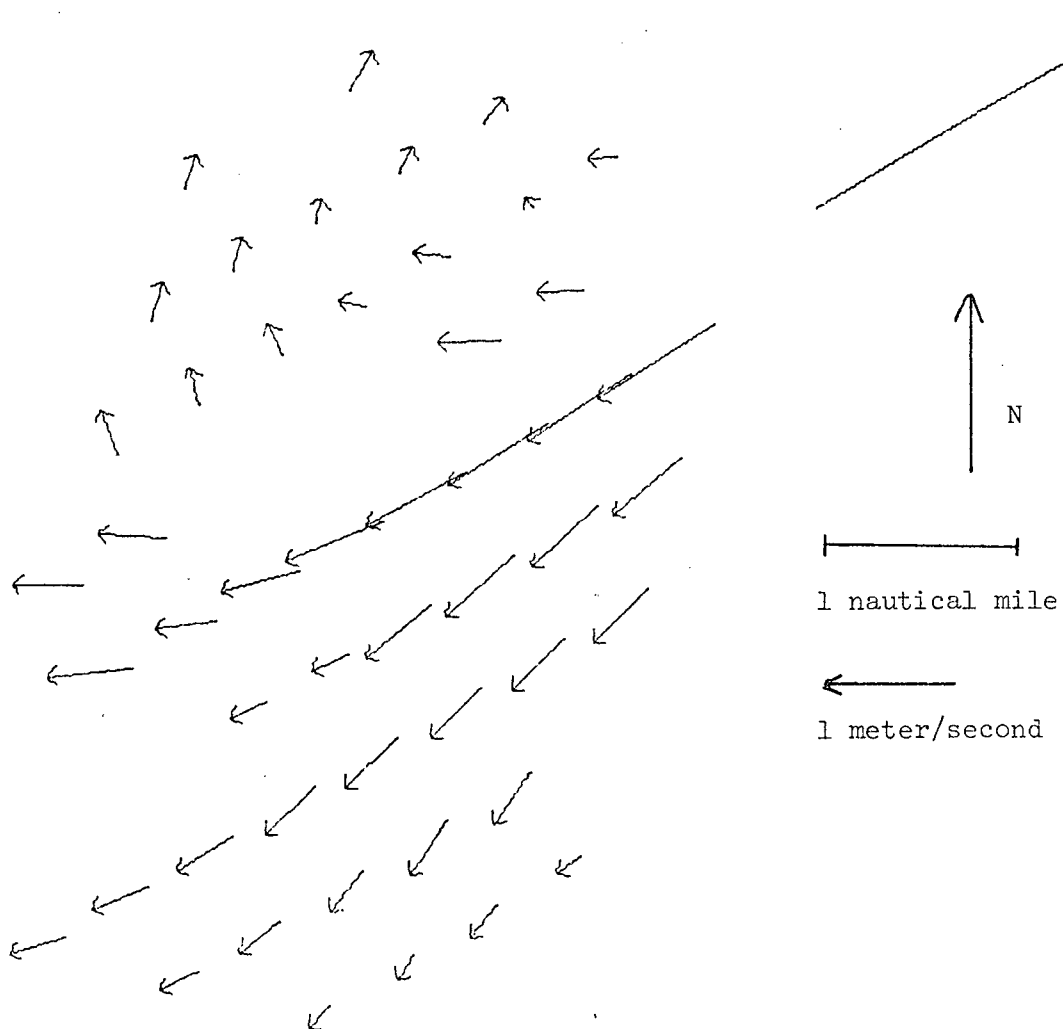


Figure 4.11 Velocity field for Set 4 (38.9 hours to 43.6 hours), on the ebb to and rise from higher low tide.

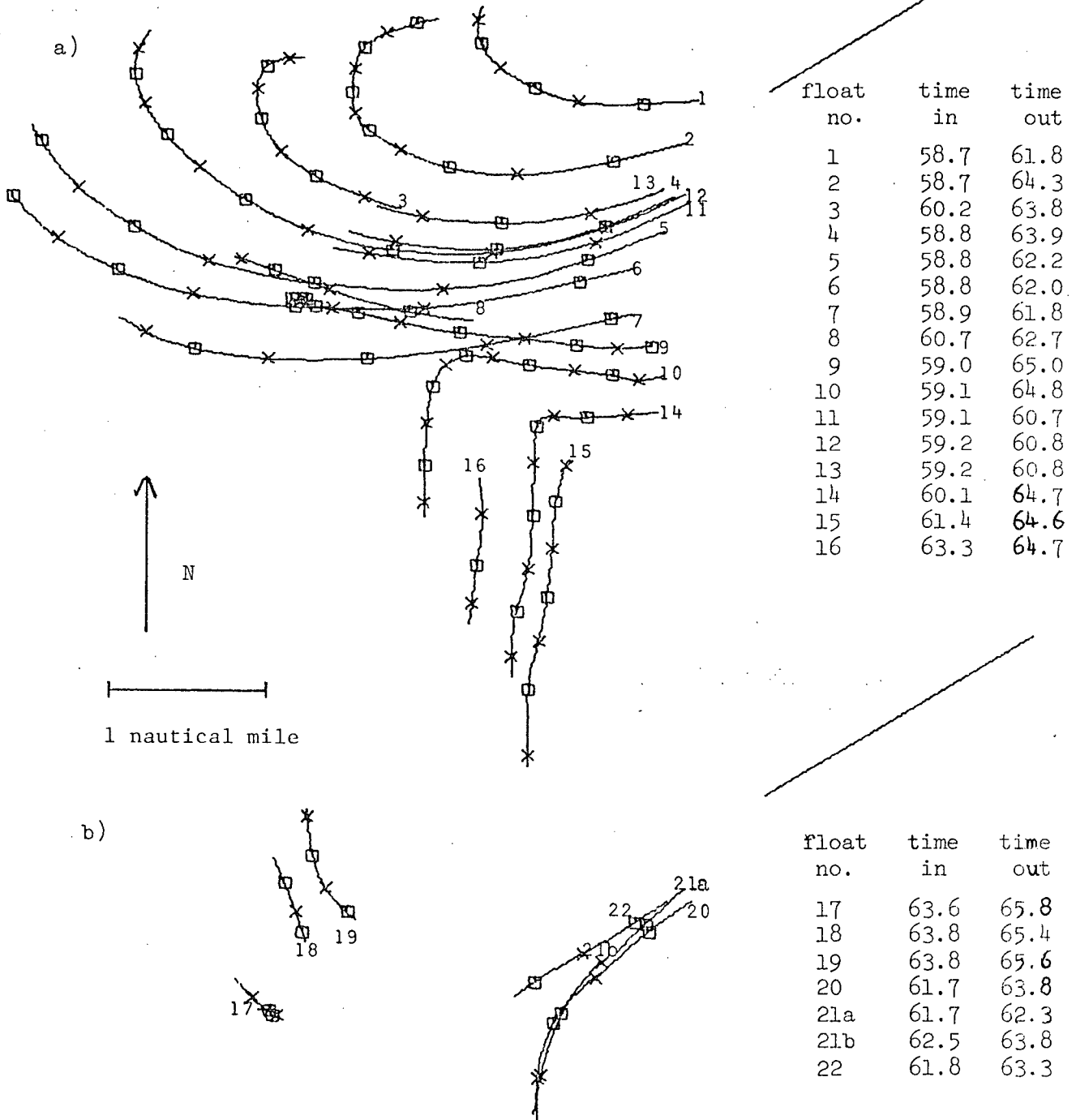


Figure 4.12 Path lines of floats in Set 7, on the rise to and ebb from lower high tide. a, 58.6 hours to 65.0 hours, when winds were northeast 7 to southwest 7. b, 61.6 hours to 65.6 hours, when winds were east 4 to southwest 7. The path lines numbered 21a and 21b indicate that the float was removed briefly for repairs.

before high water to three hours after it. Another line of floats (Figure 4.13) was put in almost two hours after high tide and removed just after low tide.

As in the analysis of Set 4, three average velocity fields were generated: one for the rising tide, one for the time near the change from flood to ebb, and one for the falling tide. The first of these (Figure 4.14) covers the time from the beginning of the set until just over an hour before high water. The winds during the period were northeast 8 to east 4. The float paths curved much more evenly to the north than in Set 4, in which the floats moved straight out and then curled north. Speeds at the core of the plume were about .8 m/s. The tidal rise in Set 4 was smaller than that in Set 7, but Set 7 began later relative to the low tide. The winds at about northeast 6 were too light to have much effect on the flow, but if anything, they tended to oppose the turning. The previous day's winds had increased fairly quickly to enhance it. By the end of the time period, the flood had slowed as high water approached and the pressure head of the river was enough to begin to overcome the force of the tide pushing it back. The southern part of the plume began to swing to the south.

Figure 4.15 shows the velocity field for the time one and one-half hours before the turn of the tide until two hours afterward. The change in the flow was very noticeable as the old part of the plume was left curling slowly around on the north side, while the main flow from the river moved off to the south with the ebbing tide. The effect was like that of swinging a hose back and forth; the water continued to move in the direction the hose was pointing when the water left it.

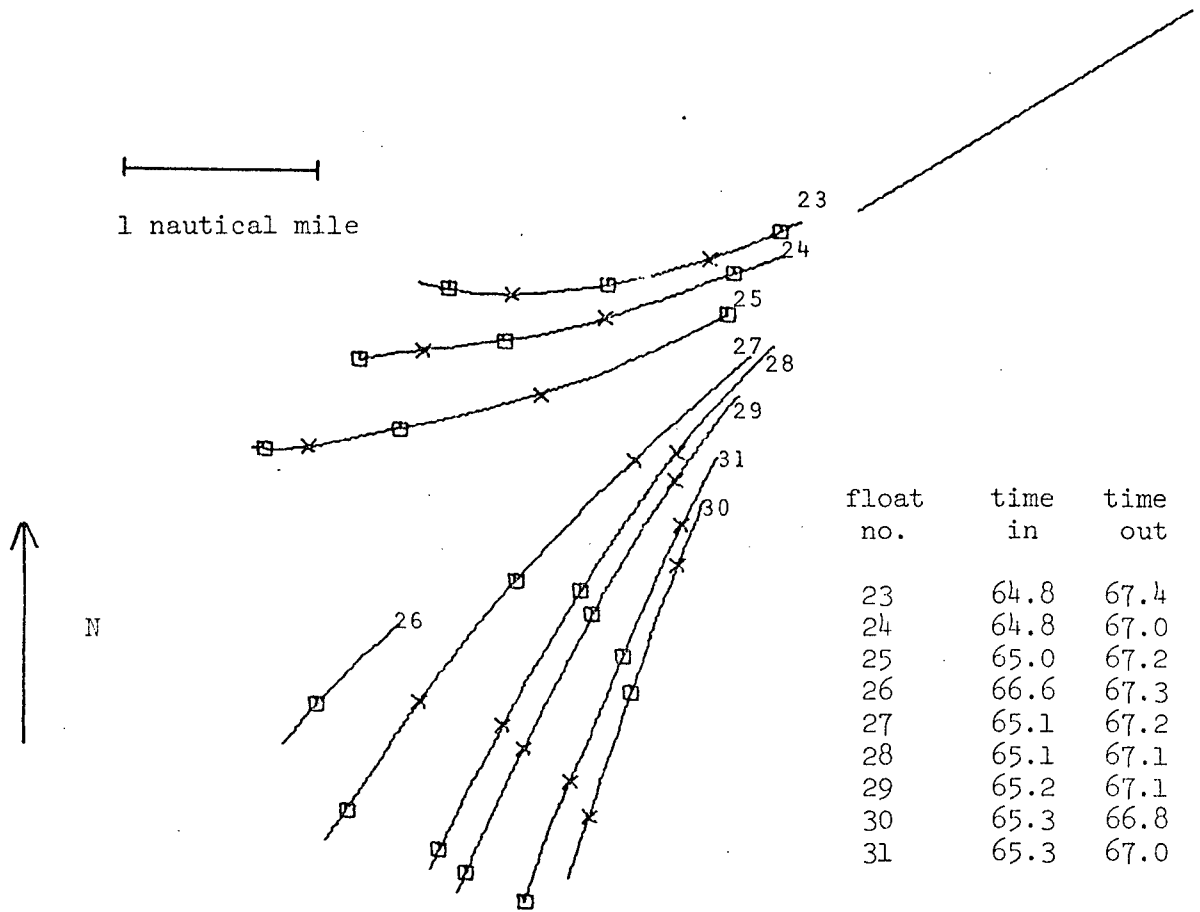


Figure 4.13 Path lines of floats in Set 7, from 64.7 hours to 67.5 hours, on the ebb from lower high tide. Winds were near southwest 6.

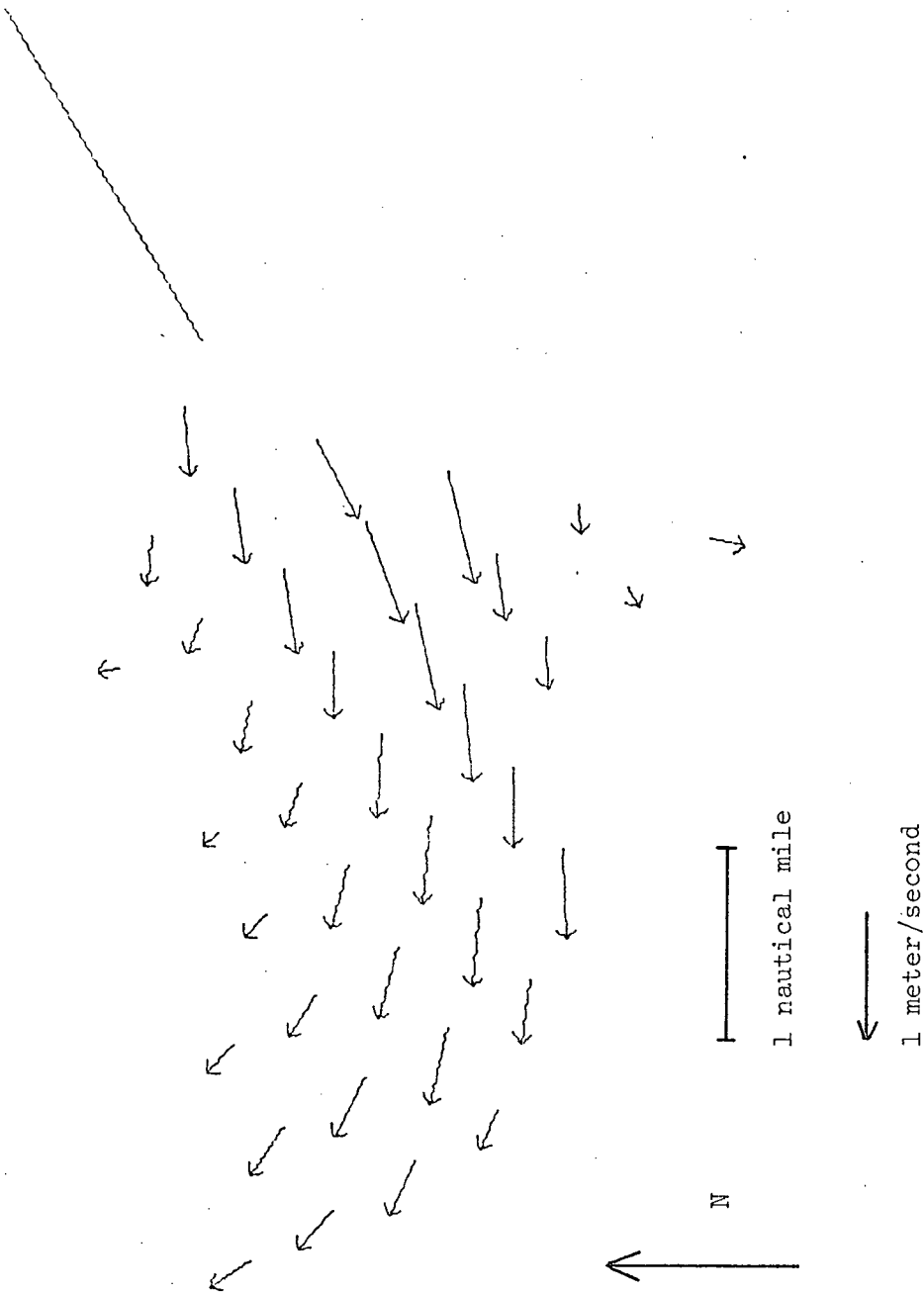


Figure 4.14 Velocity field for Set 7 (58.6 hours to 62.0 hours) on the rise to lower high tide.

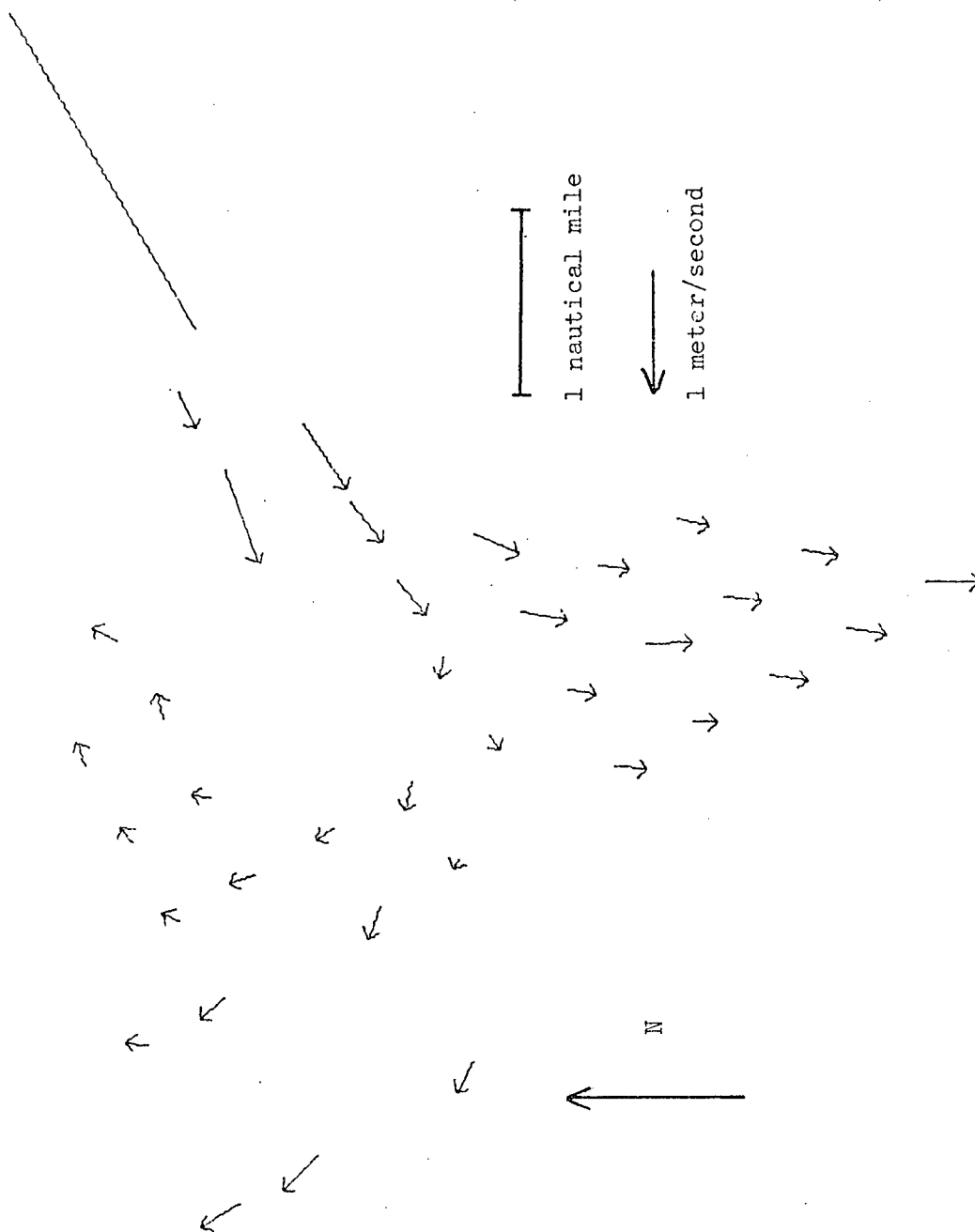


Figure 4.15 Velocity field for Set 7 (61.6 hours to 65.0 hours), near lower high tide.

Near the boundary between the old and new plumes the motion of the old plume is slowed to almost nothing by friction (Floats 9 and 17). The faster speeds near the river mouth are due to another line of floats (Figures 4 to 13) which were put in after the ebb had begun. The separation of the old and new plumes is much more pronounced than in Set 4, in which south-southeast wind inhibited turning to the south.

The difference in the flow between the flood and ebb tides in Set 7 are marked. In some areas where the speeds had been quite large during the flood they became very small during the turn to the ebb. Averaging over a longer time period in such a situation can lead to biases according to which data sampling method is used. Figure 4.16 is a combination of Figures 4.14 and 4.15 (made using distance-sampled data), while Figure 4.17 shows an average of the time-sampled data set for the same period. The speeds in the central region are somewhat slower in the time-sampled plot, especially in the square where Floats 9 and 17 remained for a long time. However, while there are differences in detail, the basic pattern is the same in both cases, giving confidence that the overall picture of the flow is representative although small details may not be.

By the time the tide began to ebb, the wind had swung around to about southwest 6. Such a light wind had little effect on the flow (Figure 4.18) which moved quite quickly to the south showing some spreading. The low velocities on the north side are due to the remnants of the slow-moving water along the boundary with the old plume at the beginning of the time period. The apparent separation into northern and

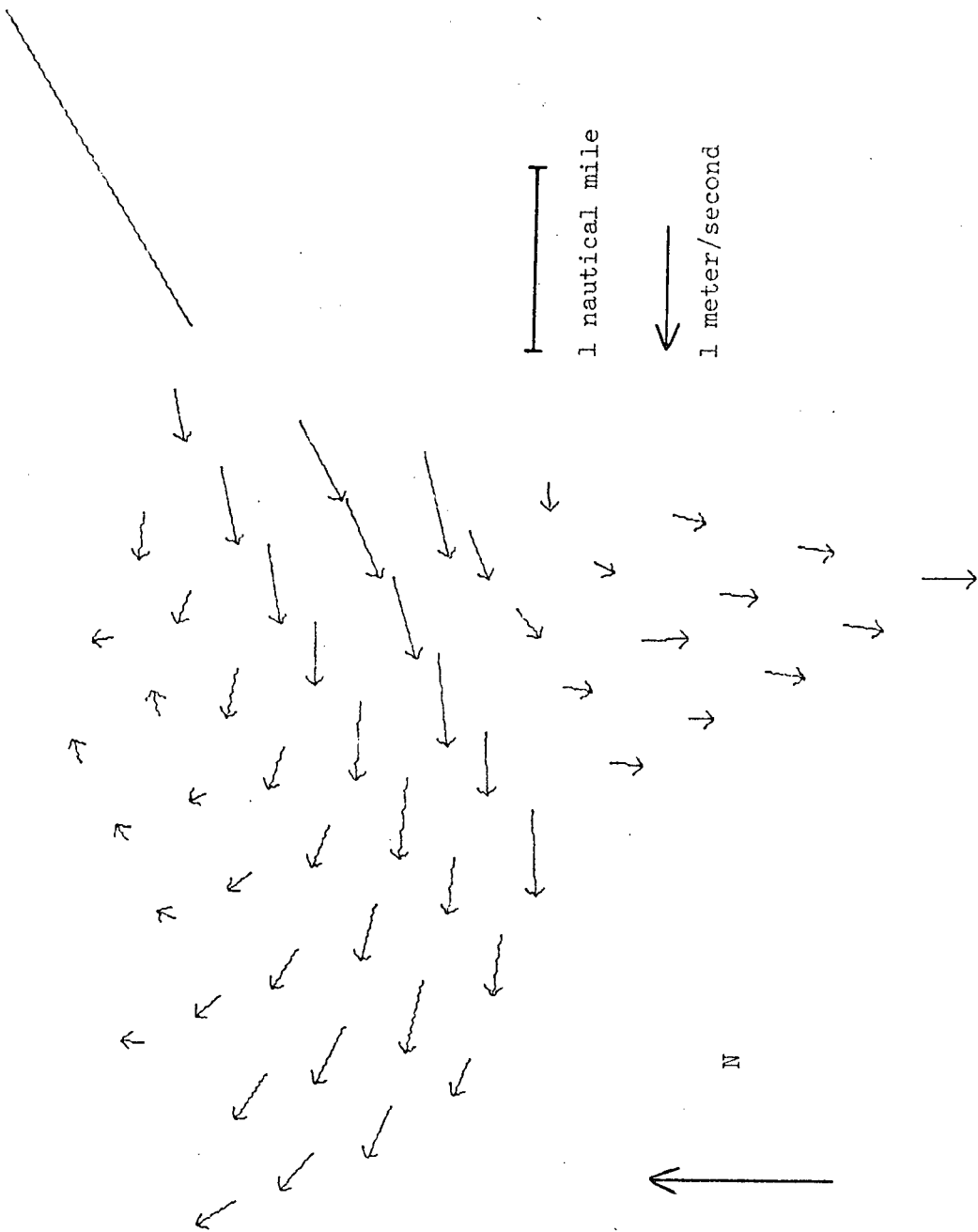


Figure 4.16 Velocity field for Set 7 (58.6 hours to 65.0 hours), on the rise to and start of the ebb from lower high tide, made from data sampled at 0.1 mile intervals.

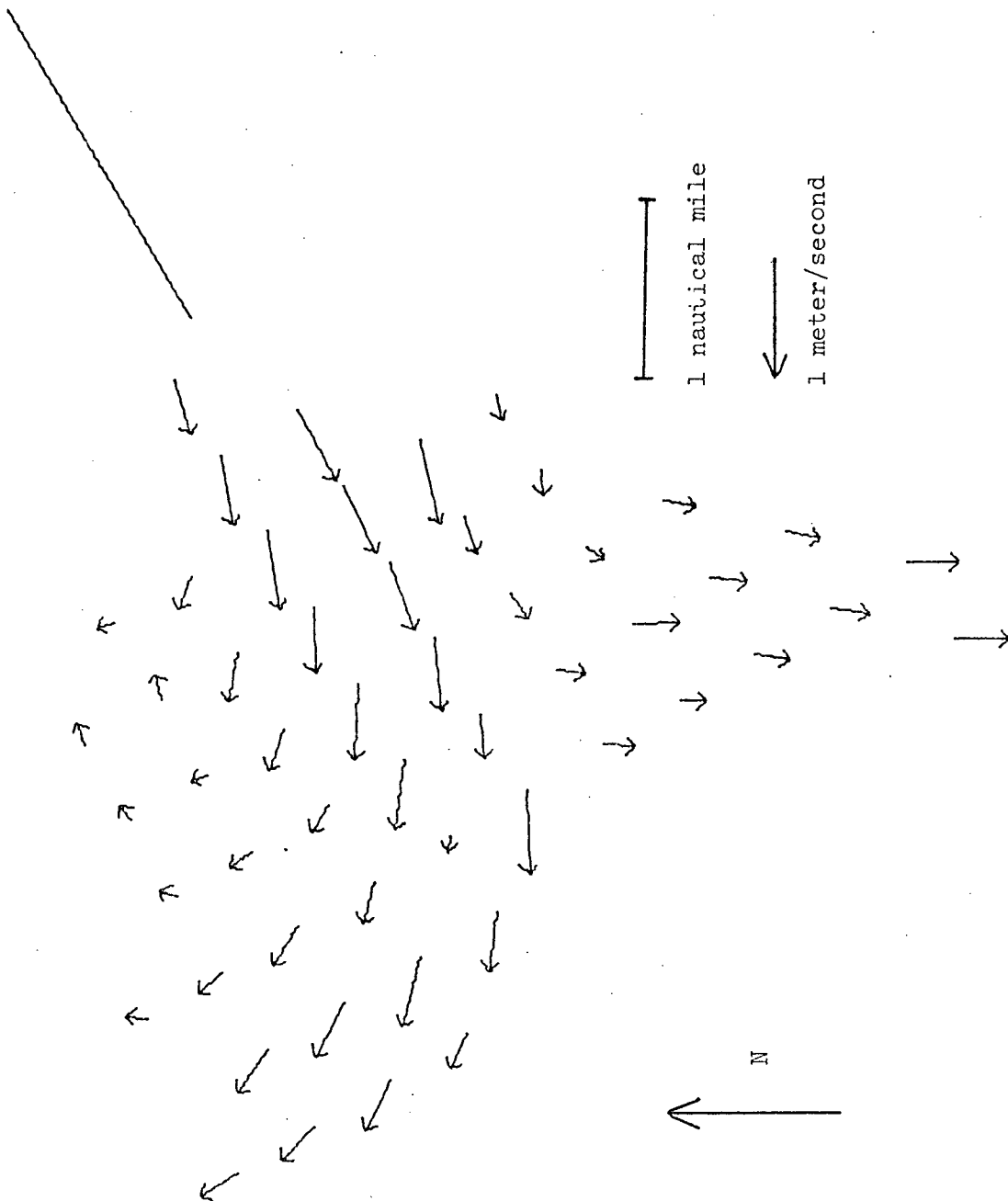


Figure 4.17 Velocity field for Set 7 (58.6 hours to 65.0 hours), on the rise to and start of the ebb from lower high tide, made from data sampled at five-minute intervals.

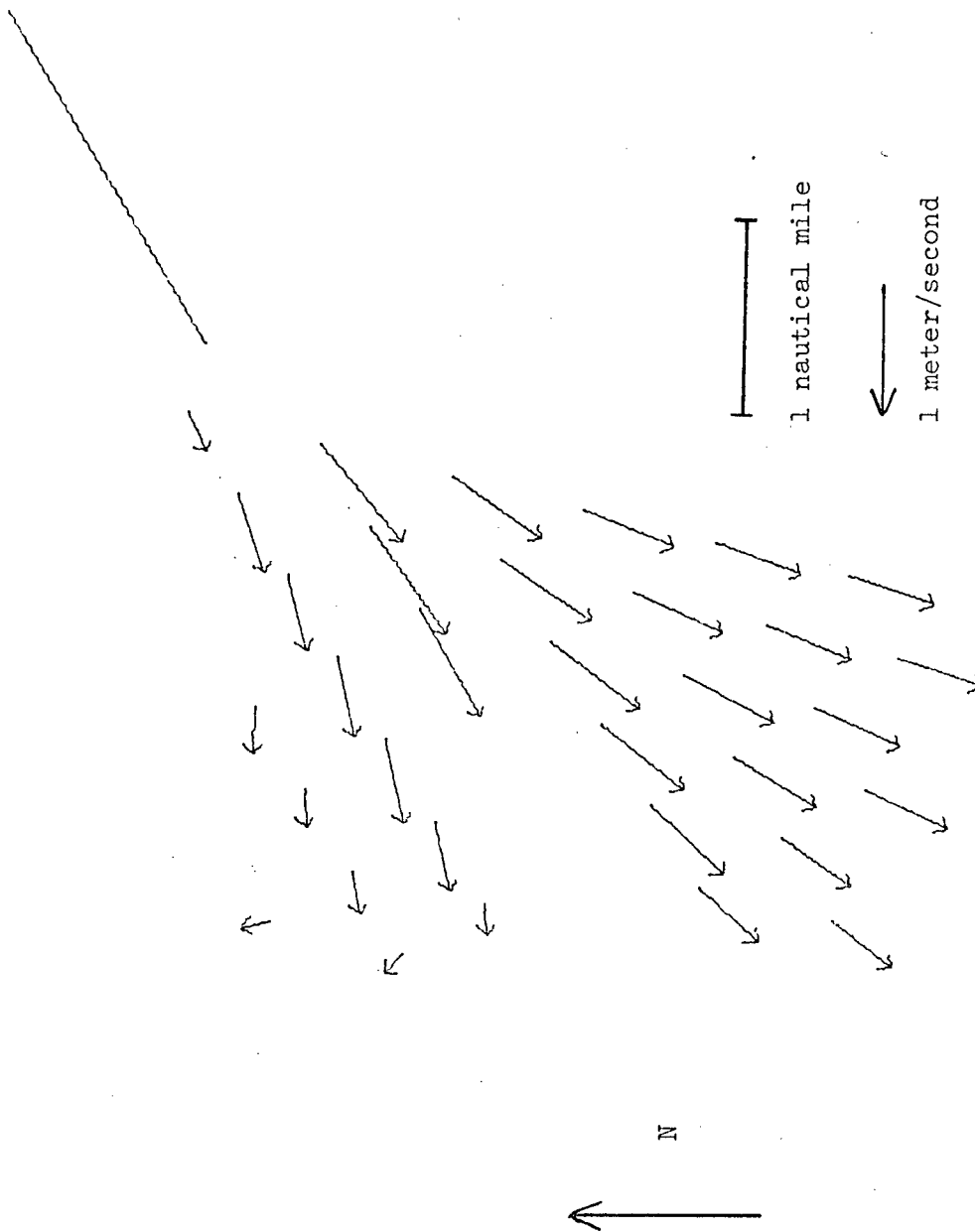


Figure 4.18 Velocity field for Set 7 (64.7 hours to 67.5 hours) on the ebb from lower high tide.

southern sections is caused by the fact that not enough floats were put in to fill up gaps in the diverging flow. While the speeds near the river mouth, at 1 m/s, were about the same as those observed in Set 4, those in the southern part of the plume were considerably larger. Speeds there averaged .7 m/s in Set 7, compared with .4 m/s in Set 4. The change in tide height was less in Set 7, but the east ll wind blowing at the end of Set 4 may have slowed the southward flow.

Set 1 comprises two lines of floats (Figure 4.19), the first of which was put in at lower high water. The second followed about two hours later and the floats remained in the water until about one hour before low tide. The ebb was a larger one than either of the two seen on the following days. The first line of floats moved out fairly straight and then turned to the south as the ebb increased, while the second line turned much closer to Sand Heads and showed more divergence. Winds during the period were southwest 4 to 8. The velocity field (Figure 4.20) was very similar to that for the ebb in Set 7 (Figure 4.18). Since the ebb during Set 1 was larger, the speeds near the river mouth were higher, reaching 1.2 m/s, but the opposing winds slowed the flow slightly so that speeds were very similar farther out.

Composite velocity fields summarize the observations. The flow on the flood tide from Sets 4 and 7 (Figures 4.9 and 4.14) has been averaged in Figure 4.21. It shows the smooth curving to the north found on this tidal phase and the beginning of the turn to the south as the river's pressure head overcame the push of the rising tide. To obtain an average flow pattern for a 'typical small ebb', the data comprising

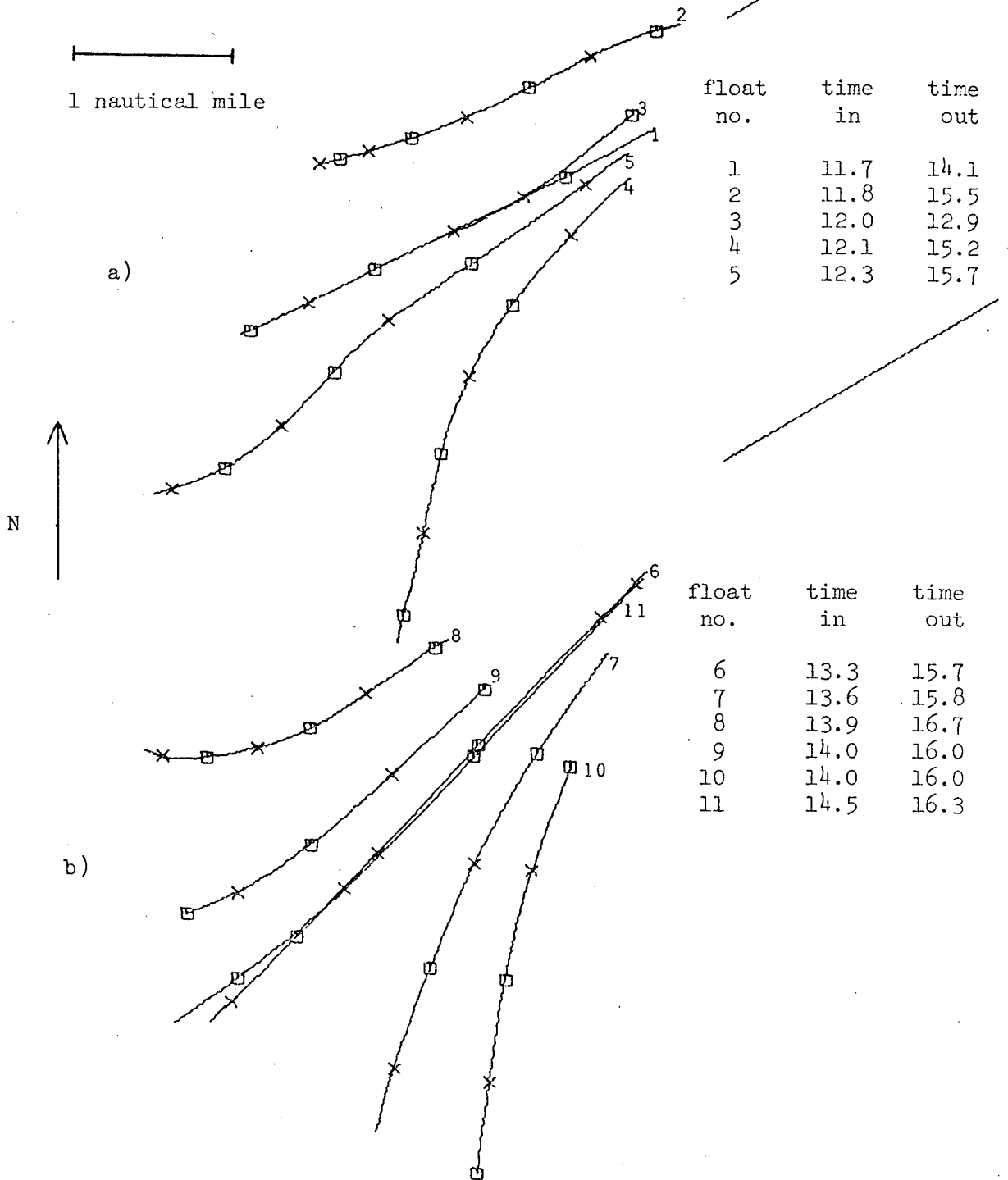


Figure 4.19 Path lines of floats in Set 1, on the ebb from lower high tide a, 11.6 hours to 15.7 hours. b, 13.3 hours to 16.7 hours. Winds were southwest 4 to southwest 8.

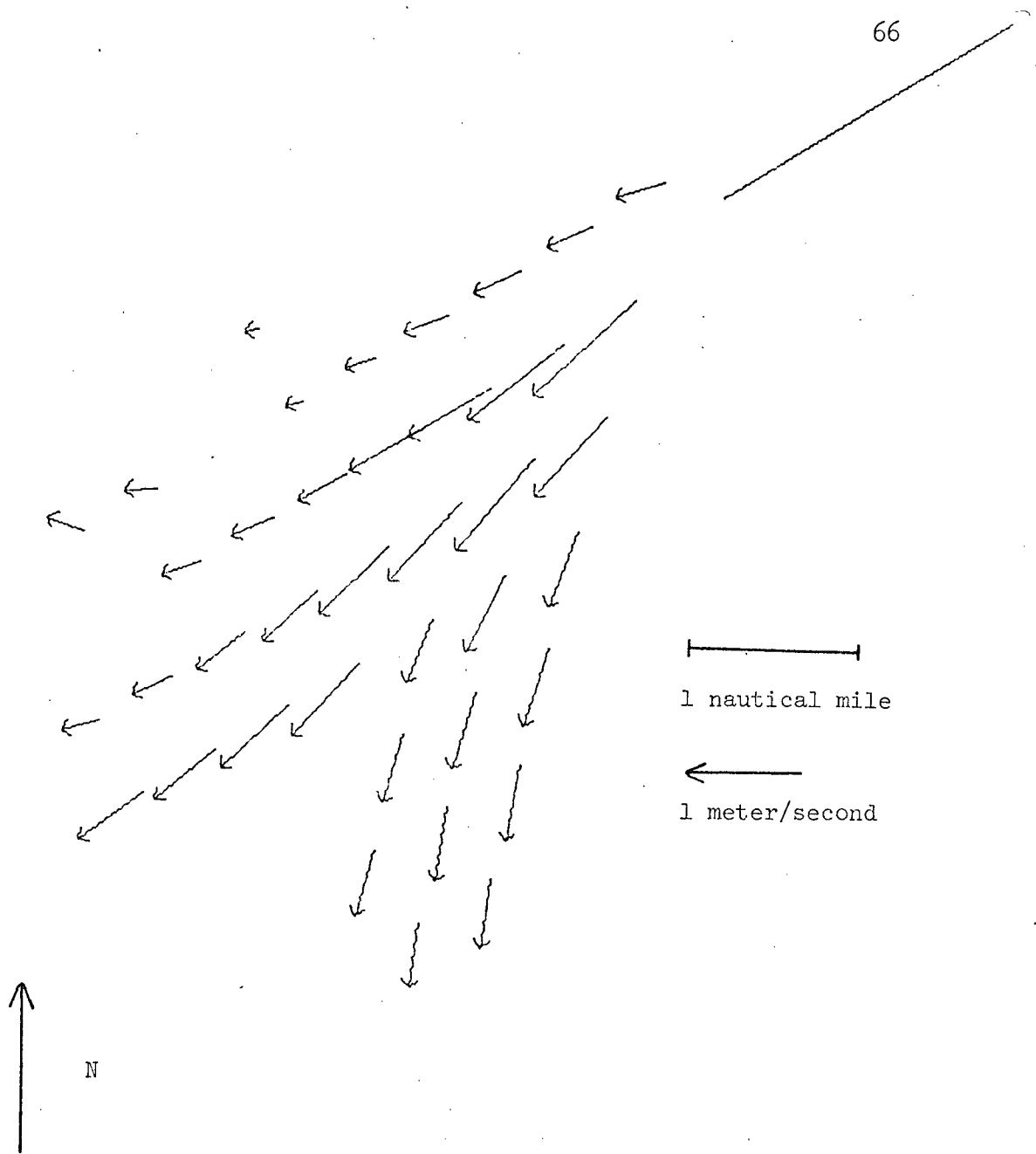


Figure 4.20 Velocity field for Set 1 (11.6 hours to 16.7 hours) on the ebb from lower high tide.

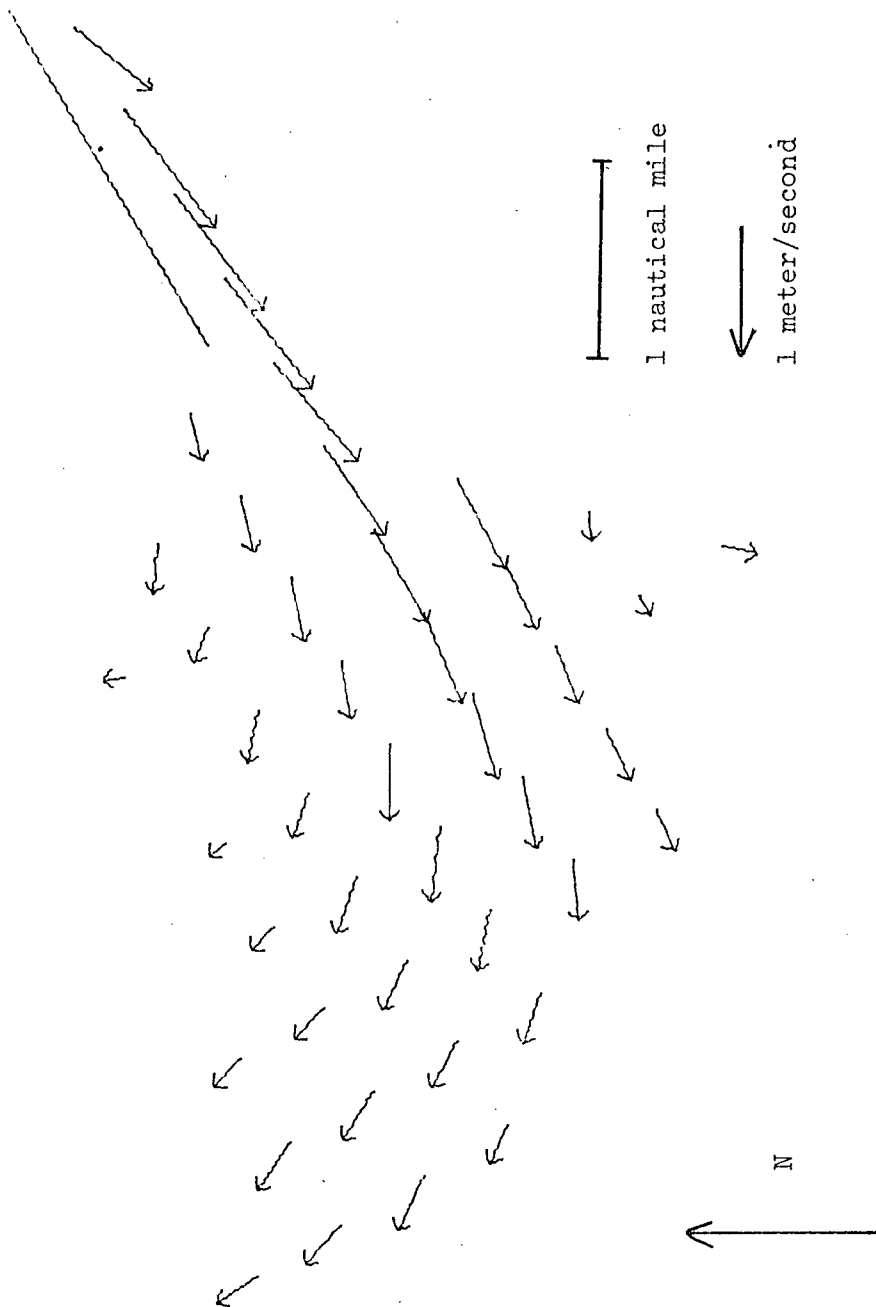


Figure 4.21 Composite velocity field averaging the data on the rise to lower high tide, from Set 4 (33.1 hours to 38.9 hours) and Set 7 (58.6 hours to 62.0 hours).

Figures 4.11, 4.18 and 4.20 were averaged to form a single velocity field. This composite field (Figure 4.22) shows the turning to the south, the curling to the north, and the decreasing speeds as distance from the river mouth increases which are characteristic of the flow on this tidal phase.

4.1.3 Sets 5, 8 and 3, near higher high water

During the nights of the first week an attempt was made to study the large floods and ebbs. Because of poor weather, the difficulties of working in the dark and the inexperience of some of the people involved, we only managed to track one line of floats each night. Set 5, collected during the second night, gives the best representation of the flow.

The floats in Set 5 (Figure 4.23) were put in the water about three and one-half hours before higher high tide, starting halfway through the flood tide. The winds were near east 11 at this time. The floats moved out and to the right until about an hour before the high tide, when they began to turn to the south. They continued moving south or southwest until they were removed, less than an hour before the lower low tide. The data may be divided into two distinct flow regimes with the division occurring about an hour before higher high tide.

The first velocity field (Figure 4.24a) shows that the river discharge was held back by the flooding tide, resulting in speeds as low as .2 m/s by the end of the time interval. The swing to the north was probably due to several factors: the flooding tide, the Coriolis force and the east 11 winds all encouraged the trend.

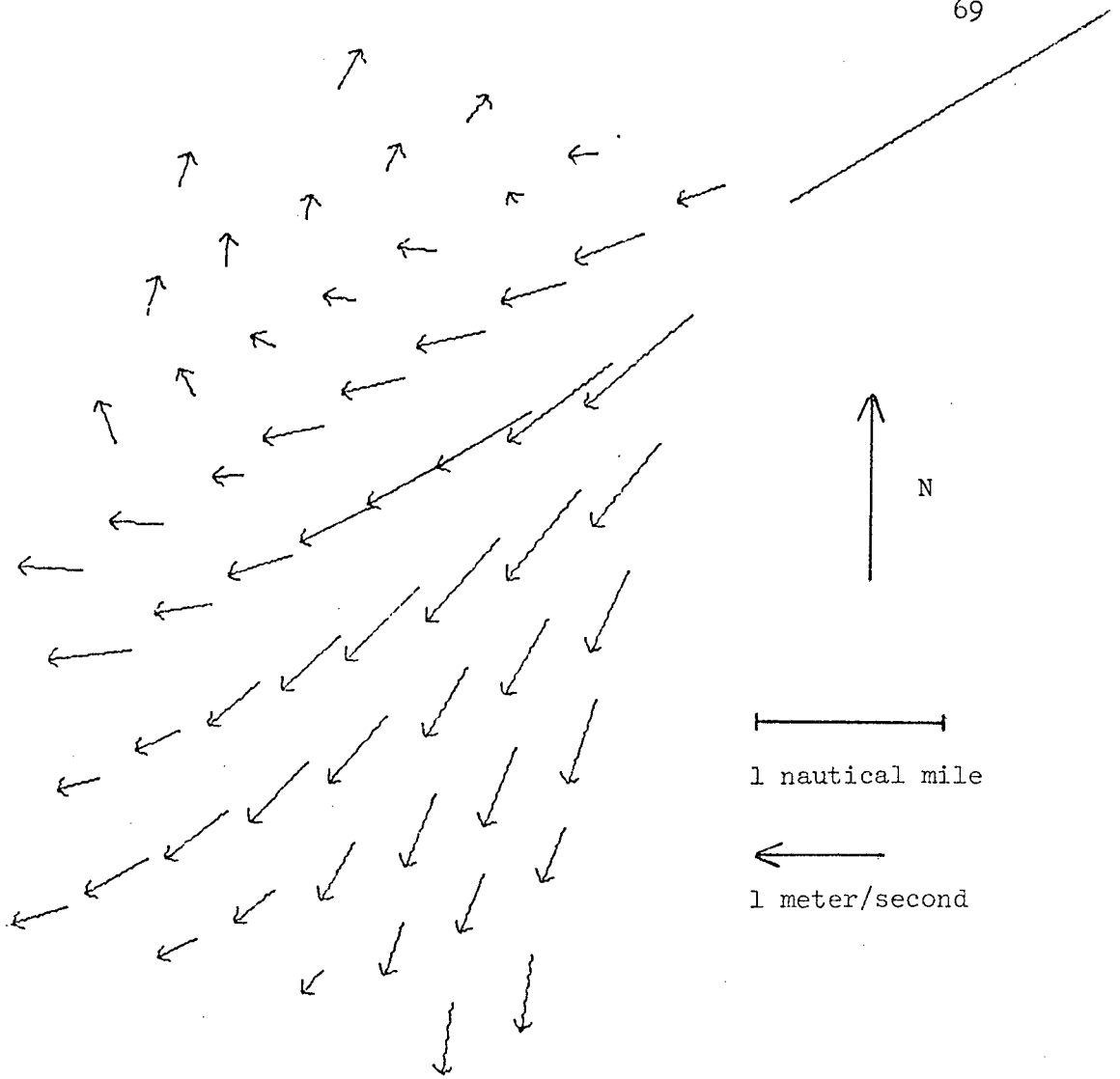


Figure 4.22 Composite velocity field averaging the data on the ebb from lower high tide, from Set 1 (11.6 hours to 16.7 hours), Set 4 (38.9 hours to 43.6 hours), and Set 7 (64.7 hours to 67.5 hours).

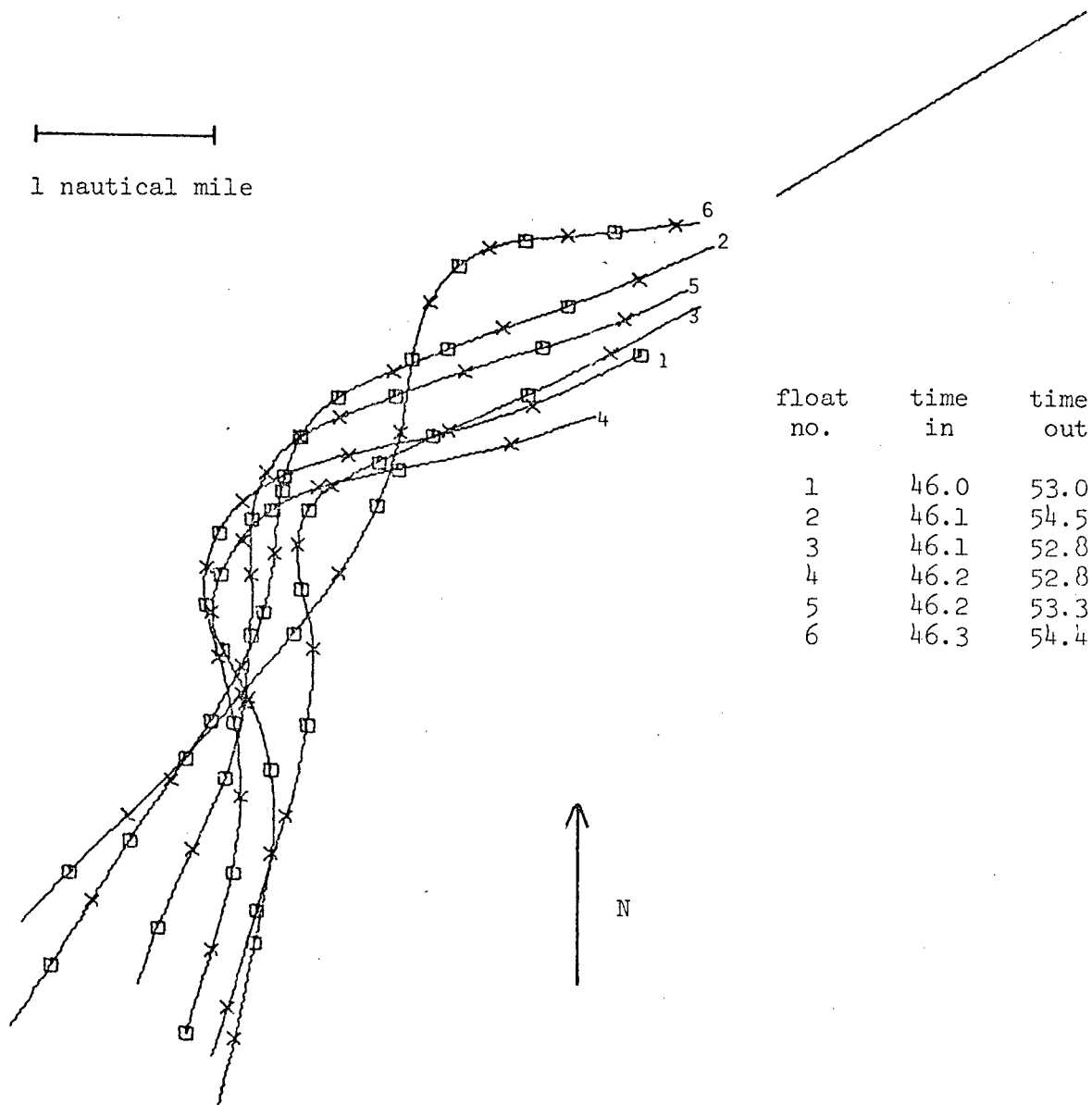


Figure 4.23 Path lines of floats in Set 5, from 45.9 hours to 54.5 hours, on the rise to and ebb from higher high tide. Winds were east 9 to northeast 15.

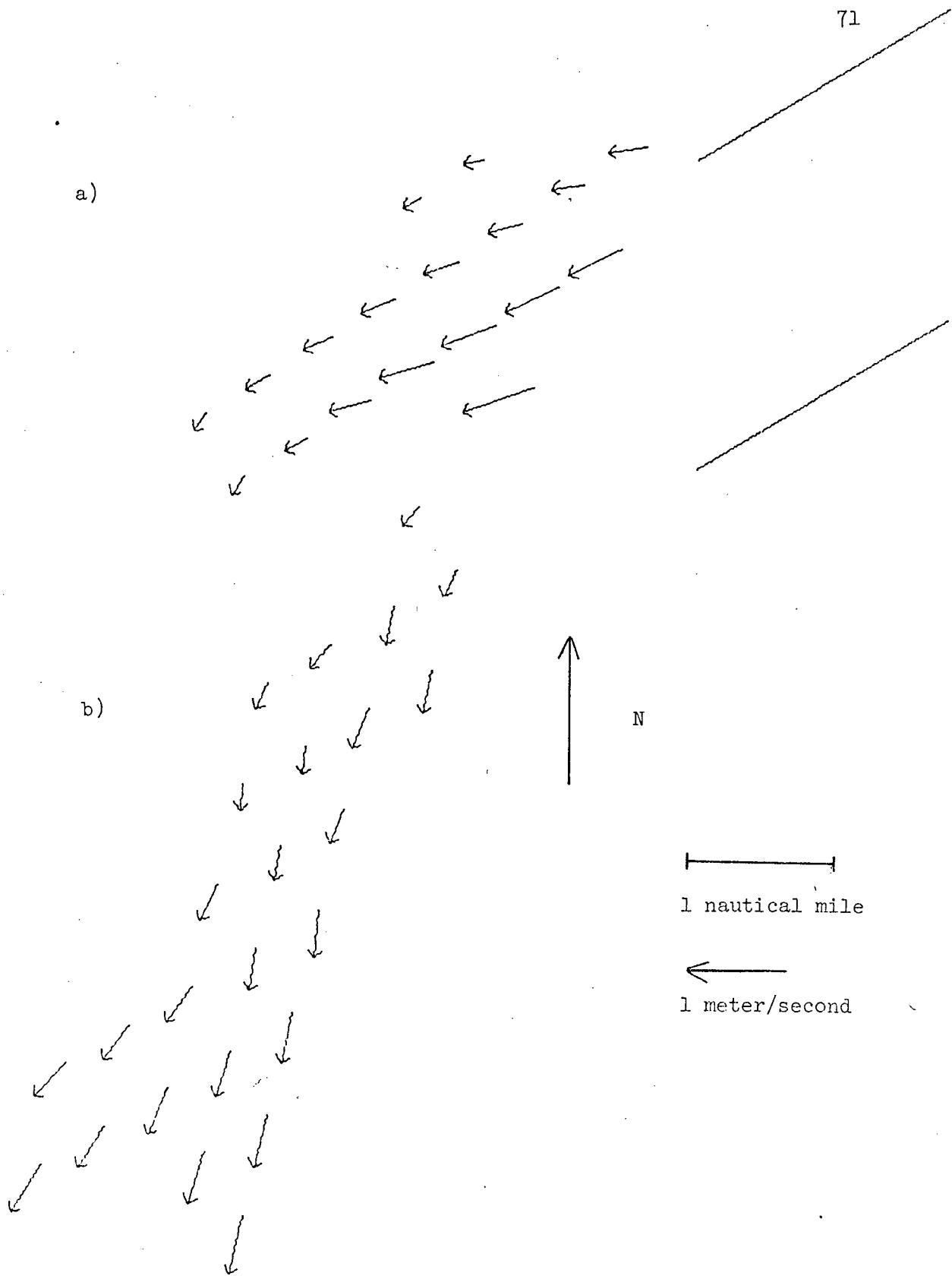


Figure 4.24 Velocity fields for Set 5. a, 45.9 hours to 49.0 hours, on the rise to higher high tide. b, 49.0 hours to 54.5 hours, on the ebb from higher high tide.

As Sets 4 and 7 demonstrated, the pressure head of the river becomes large enough to overcome the flooding tide somewhat before high water. During the time from one hour before high tide until the end of the set (Figure 4.24b) the plume turned to the south, with speeds increasing to .6 m/s as the ebb became stronger. The surface slope in the Strait and the frictional effect of the ebbing tide would act together to bring about this change in the flow direction. The shift of the wind to northeast 12, increasing to northeast 18, brought it more nearly parallel to the flow. As calculated earlier, a wind of 16 knots would add .12 m/s to the current over a period of an hour. A comparable increase in the water speed would be expected to be caused by the wind during the latter part of Set 5. Water leaving the river mouth during this time would have begun to move south immediately, forming the main part of the plume to the east of the float positions. Speeds in it would probably have been somewhat higher than those we observed at the side of the plume.

The data in Set 8, obtained during the third night, again consist of a single line of floats (Figure 4.25). They were put in slightly over four hours before the higher high tide, starting about a third of the way through the flood. Since the preceding low tide had been quite a bit higher than the one the previous evening, the flood was not as strong and the flow speeds near the river mouth (Figure 4.26) were about .8 m/s, slightly larger than the corresponding ones in Set 5 (.6 m/s). The increased speed must have been due to

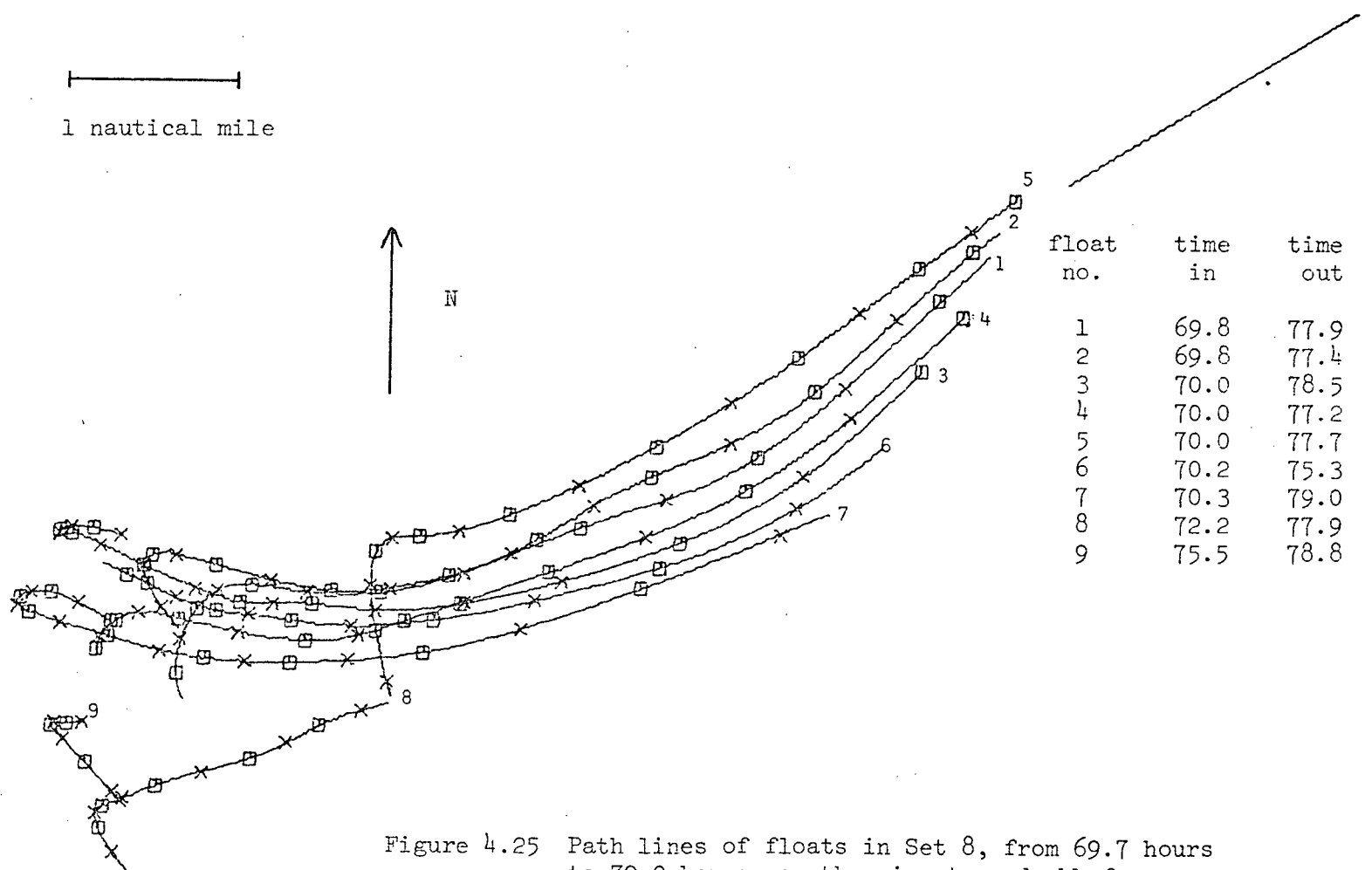


Figure 4.25 Path lines of floats in Set 8, from 69.7 hours to 79.0 hours, on the rise to and ebb from higher high tide. Winds were near southeast 5.

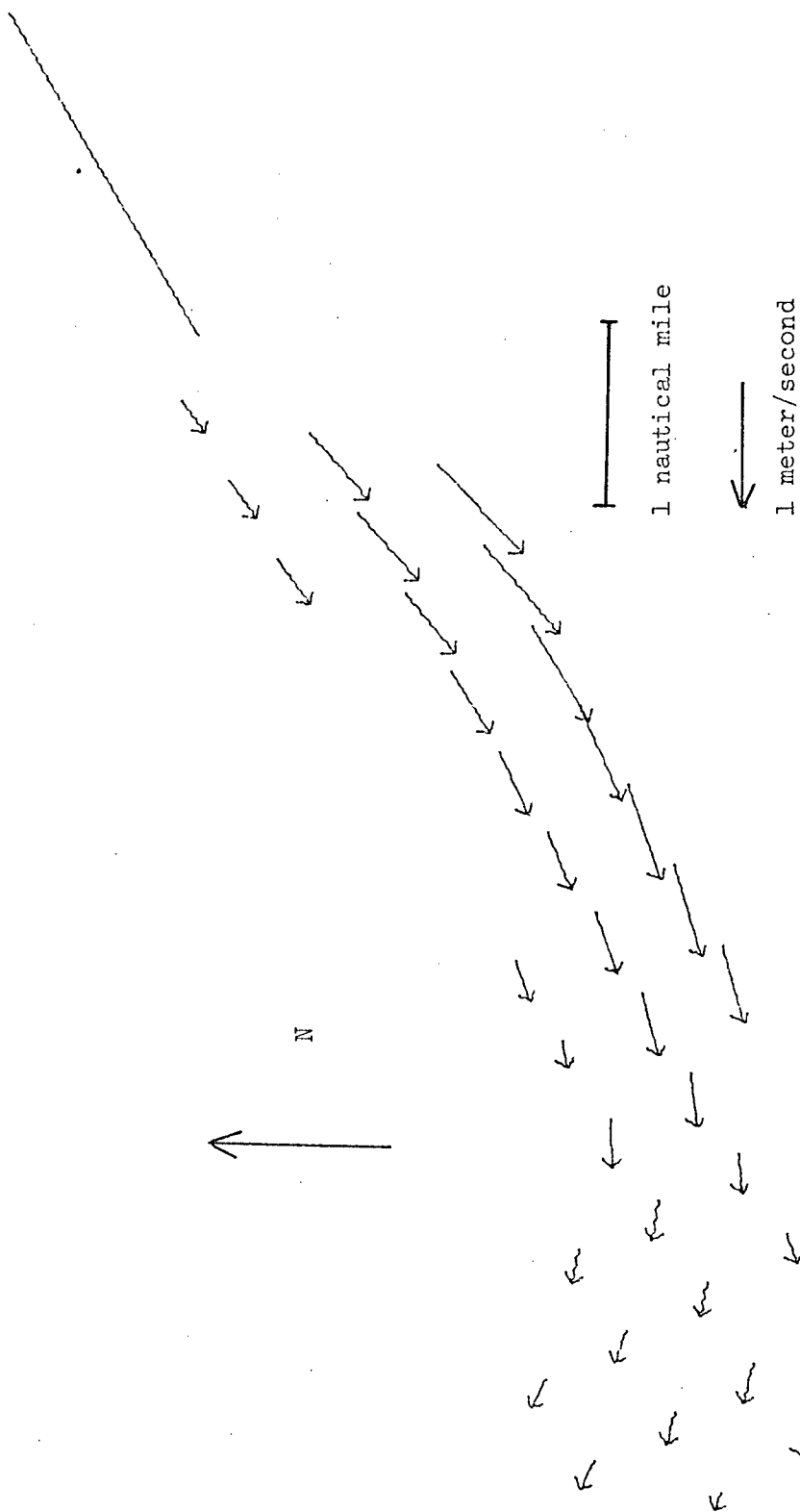


Figure 4.26 Velocity field for Set 8 (69.7 hours to 76.0 hours), on the rise to and beginning of ebb from higher high tide.

differences in the tide, since the winds during Set 8 were very light (less than 6 knots), while the winds during Set 5 should have enhanced the flow. By high water most of the floats were over five miles from Sand Heads. They were left moving out with a slight curve to the north, while the main plume near the river mouth probably turned to the south as observed in Set 7. The floats continued outward, curving to the right under the influence of Coriolis force and slowing because of the frictional drag between the surface and lower layers. Finally, they appeared to stall, probably because the fresh water layer had spread out so thinly that the floats were influenced considerably by the lower layer of salt water. Two to three hours after higher high tide the floats began to move again as the ebb in the Strait became stronger (Figure 4.27). Even after this change, the speeds were still small (.2 m/s) but appeared to be increasing.

On the first night, the floats in Set 3 (Figure 4.28) were installed less than two hours before higher high tide. The winds at the time were northwest 12, so the floats began to move to the south quite soon. The situation corresponds to the second parts of Sets 5 and 8, which took place on the ebbing tide. The winds dropped to 5 knots for a few hours, but then rapidly increased to northwest 19 by 28.0 hours. The rough seas which accompanied the wind made work very difficult, so float tracking stopped by 27.0 hours. Float 1 could not be located, but later washed up on Mayne Island, on the west side of the Strait of Georgia.

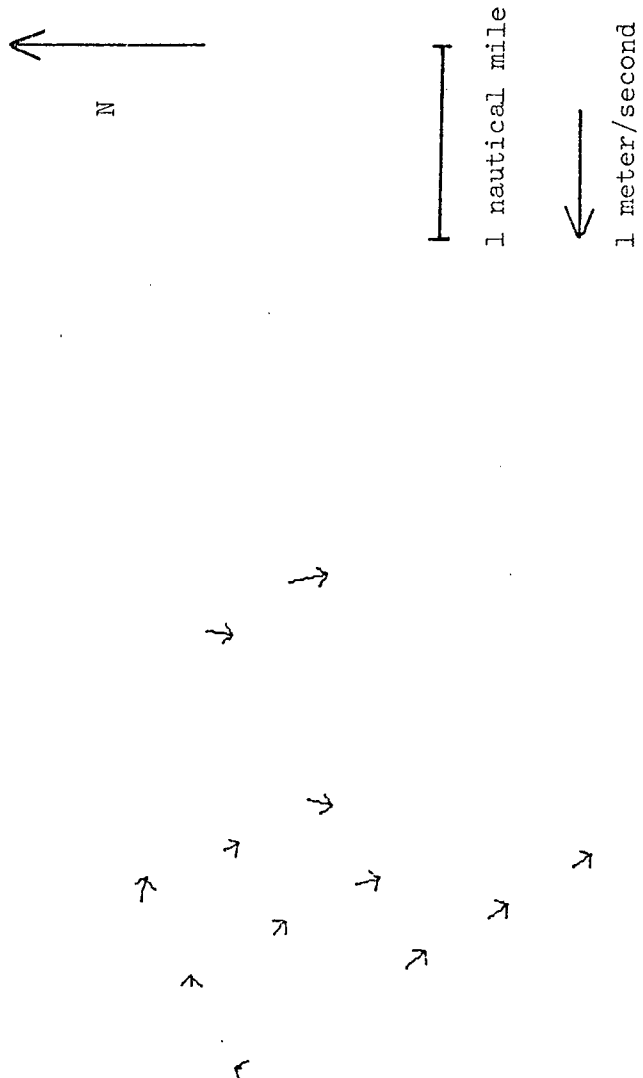


Figure 4.27 Velocity field for Set 8 (76.0 hours to 79.0 hours) on the ebb from higher high tide.

1 nautical mile

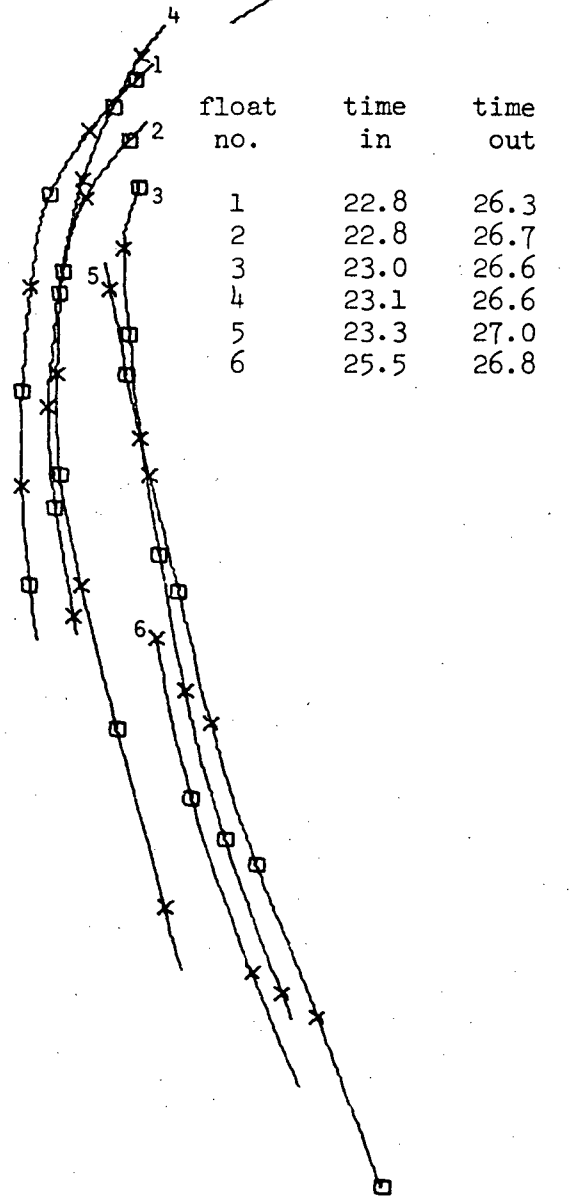
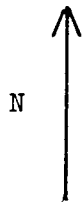


Figure 4.28 Path lines of the floats in Set 3, from 22.8 hours to 27.0 hours, on the ebb from higher high tide. Winds were northwest 7 to northwest 19.

The velocity field (Figure 4.29) appears to have been strongly influenced by the wind, since the direction of flow became nearly parallel to it and the flow speed increased. Of course, the ebbing tide also encouraged the accelerating flow to the south; speeds increased from .4 m/s near Sand Heads to 1 m/s at the end of the observations. When the path lines are compared with a hydrographic chart of the area it seems that the floats followed the curvature of the banks of the river delta. A more typical ebb without such strong wind effects would be expected to resemble Set 5, showing more divergence of the flow, and less sharp turning to the south.

Composite velocity fields of the flow for the second and third nights have been prepared for the time before the flow turned (Figure 4.30) and for the time after the turn (Figure 4.31). Set 3 has been omitted from the composite since it represents a fairly different situation.

4.2 Week 2 - tracks and velocities

The experimental work during the second week was done only during the large ebbs and floods. On the basis of our experience the previous week it was clear we could not get good coverage during such tidal periods and maintain 24-hour operations with the vessels and personnel available. Fortunately, these tidal periods occurred during the daylight which made the work somewhat easier. Figure 4.32 shows the tidal height, the wind speed and direction, and the times when data were obtained. Time is in hours, measured from midnight PDT June 4, 1974. In order to maintain continuity of the data through the lower low tides, we will examine it beginning at high tide.

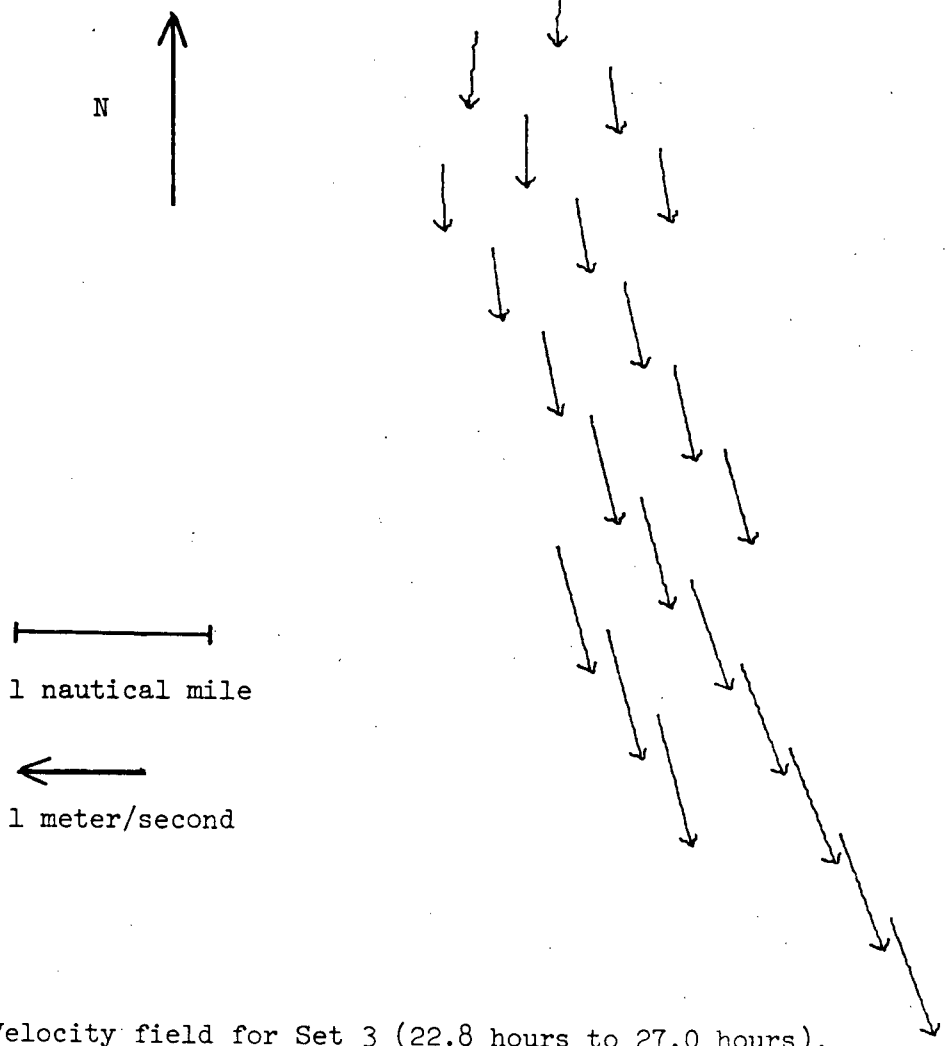


Figure 4.29 Velocity field for Set 3 (22.8 hours to 27.0 hours), on the ebb from higher high tide.

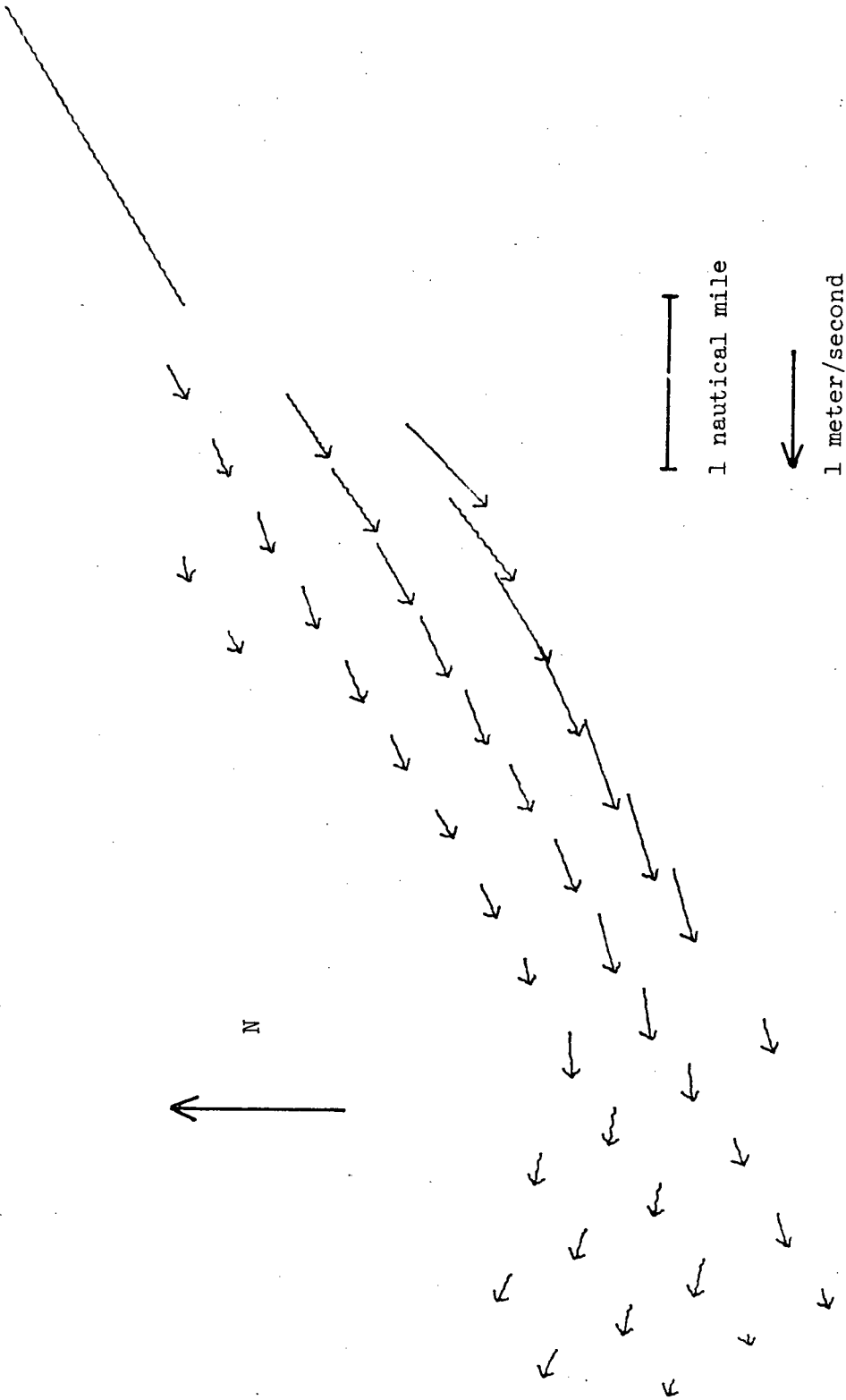


Figure 4.30 Composite velocity field averaging the data on the rise to higher high tide, from Set 5 (45.9 hours to 49.0 hours) and Set 8 (69.7 hours to 76.0 hours)

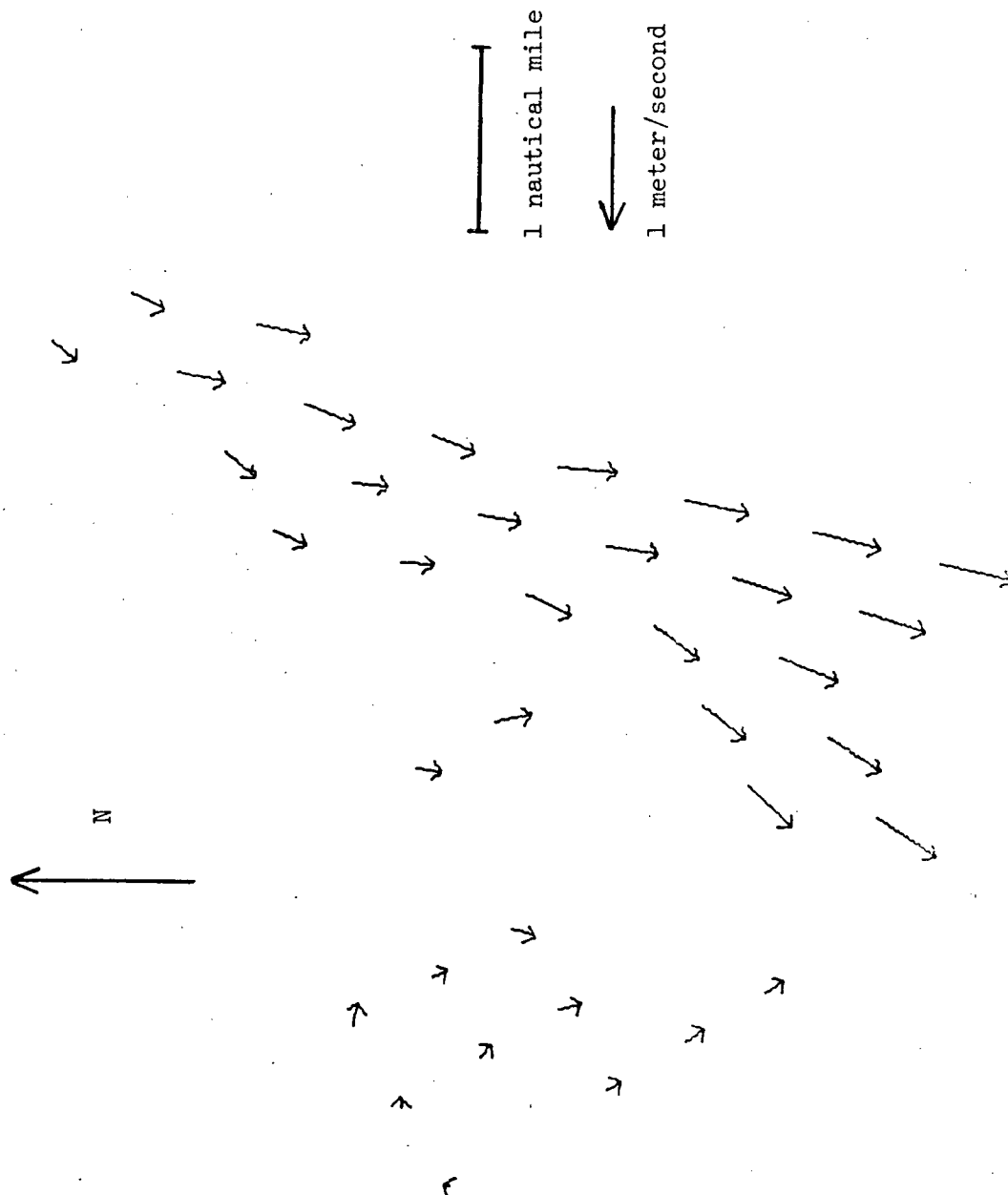


Figure 4.31 Composite velocity field averaging the data on the ebb from higher high tide, from Set 5 (49.0 hours to 54.5 hours) and Set 8 (76.0 hours to 79.0 hours).

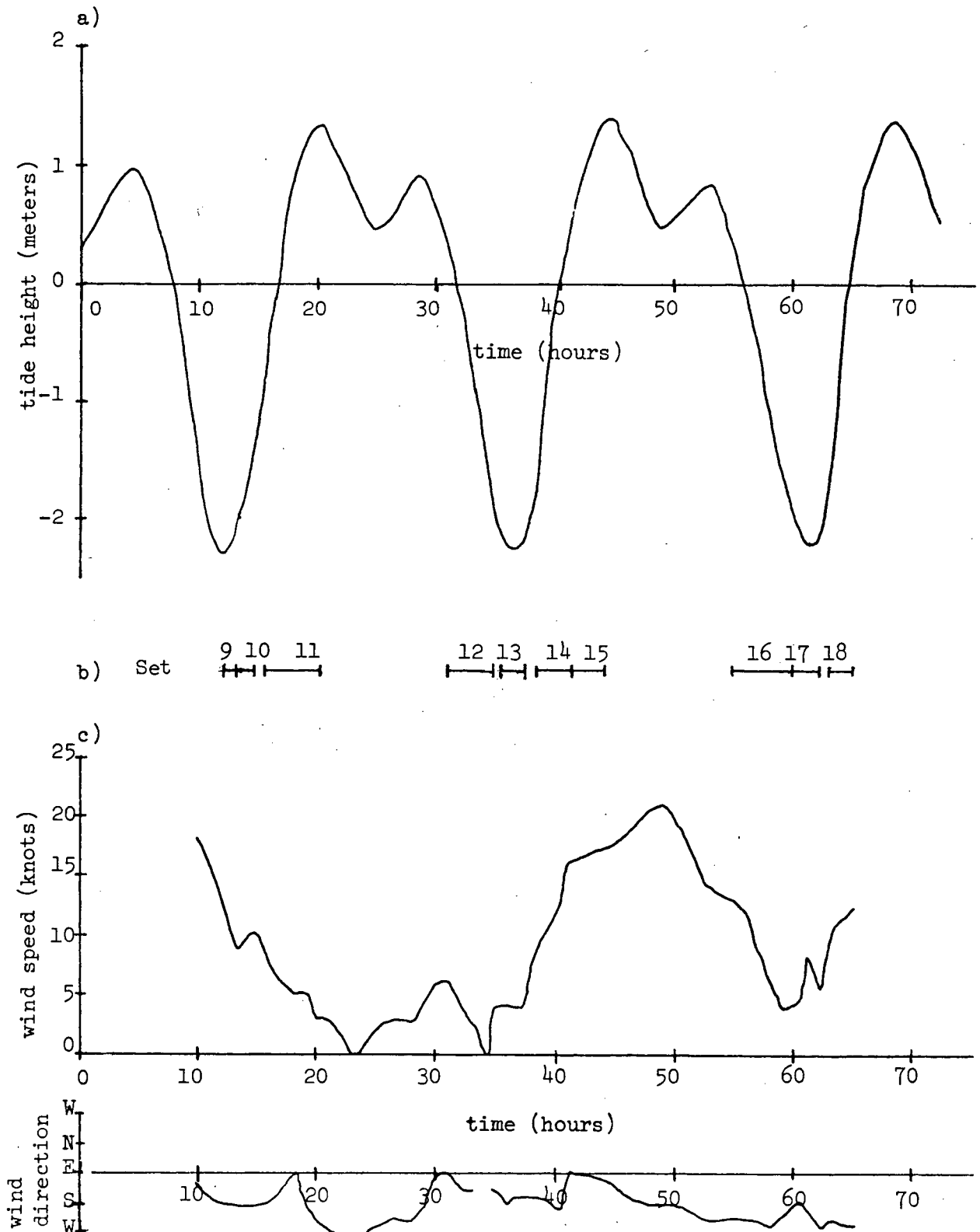


Figure 4.32 a, Tide height at Tsawwassen. b, times when the sets of data were taken, and c, wind speed and direction, during the second week of the experiment. Time is measured in hours from midnight, PDT, June 4, 1974.

4.2.1 Sets 12 and 16 (before 59.0 hours), first part of large ebbs

The data comprising Sets 12 and 16 were obtained during the ebb tide on the second and third days of the week's work. No data were collected during this tidal phase on the first day because of high winds. Set 12 consists of two lines of floats (Figures 4.33a and 4.33b). The first line was installed almost two hours after the high tide, with the second line following over an hour later. The floats were left in the water until about one and one-half hours before the lower low tide.

The winds were very light during the ebb, from east 6 to calm. The velocity field for the first two hours of the set is Figure 4.34a. The speeds, which were about 0.8 m/s near Sand Heads, were somewhat smaller than those at the beginning of the small ebbs the previous week. This difference was probably due to the fact that the lower high tides in the second week were higher, giving the river less of a pressure head. The floats moved out without much curving, though there was some divergence to the north and south. The floats in the centre moved out more quickly than those on the sides, so that they were quite far out by the time the northern float began to turn south under the influence of the increasing ebb.

By the time the second line of floats was put in, the flow had begun to swing slightly to the south and the speed had increased considerably, to 1.1 m/s near Sand Heads (Figure 4.34b). The floats in the second line appear to have been put in to the north of the plume axis, since they curved gradually to the north and showed no sign of swinging toward the south as is typical of flow on an ebb tide. It seems likely that the speed of the water leaving the river mouth would have continued to increase with the ebbing tide until reaching a maximum about an hour

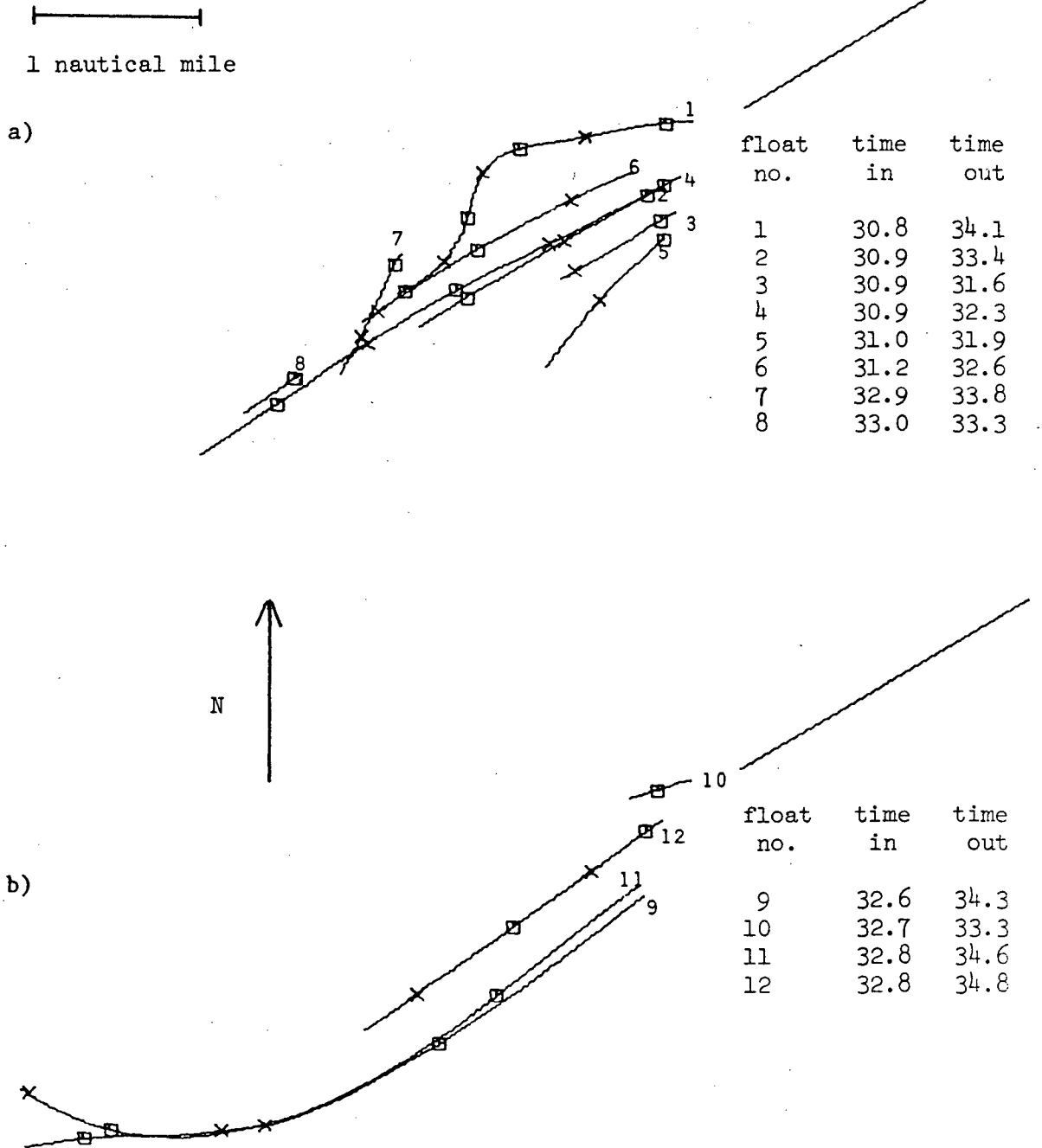


Figure 4.33 Path lines of floats in Set 12, at the start of the large ebb a, 30.8 hours to 34.1 hours. b, 32.5 hours to 34.8 hours. Winds were east 6 to calm.

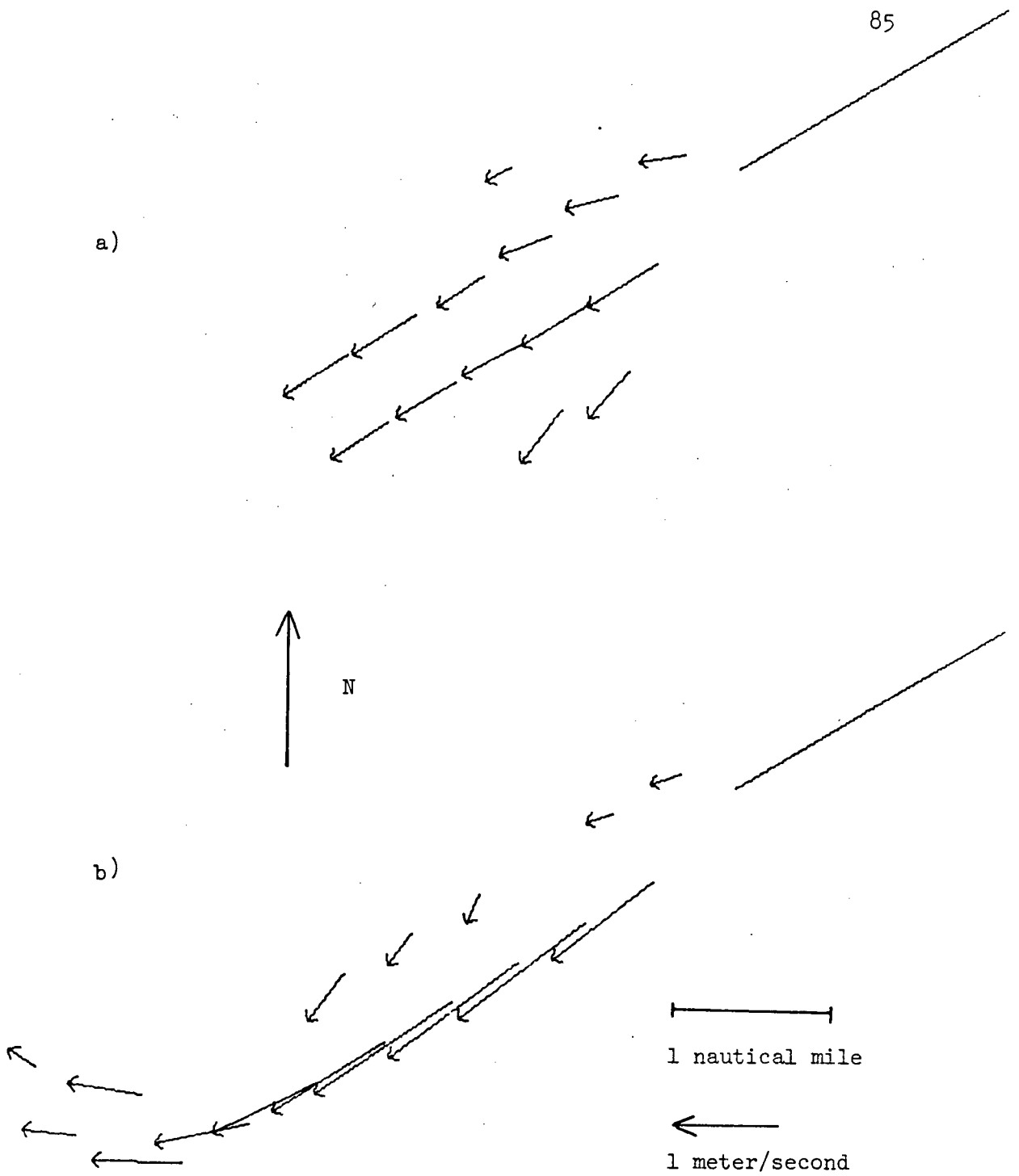


Figure 4.34 Velocity fields for Set 12, at the start of the large ebb. a, 30.8 hours to 32.7 hours. b, 32.6 hours to 34.8 hours.

before the lower tide. The turning to the south would have decreased somewhat before that time.

Set 16, collected the next day, gives better coverage of the ebb. In the time from high water until about two hours before lower low water, three lines of floats were put in the water (Figures 4.35a, 4.35b and 4.38a). The very end of the second line and most of the third line will be considered with Set 17, which covers the end of the ebb. The three lines were put in about one hour, three hours, and four and one-half hours after high tide.

The initial velocity field (Figure 4.36a) is very similar to that for the beginning of Set 12, although there was less turning to the north. The second field (Figure 4.36b) shows speeds similar to those in the second part of Set 12, but the flow direction was more southerly. The winds which were southwest 13 to southwest 5 probably enhanced the turn to the south. The larger speeds (about 1.8 m/s) near Sand Heads are derived from the beginning of the third line of floats. The speeds of the floats in the second line were about 1.5 m/s there.

Figure 4.37 is an average velocity field for the early part of the ebbing tide, including Set 12 and Set 16 before 59.0 hours. It shows the features characteristic of the flow at this phase of the tide. Initially, there is a slight swing to the north perhaps caused by the end of the flooding tide as well as the Coriolis force. The flow swings to the south but the speeds remain near 1 m/s decreasing very slowly.

4.2.2 Sets 16 (after 59.0 hours), 17, 13 and 9, end of large ebbs

As lower low tide was approached, the river reached its

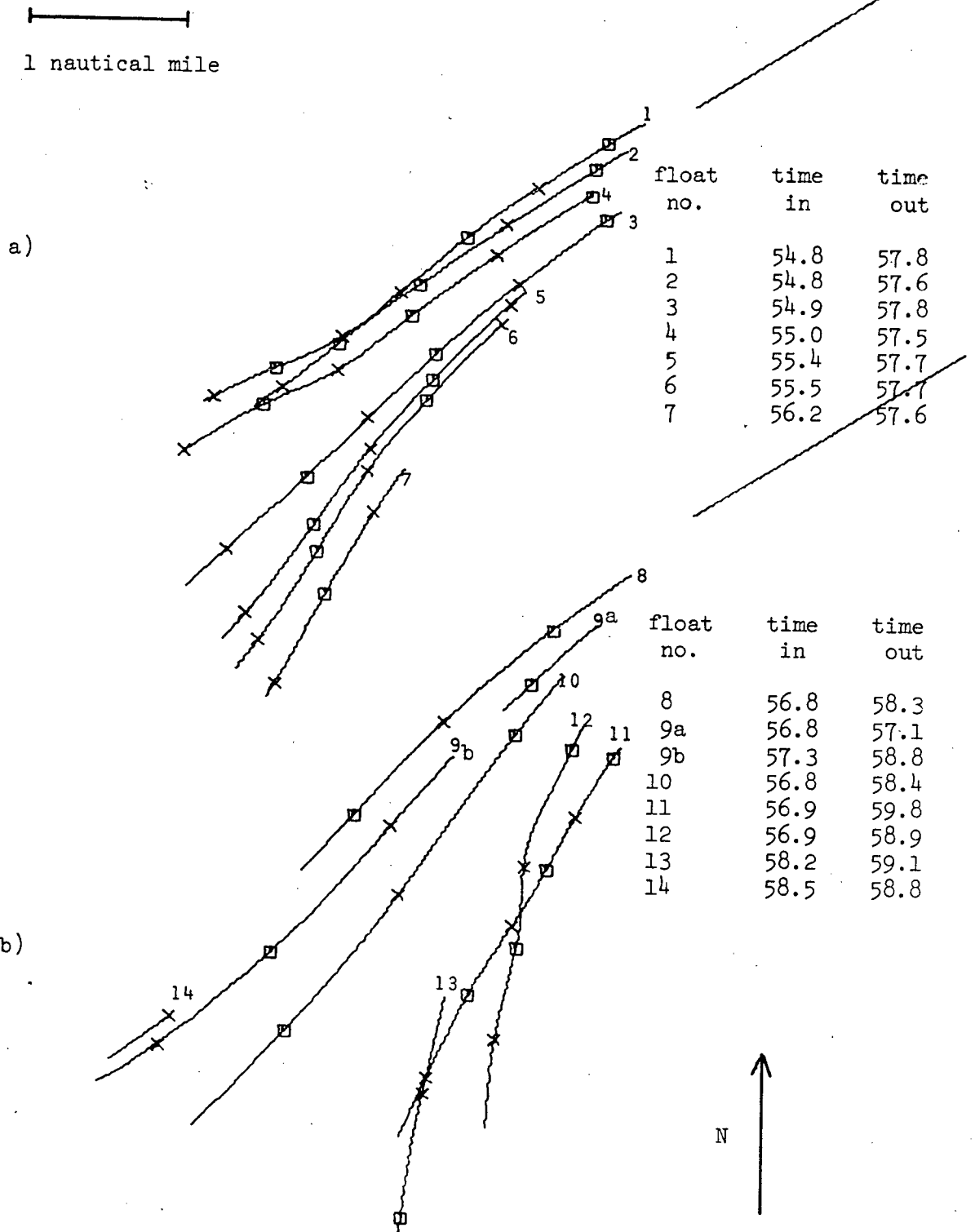


Figure 4.35 Path lines of floats in Set 16, at the start of the large ebb. a, 54.7 hours to 57.8 hours. b, 56.7 hours to 59.9 hours. Winds were southwest 15 to southwest 4. The path lines numbered 9a and 9b indicate that the float was removed briefly for repairs.

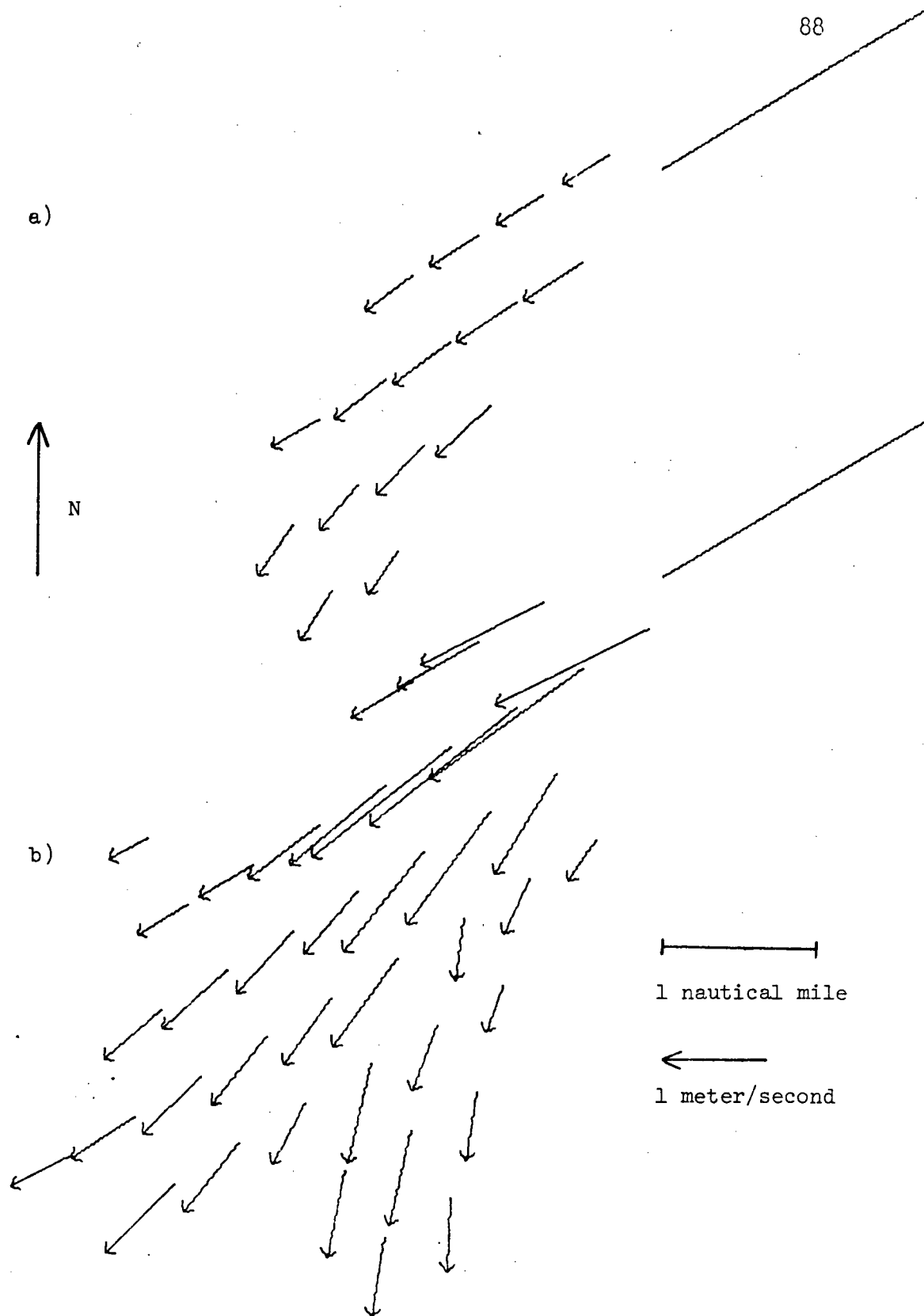


Figure 4.36 Velocity fields for Set 16, at the start of the large ebb. a, 54.7 hours to 56.7 hours. b, 56.3 hours to 59.0 hours.

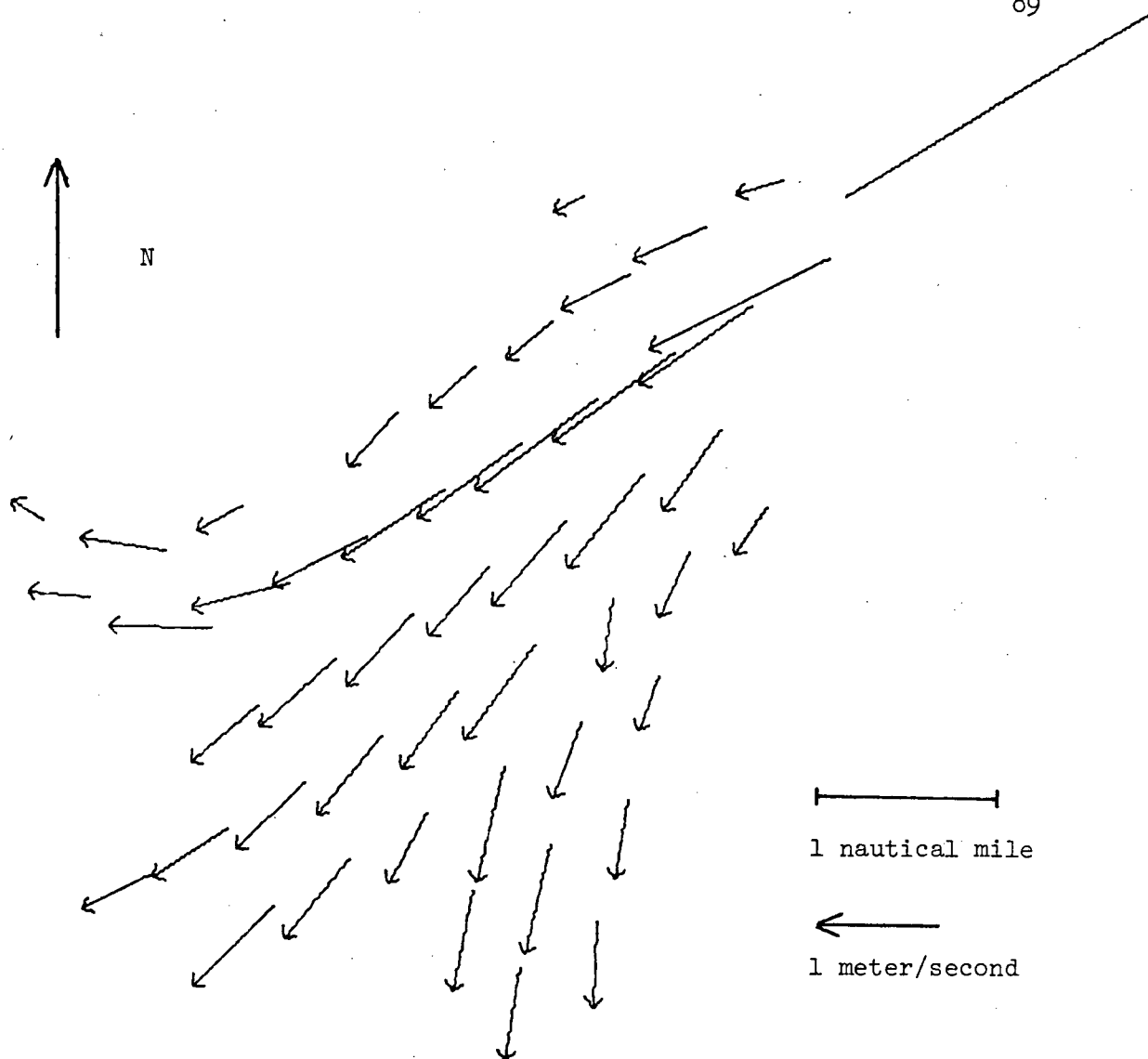
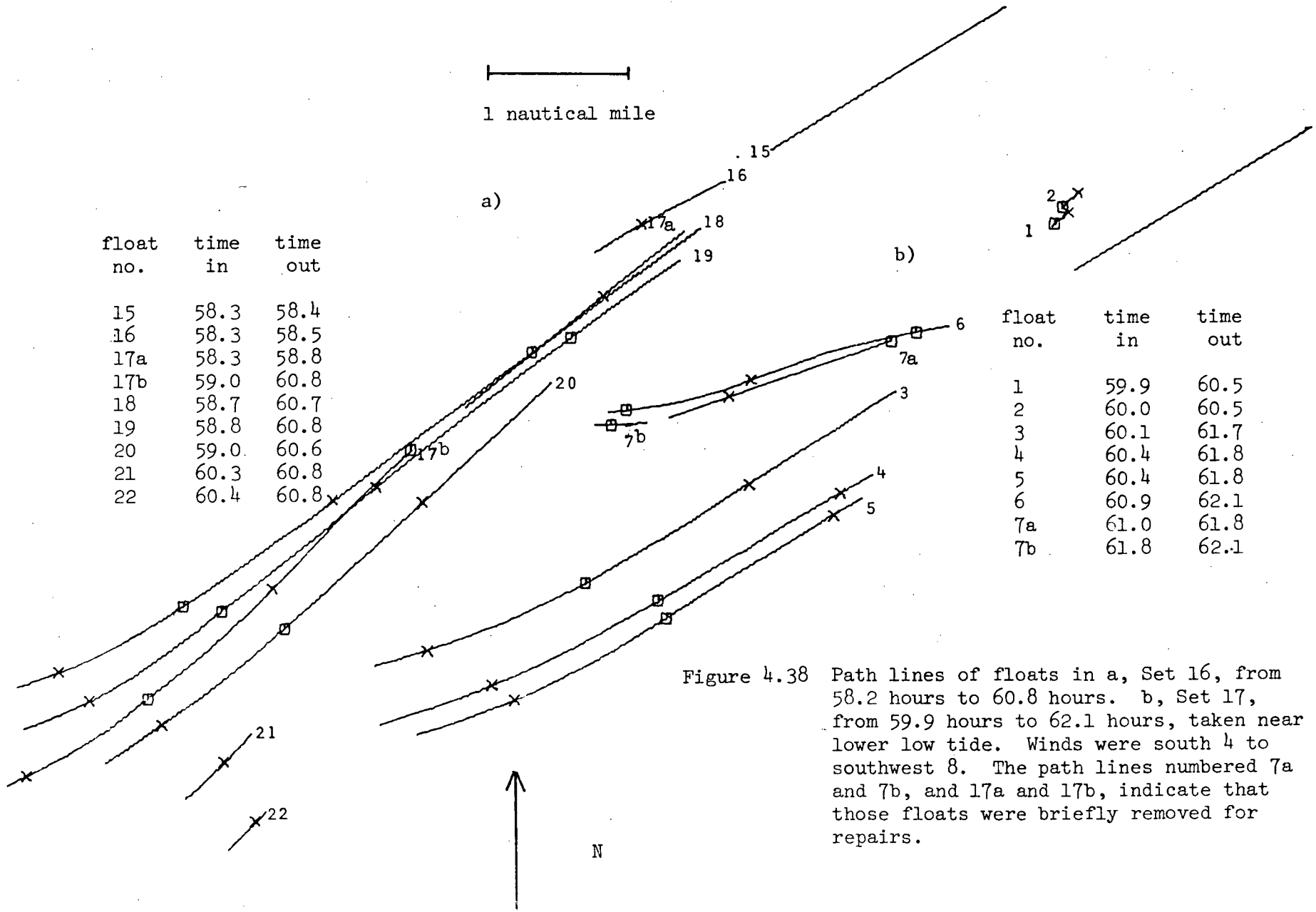


Figure 4.37 Composite velocity field averaging the data from Set 12 (30.8 hours to 34.8 hours) and Set 16 (54.7 hours to 59.0 hours), taken at the beginning of the large ebb tide.



float no.	time in	time out
15	58.3	58.4
16	58.3	58.5
17a	58.3	58.8
17b	59.0	60.8
18	58.7	60.7
19	58.8	60.8
20	59.0	60.6
21	60.3	60.8
22	60.4	60.8

float no.	time in	time out
1	59.9	60.5
2	60.0	60.5
3	60.1	61.7
4	60.4	61.8
5	60.4	61.8
6	60.9	62.1
7a	61.0	61.8
7b	61.8	62.1

Figure 4.38 Path lines of floats in a, Set 16, from 58.2 hours to 60.8 hours. b, Set 17, from 59.9 hours to 62.1 hours, taken near lower low tide. Winds were south 4 to southwest 8. The path lines numbered 7a and 7b, and 17a and 17b, indicate that those floats were briefly removed for repairs.

maximum outflow. The flow in the plume during this tidal phase was measured on the third day in Set 16 (after 59.0 hours) and Set 17, and on the second day in Set 13. On the first day two floats were put in the river beside the jetty just after lower low tide (Set 9). Their velocities will be examined as well.

The end of Set 16 and Set 17 cover the time interval from about two hours before lower low water until about one hour after it. The last two floats from the second line of Set 16 (Figure 4.35b) remained in the water for a short while, and those of the third line (Figure 4.38a) were removed half an hour before low water. A new line of floats (Figure 4.38b) was put in the water about an hour before the lower low tide. Floats 1 and 2, put in north of Steveston Jetty, moved very slowly back parallel to the jetty, while the floats put in the main part of the plume moved out straight at quite a high speed, as the velocity field (Figure 4.39) shows. The speeds (about 1.7 m/s near Sand Heads) are considerably higher than they were in Sets 2 and 6, and the floats moved out farther before beginning to curve to the north. These differences are due to the floats in Set 17 being put in slightly before the time of maximum outflow while those in Sets 2 and 6 went in somewhat after, as well as to the height of the low tide being considerably lower. As the sideways pull of the ebb tide slackened the velocities of the floats from the end of Set 16 also swung right to become nearly parallel to the jetty. The winds during the three-hour period were light, being south 4 to southwest 8.

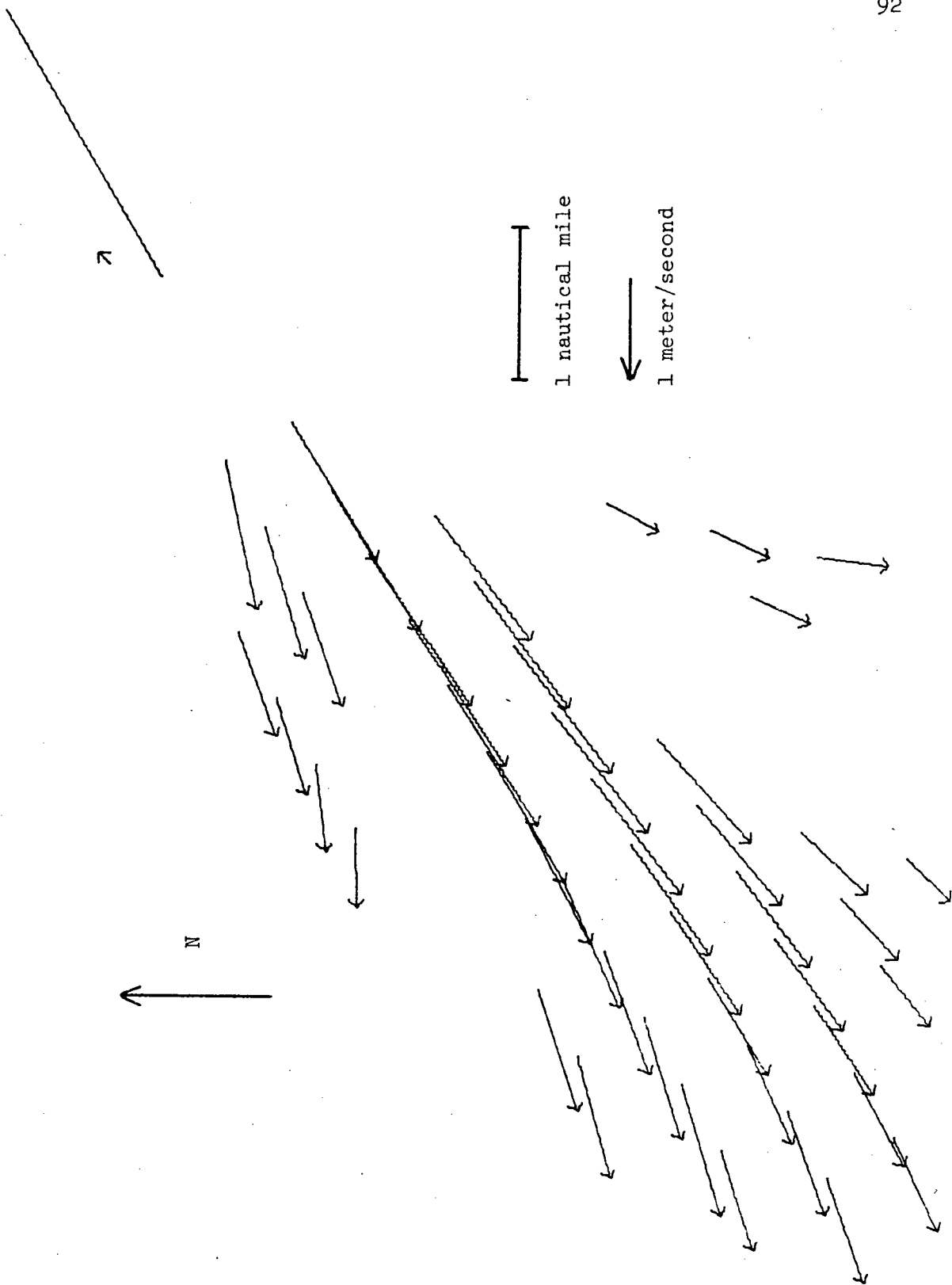


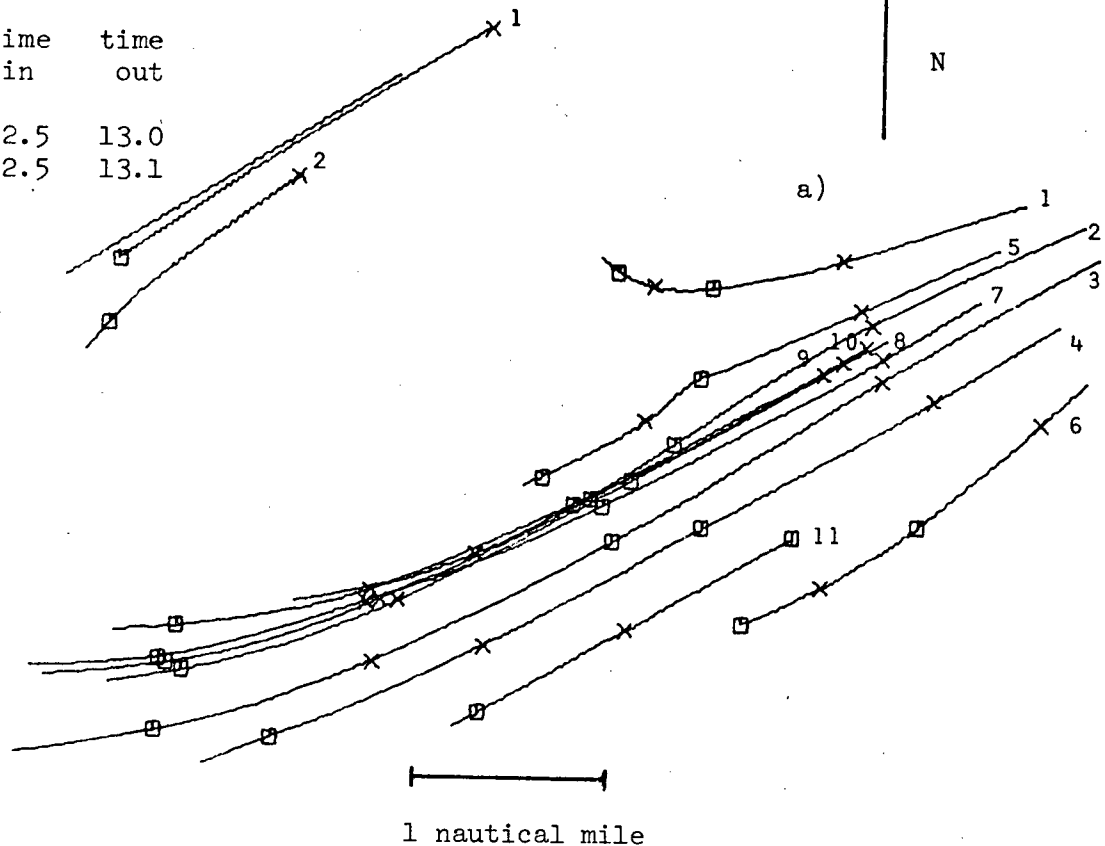
Figure 4.39 Velocity field for Sets 16 and 17 (59.0 hours to 62.1 hours), taken near lower low tide.

Set 13, which began almost two hours before lower low water on the second day, follows the end of Set 12 with a gap of only a few minutes. The float tracks are shown in Figure 4.40a, and the velocity field in Figure 4.41a. Although the winds were very light (southeast 4), the floats initially moved somewhat to the north. This may be due to spreading of the plume and the fact that those floats were on the northern side of it. The initial speeds of 2.1 m/s near Sand Heads were somewhat higher than those in Set 17 (1.7 m/s), but at distances of three miles or more from Sand Heads, speeds in the two sets became very similar. By the time the floats were removed about a half hour after lower low water, the Coriolis force and the effect of the lower salt water layer, which was being pushed up the Strait by the flooding tide, had begun to turn the flow to the right.

Set 9 consists of two floats which were put in the river beside the jetty on the first day (Figure 4.40b) at about one-half hour after lower low water, but while the river's pressure head was still quite large. Float 1 remained quite close to the jetty but Float 2 gradually moved away. It would probably have been in the "southern side" of the plume if it had stayed in the water long enough to move out into the Strait. The floats moved very quickly, at 2.5 to 2 m/s in the river, (Figure 4.41b), but slowed slightly as they approached the Strait. The slowing was probably due to frictional drag with the lower layer, which had by then begun to be pushed up the Strait by the flooding tide. The surface layer had become thin enough that this drag force was felt by the floats.

float no.	time in	time out
1	12.5	13.0
2	12.5	13.1

b)



float no.	time in	time out
1	35.2	37.3
2	35.2	36.9
3	35.2	37.3
4	35.3	37.2
5	35.3	37.1
6	35.3	37.0
7	35.3	37.3
8	35.4	37.3
9	35.5	37.2
10	35.5	37.2
11	36.0	37.1

Figure 4.40 Path lines of floats in a, Set 13, from 35.1 hours to 37.4 hours, when winds were calm to south 4, and b, Set 9, from 12.1 hours to 13.1 hours, when winds were near south 10. The data were taken near lower low tide.

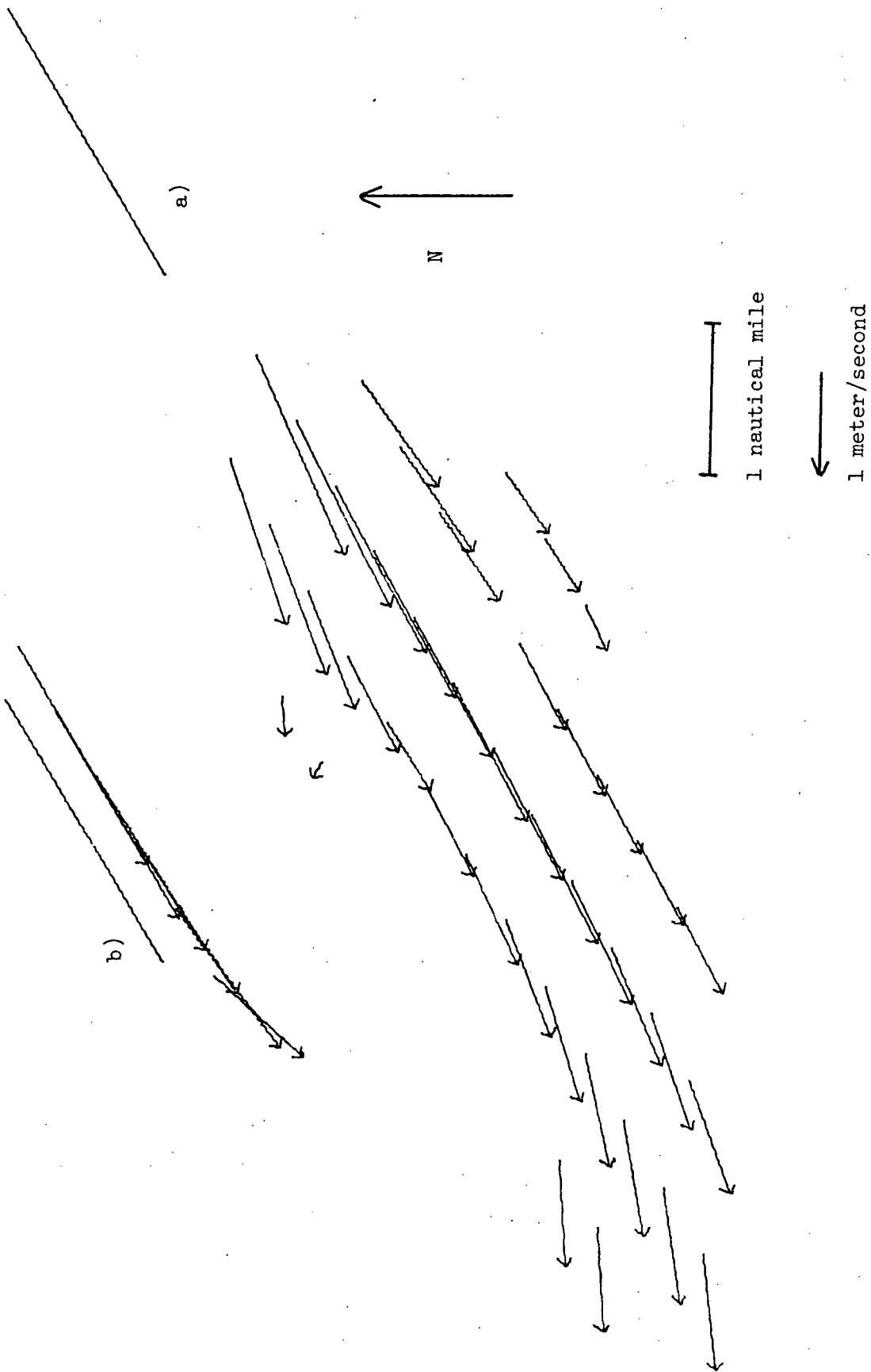


Figure 4.41 Velocity fields for data near lower low tide. a, Set 13 (35.1 hours to 37.4 hours) and b, Set 9 (12.1 hours to 13.1 hours).

The composite flow field (Figure 4.42) is an average of Sets 9, 13, 16 (after 59.0 hours) and 17. It shows the typical features of flow near lower low water. Because of the river's large pressure head, the flow is quite rapid, and moves away from the river mouth with little spreading and only a very gradual curvature to the north. The radius of the inertial circle for a 2 m/s current is about 11 nautical miles, which is consistent with the observed curvature.

4.2.3 Sets 10, 14 and 18, early part of large flood

As the tide began to rise from lower low water, the water moving up the Strait aided the Coriolis force in swinging the river plume to the north. Sets 10, 14 and 18 were all collected on the rising tide, starting one to one and one-half hours after lower low water. The path lines for these sets are shown in Figures 4.43a, 4.43b, and 4.45a. Figures 4.44a, 4.44b, and 4.45b are the corresponding velocity fields.

In all three cases, the floats initially moved out fairly straight from Sand Heads, but the effect of the flooding tide combined with the Coriolis force to turn the flow increasingly northward. Floats on the south side of the plume were caught between the flooding Strait water and the outward moving river water and slowed rapidly. In Set 18, Float 11 moved very slowly at first, but was later pushed north more sharply than the faster moving floats near the centre of the plume, cutting across their path lines. By that time the central floats were more than a mile farther out. Floats on the north side of the plume tended to move quite slowly also, and to be pushed north by both the

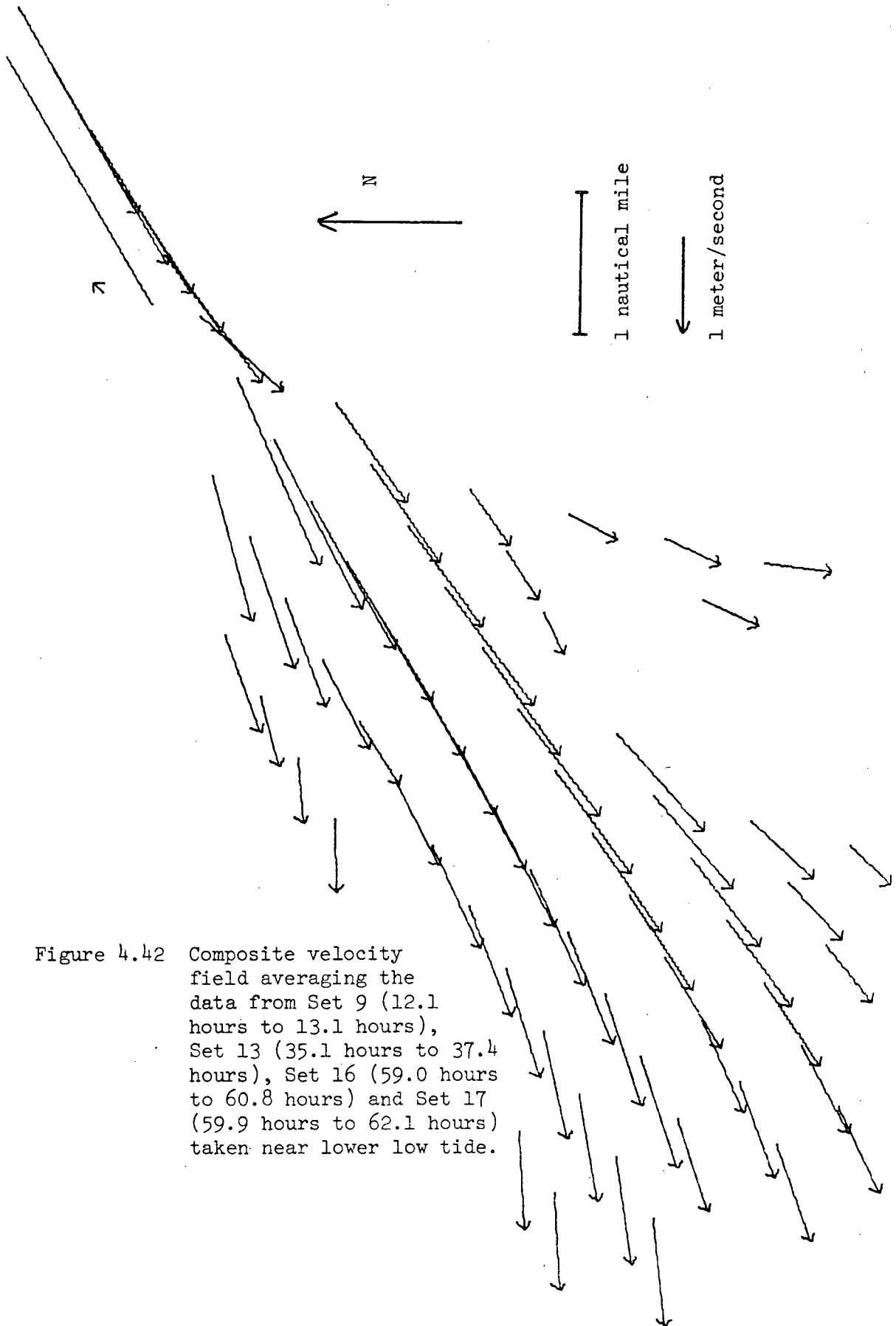
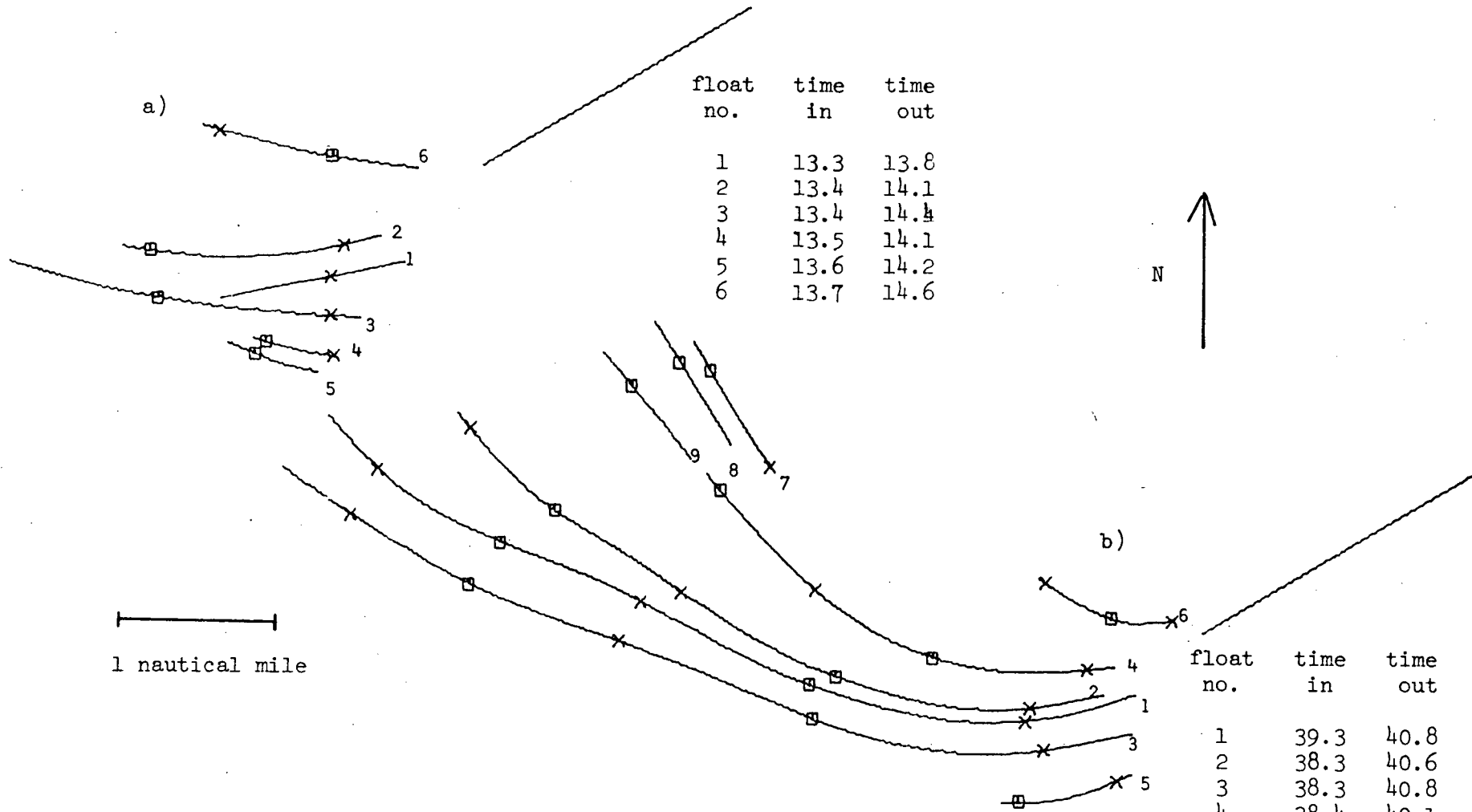


Figure 4.42 Composite velocity field averaging the data from Set 9 (12.1 hours to 13.1 hours), Set 13 (35.1 hours to 37.4 hours), Set 16 (59.0 hours to 60.8 hours) and Set 17 (59.9 hours to 62.1 hours) taken near lower low tide.

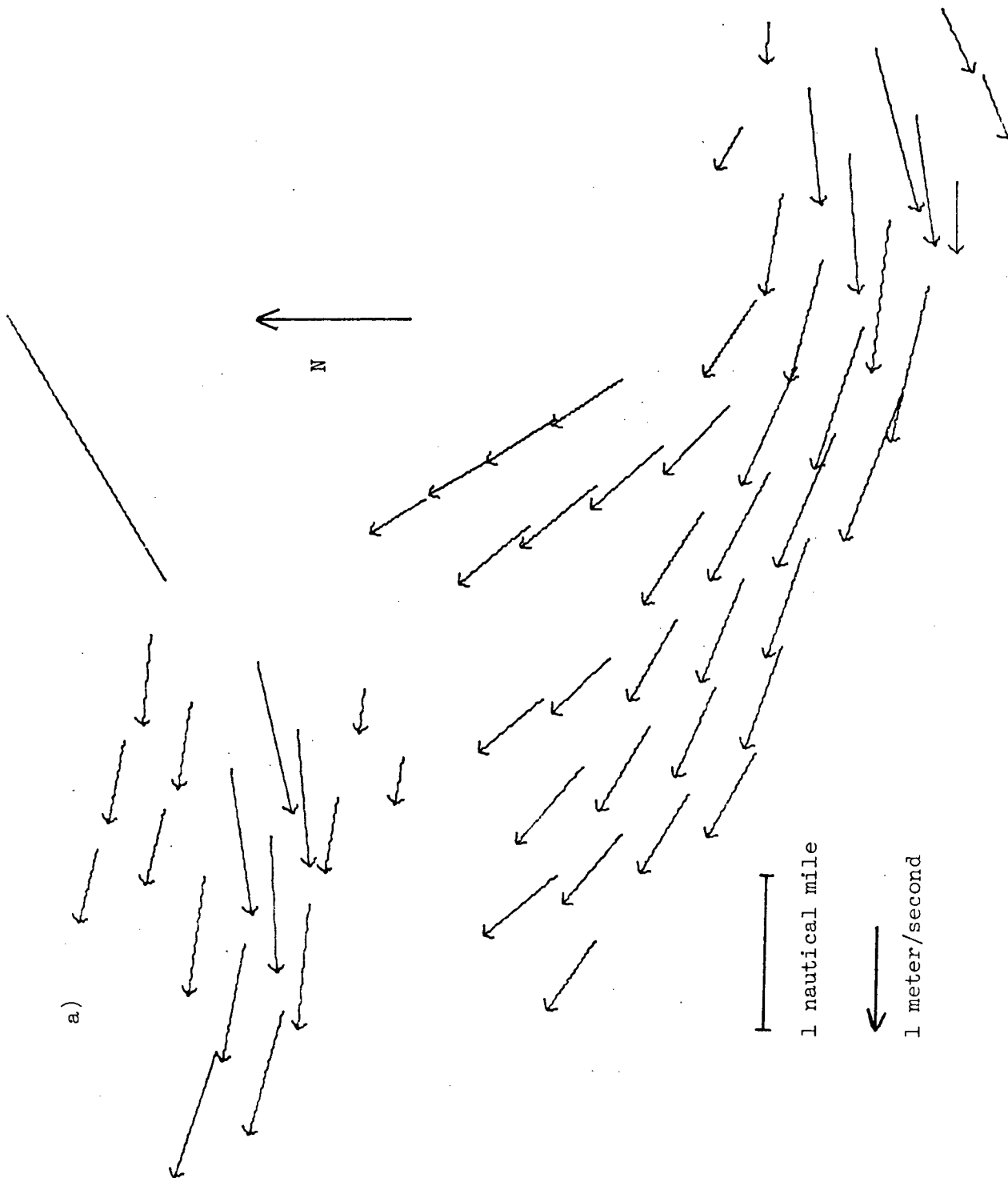


float no.	time in	time out
1	13.3	13.8
2	13.4	14.1
3	13.4	14.4
4	13.5	14.1
5	13.6	14.2
6	13.7	14.6

float no.	time in	time out
1	39.3	40.8
2	38.3	40.6
3	38.3	40.8
4	38.4	40.1
5	38.4	39.1
6	38.5	39.6
7	40.5	39.6
8	40.6	41.3
9	40.7	41.2

Figure 4.43 Path lines of floats in a. Set 10, from 13.3 hours to 14.6 hours, when winds were near south 10, and b. Set 14, from 38.2 hours to 41.3 hours, when winds were southeast 4 to east 12. The data were taken near the beginning of the large flood to higher high tide.

Figure 4.44 Velocity fields for data near the beginning of the large flood to higher high tide. a, Set 10 (13.3 hours to 14.6 hours) and b, Set 14 (38.2 hours to 41.3 hours).



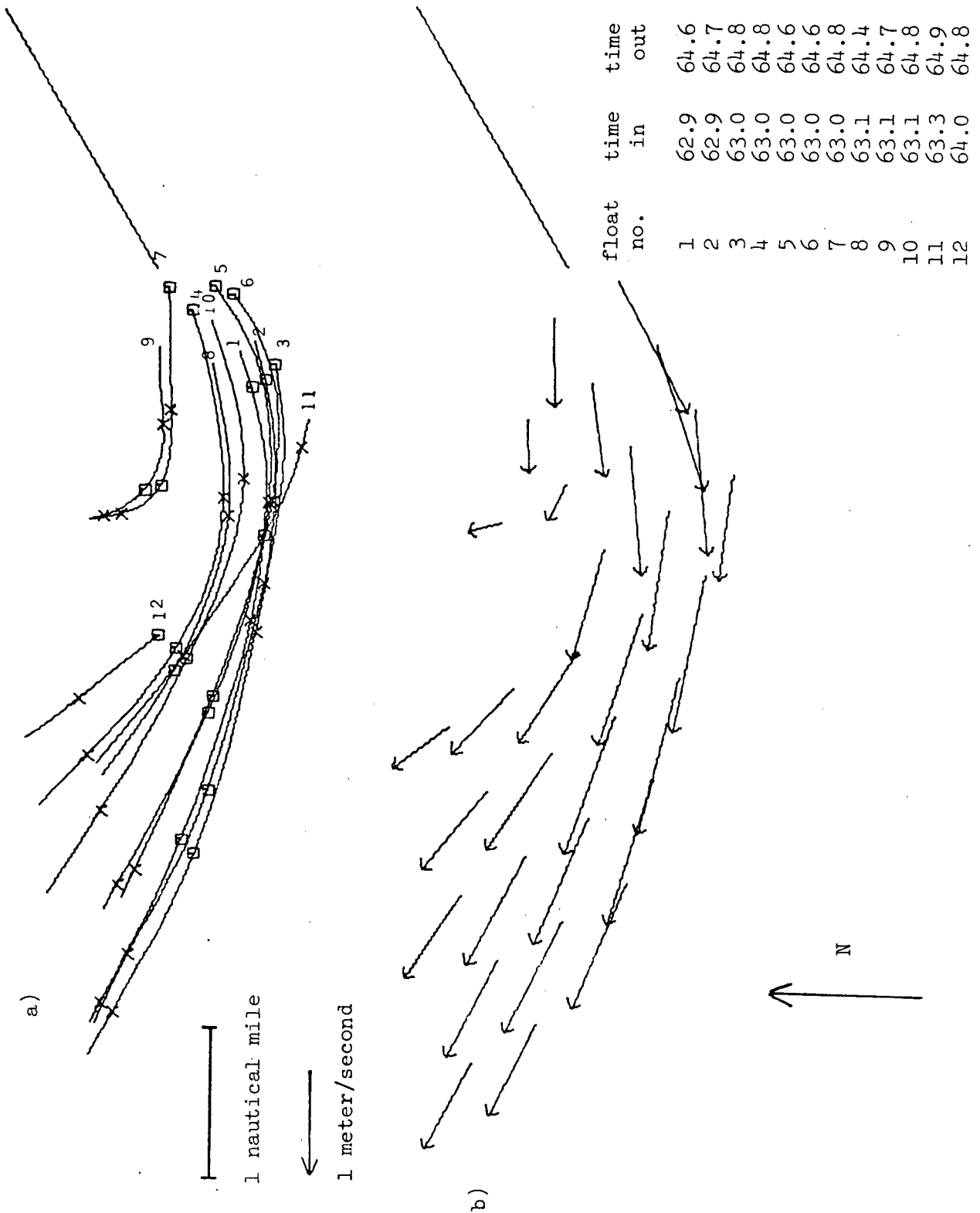


Figure 4.45 a, Path lines and b, Velocity field for Set 18 (62.8 hours to 64.9 hours) taken near the beginning of the flood to higher high tide, when winds were southwest 6 to southwest 14.

flooding tide and the Coriolis force. The central floats maintained quite high speeds, since the water level in the Strait was low and the river had quite a large pressure head when they left Sand Heads. Winds were similar on the three days: south 10 during Set 10, south-southeast 8 to east 15 during Set 14, and southwest 10 to west-southwest 12 during Set 18. On each day the wind had a component which encouraged the flow to the north with the tide.

The average velocity field for the three sets (Figure 4.46) shows the basic features of the flow at the start of full flood. The speeds at the centre of the plume are large (near 1.5 m/s) because of the river's pressure head, and they decrease quite slowly as the floats move away from the river mouth. Frictional drag slows the floats near the north and south edges of the plume. There is gradual curving to the north, caused by the increasing strength of the flood tide, the Coriolis force and the encouragement of the wind.

4.2.4 Sets 11 and 15, approach to higher high water

The higher high tides during the second week reached about the same water levels as the higher high tides observed at night during the first week. Observations were made on the rise to higher high water on the first and second days of the week, yielding Sets 11 and 15. Even though the tidal heights were similar to those in Week 1, the preceding low tides were much lower, so the force of the tide flooding up the Strait was considerably larger.

Set 11 consists of an initial group of three floats (Figure 4.47a) put in over four hours before high water, followed by a

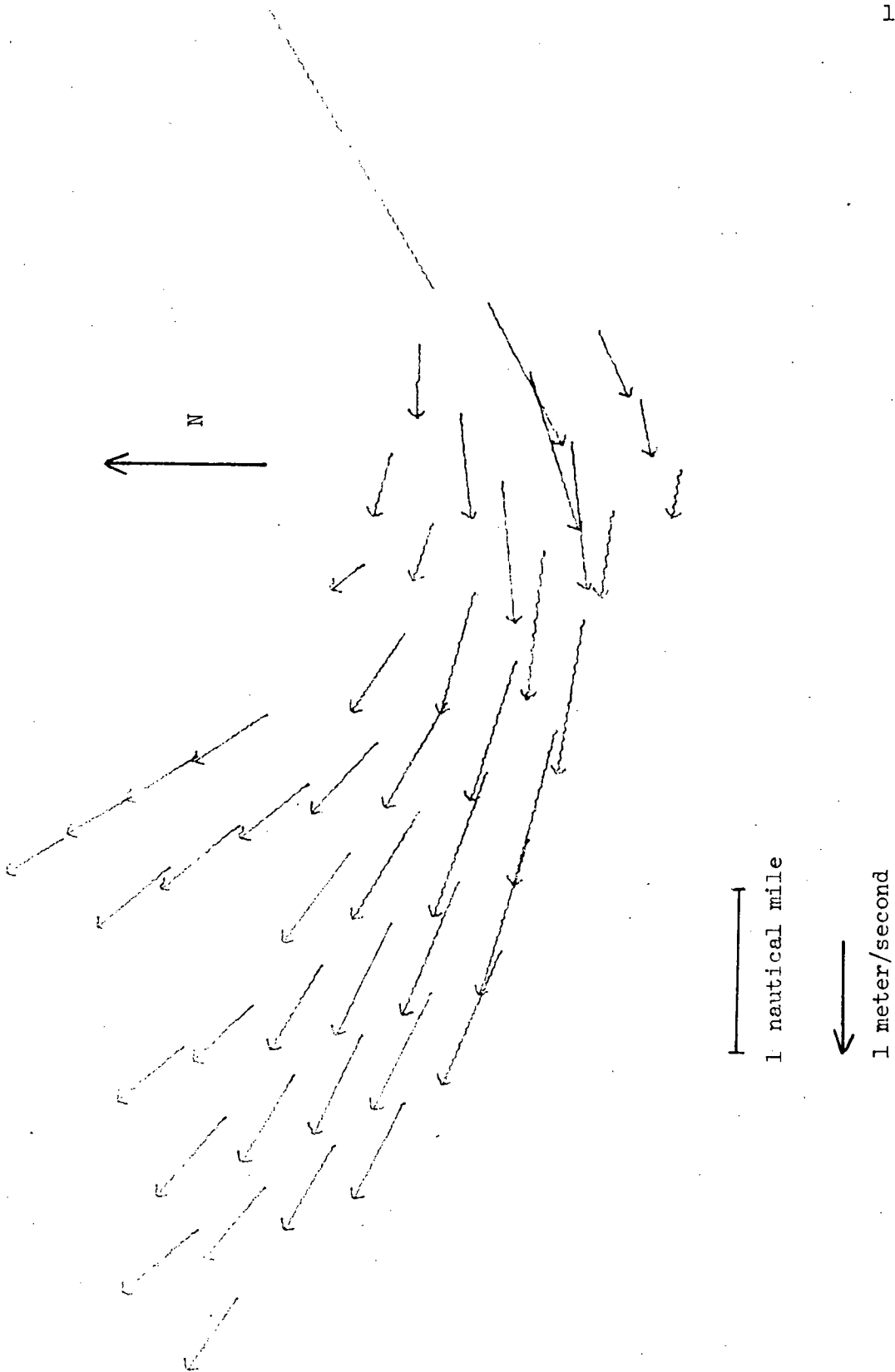
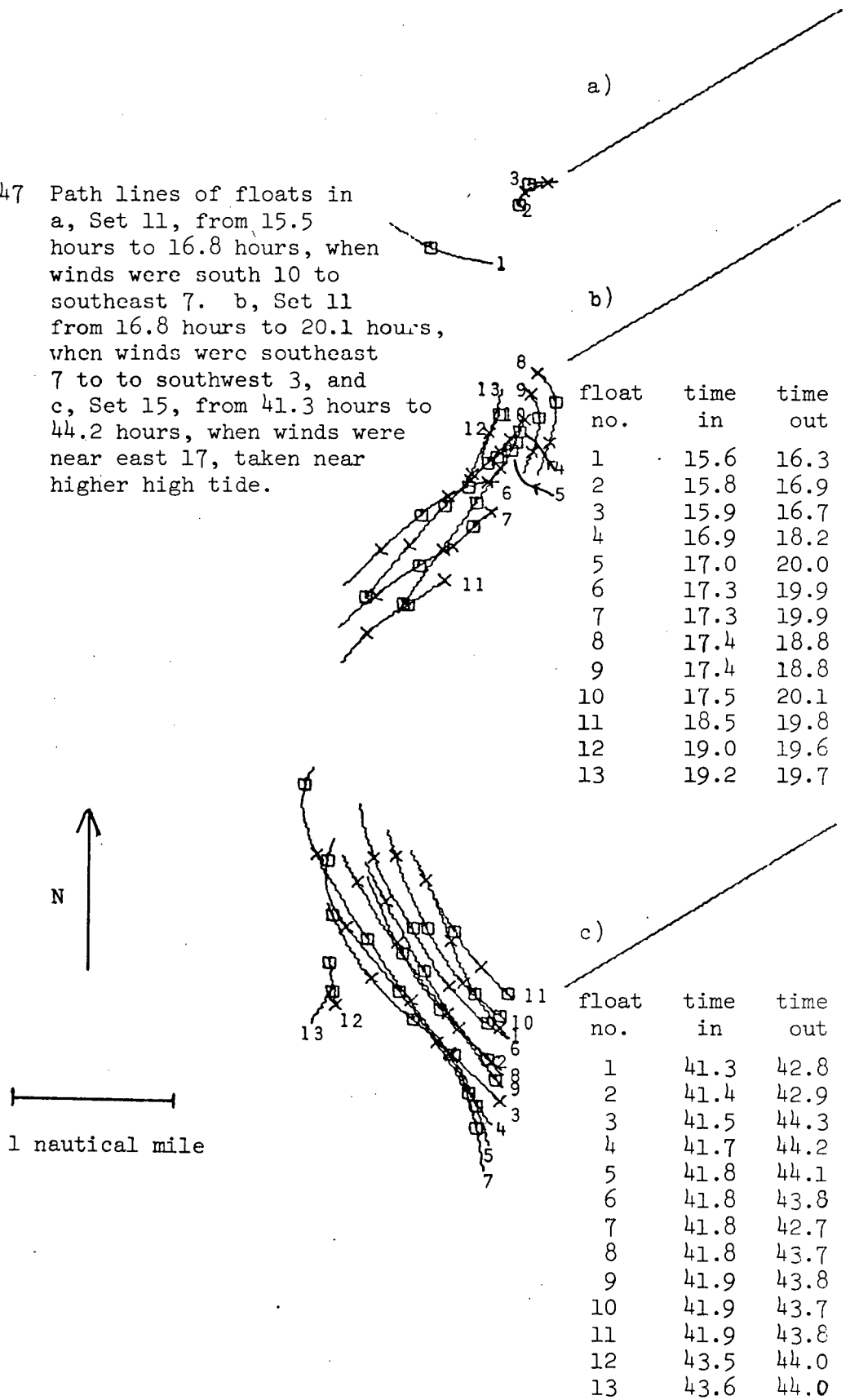


Figure 4.46 Composite velocity field averaging data from Set 10 (13.3 hours to 14.6 hours), Set 14 (38.2 hours to 41.3 hours) and Set 18 (62.8 hours to 64.9 hours), taken near the beginning of the flood to higher high tide.

Figure 4.47 Path lines of floats in a, Set 11, from 15.5 hours to 16.8 hours, when winds were south 10 to southeast 7. b, Set 11 from 16.8 hours to 20.1 hours, when winds were southeast 7 to to southwest 3, and c, Set 15, from 41.3 hours to 44.2 hours, when winds were near east 17, taken near higher high tide.



larger group (Figure 4.47b) put in from three hours to one hour before the high tide. The floats in Set 15 (Figure 4.47c) were put in about three hours before the high tide. The flow patterns observed on the two days are quite different, but most of the differences may be attributed to the strong southeast wind which was blowing on the second day.

The velocity fields for the two parts of Set 11 are shown in Figures 4.48a and 4.48b. The river outflow was decreasing as the water level in the Strait rose. Float 1 was far enough out to be pushed north by the flooding tide, but Floats 2 and 3 were caught north of the main flow near Sand Heads, and moved very slowly. The next group of floats moved quite straight out from the river mouth, but was greatly slowed by the rising water level in the Strait. Speeds were 0.2 to 0.3 m/s. The winds during the period were quite light: south 8 to east 5 to southwest 3. Initially they may have been strong enough to push Float 1 more to the north, but after that they probably had little effect.

When the floats comprising Set 15 (Figure 4.47c) were put in the water the rising water level in the Strait made the flow speed of the water leaving the river mouth quite low. In this situation the wind, which was east 16 to southeast 18, was able to exert a dominant force on the water in the surface layer. The velocity field (Figure 4.48c) shows that the flow was pushed northwest by the wind, with a little help from the Coriolis force. The wind stress increased the speed of the floats from 0.3 to 0.5 m/s. This finding is consistent

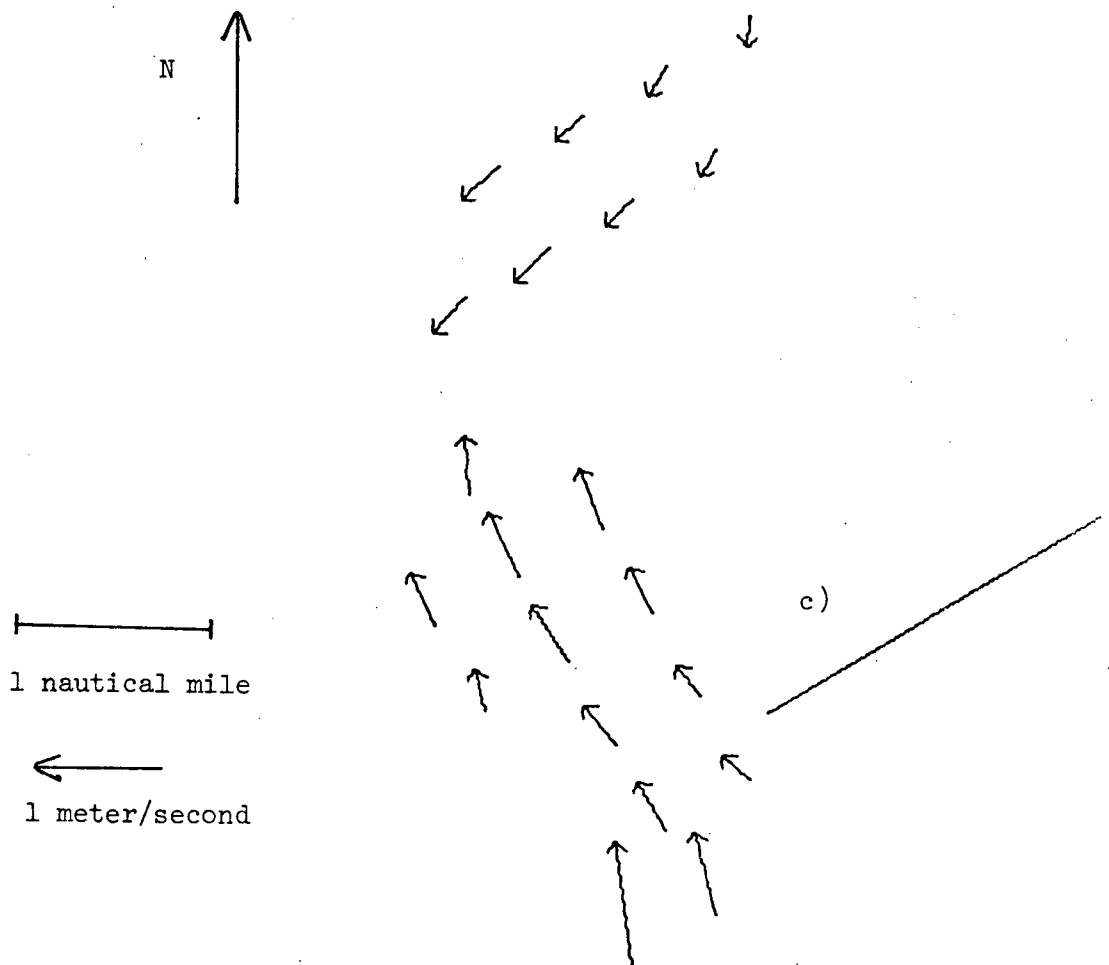


Figure 4.48 Velocity fields for data taken near higher high tide. a, Set 11 (15.5 hours to 16.8 hours). b, Set 11 (16.8 hours to 20.1 hours) and c, Set 15 (41.3 hours to 44.2 hours).

with the earlier calculation of the effects of wind drag acting on a three-meter-deep surface layer. The 16 knot wind would produce a .2 m/s increase in speed over about two hours.

Since the flow patterns in the two data sets are so different it seems that there is nothing to be gained by averaging them together. Set 11 gives the better representation of the flow near higher high water, since it is not strongly altered by wind effects.

4.3 Average velocity components versus distance from Sand Heads

Another way of presenting the data is to plot average velocity components (parallel and perpendicular to the Steveston Jetty) as a function of distance from Sand Heads. To retain some of the features of the cross stream variation, the float tracks have been arbitrarily divided into three groups - those on the north side of the plume, those in its central region, and those on the south side. For each float track, distance was calculated as the distance from Sand Heads (the origin of the graphs) to the start of the track plus the distance travelled along the track. (Note that this is not the same as the displacement from Sand Heads.) The data used are those sampled at 0.1 mile intervals along each track.

Each of the graphs of velocity components versus distance (Figures 4.49 to 4.54) corresponds to one of the composite velocity fields found earlier in the chapter. All float tracks or parts of tracks falling within the specified time intervals were averaged to produce the plots for the three regions. As in the previously displayed velocity fields, some of the apparent features of the flow are probably

artifacts caused by floats being put in and taken out at different times and places, and by the lack of simultaneity in the data sets. The standard deviation was calculated for each average, using the formula

$$\left(\frac{\sum_{i=1}^n v_i^2 - \left(\frac{\sum_{i=1}^n v_i}{n} \right)^2}{n-1} \right)^{\frac{1}{2}}$$

where v_i is a value of the downstream of cross-stream velocity component. To give an indication of the scatter in the data being averaged, typical values of this standard deviation are shown beside each graph. Since the averaged quantities were observed at slightly different times and locations, they are not expected to be measurements of exactly the same thing. The standard deviation is, therefore, probably a better estimate of error than the standard error of the mean, which would be calculated by dividing the standard deviation by $(n)^{\frac{1}{2}}$.

4.3.1 Week 1

In the first week's data, Sets 2 and 6 cover the times near low tide and hence the times of the largest discharge. All the floats involved seemed to remain in the central region of the plume, so only points for that region have been plotted in Figure 4.49. The corresponding velocity field was shown in Figure 4.6. The most significant feature of the graph is the trend toward decreasing speed. This tendency was probably caused by the frictional drag of the underlying salt water on the surface layer forming the plume. Winds during both sets were light enough (6-8 knots) to have little effect. The trend of the cross-stream component to become

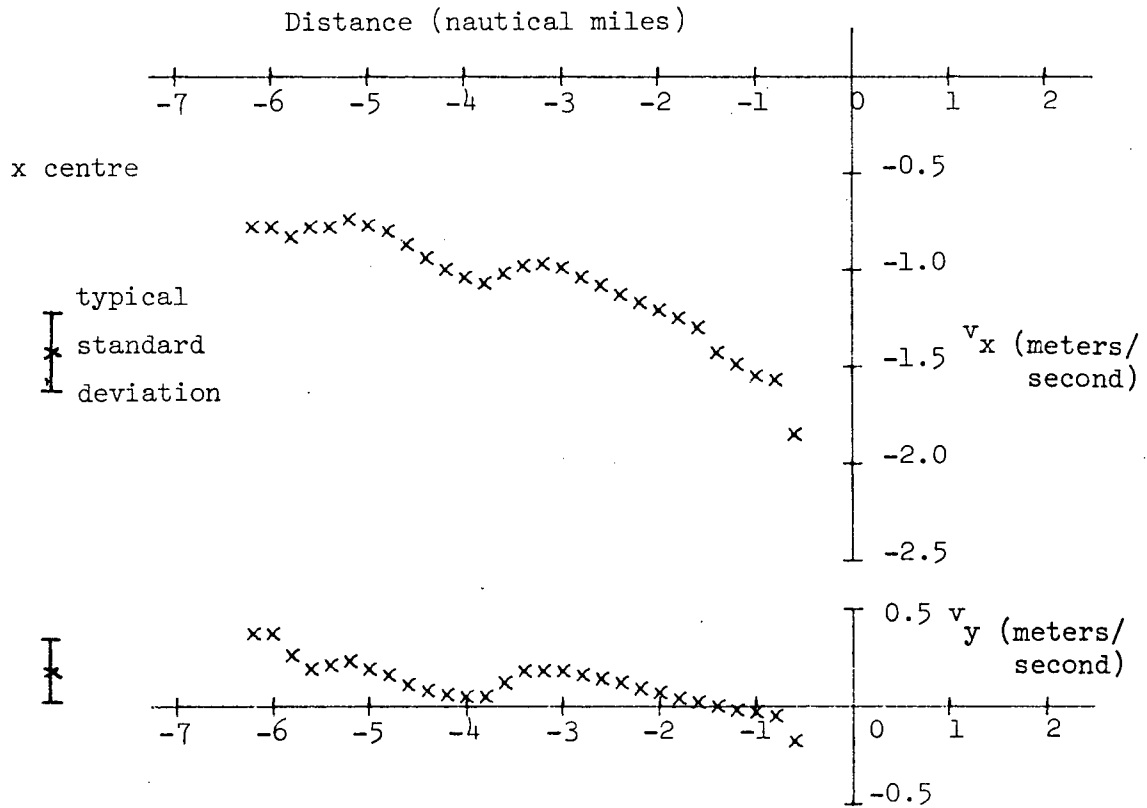


Figure 4.49 Velocity components (v_x downstream and v_y cross-stream) as a function of distance from Sand Heads, for the northern, central and southern regions of the plume. Set 2 (17.0 hours to 19.4 hours) and Set 6 (57.0 hours to 58.5 hours) were taken near lower low water during equatorial tides.

more positive has less significance, since most of the points fall within one standard deviation of zero. The effects of the flooding tide and the Coriolis force would, however, tend to produce such a change. The points for both components are generally within one standard deviation of falling along a straight line.

Figure 4.50, which corresponds to Figure 4.21, displays the average velocity components for the times when the tide was rising from low to lower high tide. The effects of the flooding tide are found in the positive (northward) values of cross-stream velocity components for most regions of the plume and in the speeds which are generally at least 50% smaller than those measured at the end of the ebb tide. Again the graph shows a fairly linear decrease in the downstream velocity component. The seeming increase in the downstream component for the north side of the plume near the origin is probably a result of more quickly moving floats being installed farther from Sand Heads than the initial slow moving ones.

Figure 4.51 is the graph for the small ebb tides, corresponding to Figure 4.22. While the flow speeds are somewhat larger than those for the rising tide, they are still appreciably smaller than those in Figure 4.49. The data for it were obtained at the end of the ebb phase of the tides which fell to a lower level. The lower tide height during Sets 2 and 6 would permit a larger outflow and thus higher speeds. Many of the floats averaged in plotting velocity components for the north side of the plume were curling sharply to the north. Some of them (Set 4) turned far enough to give the downstream component positive values

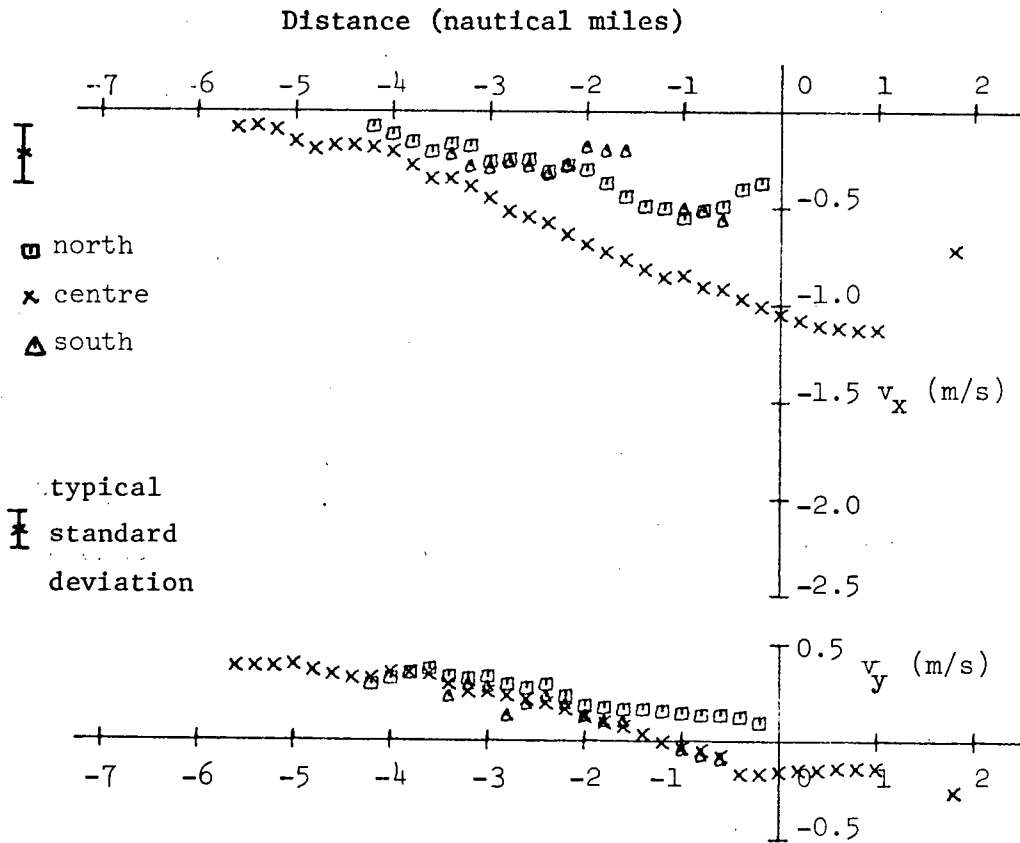


Figure 4.50 Velocity components (v_x downstream and v_y cross-stream) as a function of distance from Sand Heads, for the northern, central and southern regions of the plume. Set 4 (33.1 hours to 38.9 hours) and Set 7 (58.6 hours to 62.0 hours) were taken on the rise to lower high water during equatorial tides.

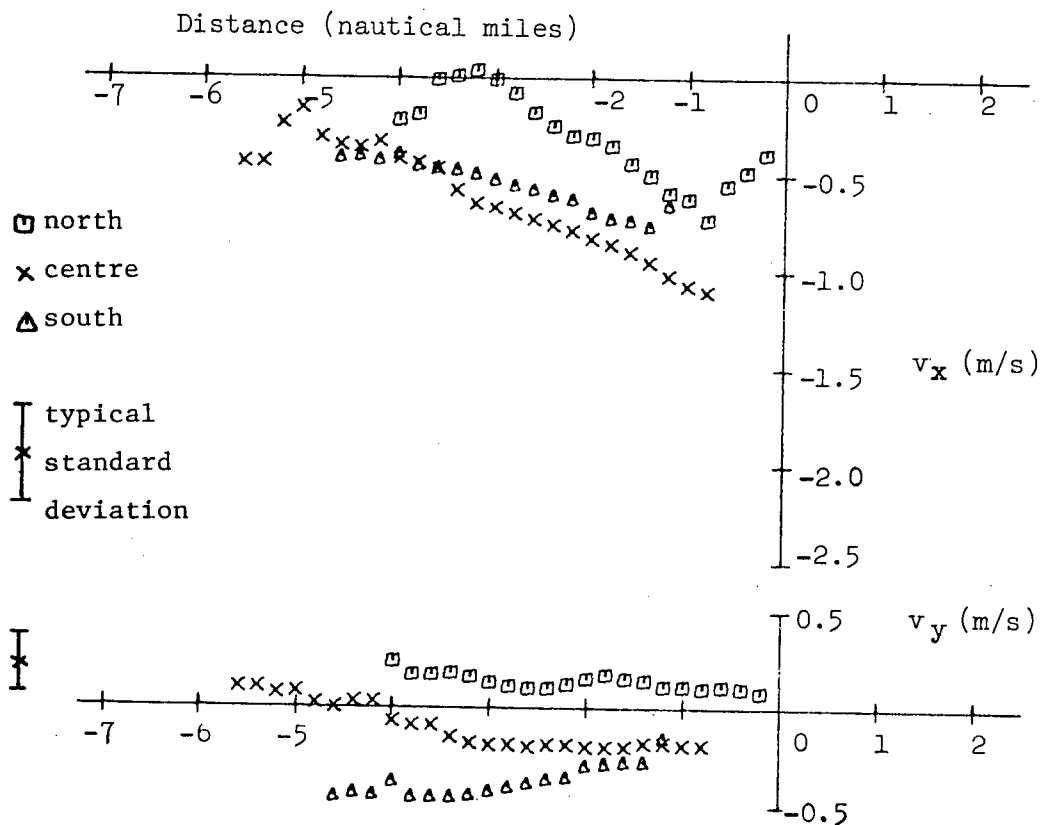


Figure 4.51 Velocity components (v_x downstream and v_y cross-stream) as a function of distance from Sand Heads, for the northern, central and southern regions of the plume. Set 1 (11.6 hours to 16.7 hours), Set 4 (38.9 hours to 43.6 hours) and Set 7 (64.7 hours to 67.5 hours) were taken on the ebb from lower high water during equatorial tides.

at a distance of about three miles from Sand Heads along the float tracks. These floats were then removed from the water so the average values for greater distances still show outward motion. The cross-stream components exhibit the divergence of the plume, with the points for the north and south sides showing definite tendencies in those respective directions. In the central region the graph initially indicates a southward component of the motion, as would be expected on an ebbing tide. The positive values at distances greater than four miles are due to the floats in Set 4, which remained in the water for up to two hours after the tide turned to the flood.

It was felt that Sets 3, 5 and 8, obtained on the rises to and falls from higher high tide during the nights of the first week, were sufficiently sparse in coverage and different in character that velocity versus distance graphs would probably not be representative. These sets have thus been omitted from this section.

4.3.2 Week 2

The study of the second week's data began with Sets 12 and 16, obtained during the early stages of the ebb from high to lower low tide, for which the composite velocity field is Figure 4.37. The velocity versus distance graph for these sets, Figure 4.52, shows speeds which are larger than those found on the small ebbs during the previous week (Figure 4.51), but speeds comparable to the end of the larger ebb (Figure 4.49). The floats in the central region of the plume move considerably faster than those on each side, which are presumably slowed by lateral friction with the water outside the plume, as well as friction

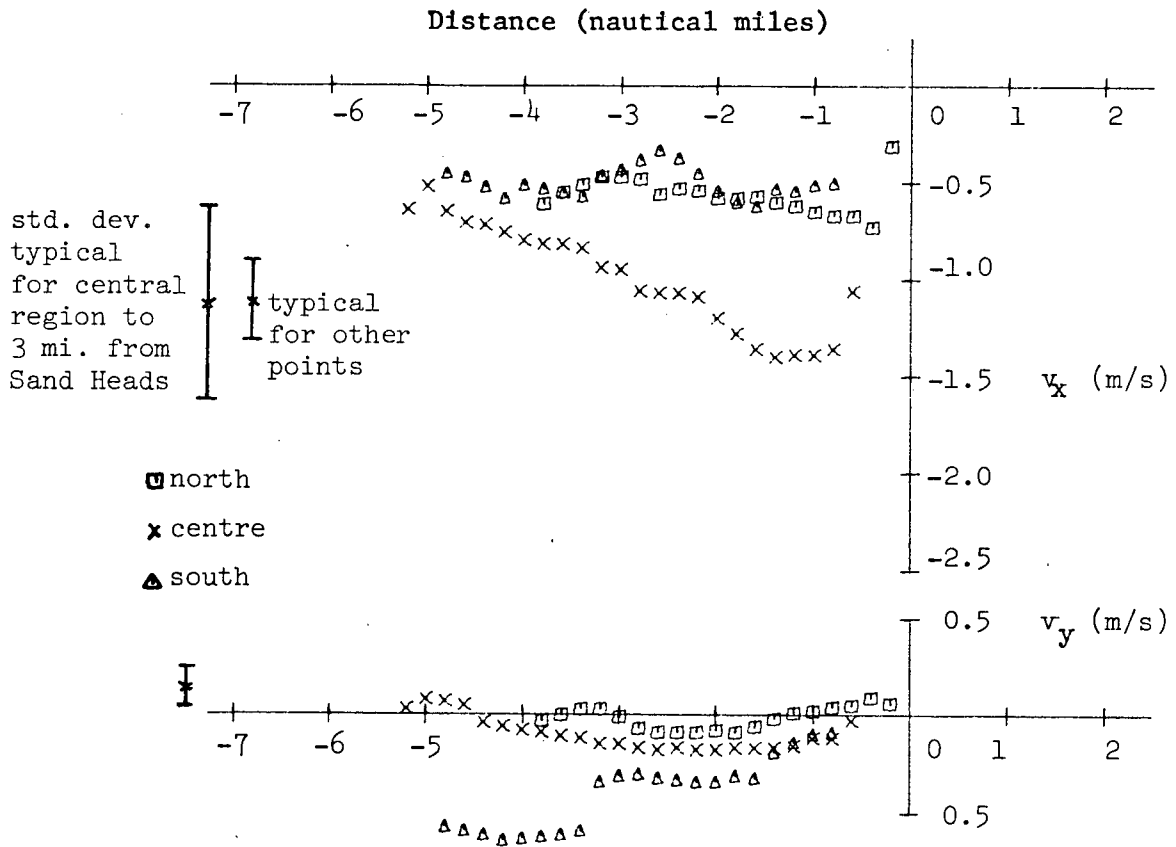


Figure 4.52 Velocity components (v_x downstream and v_y cross-stream) as a function of distance from Sand Heads, for the northern, central and southern regions of the plume. Set 12 (30.8 hours to 34.8 hours) and Set 16 (54.7 hours to 59.0 hours) were taken at the start of the ebb from lower high water during tropic tides.

from below. The cross-stream components show that the plume gradually diverges, especially by turning to the south under the influence of the ebbing tide. The sudden increase in this component in the southern region of the plume at 3.4 miles from Sand Heads is caused by the installation at that point of a quickly moving float, and by a slower moving float being just that far out at 59.0 hours, the end of the time interval for this graph, so its effects on the average are not seen beyond there.

Figure 4.53 displays the velocity versus distance graph for Sets 9, 13, 16 (after 59.0 hours) and 17, which cover the times near the lower low tides at the end of the large ebbs. As one would guess from looking at the composite velocity field in Figure 4.42, the speeds in the central region are larger than those observed on any other tidal phase. The very low tide height gives the river an exceptionally large pressure head and correspondingly high outflow speed. Even the floats on the north and south sides of the plume move relatively fast in comparison with those on other tidal phases. Initially, the central floats show a positive cross-stream velocity component, which may be caused by the Coriolis force. Under the influence of the ebbing tide, the central floats then show a smaller negative cross-stream component, which becomes positive again as the tide turns and begins pushing up the Strait.

The final graph of velocity versus distance, Figure 4.54, displays the averages for Sets 10, 14 and 18. The composite velocity field for these data, which were obtained on the rising tide just after lower low water, is Figure 4.46. The rapid rise in the tide height was

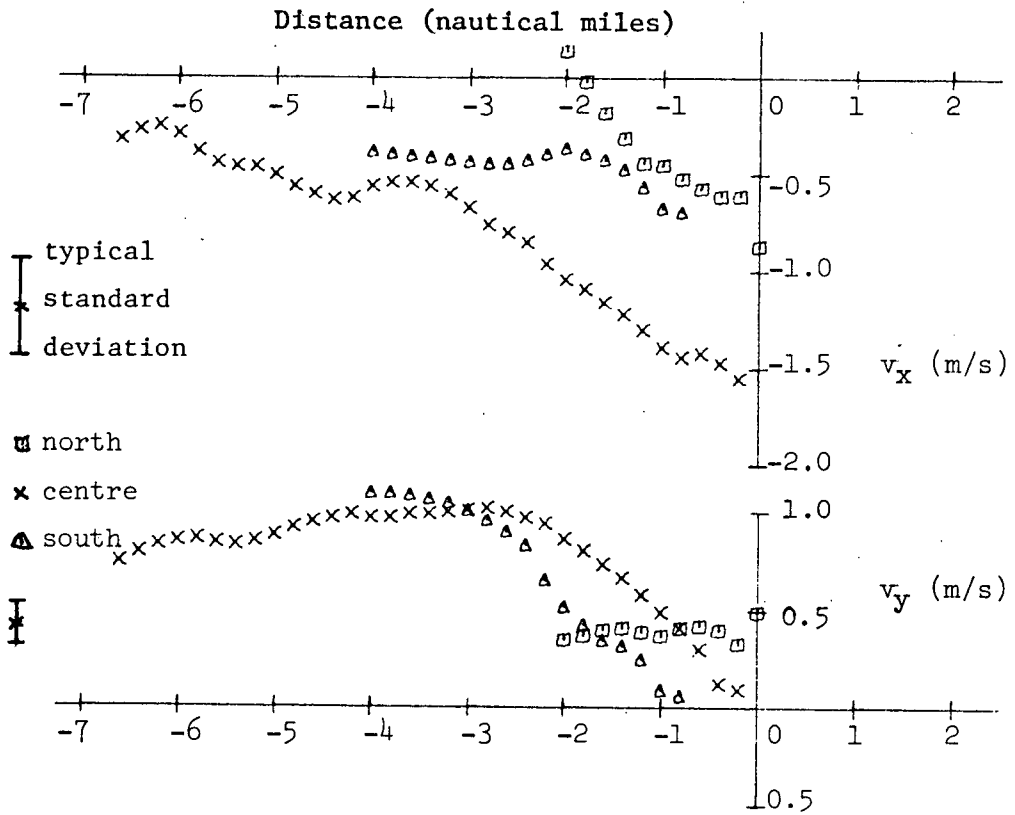


Figure 4.54 Velocity components (v_x downstream and v_y cross-stream) as a function of distance from Sand Heads, for the northern, central and southern regions of the plume. Set 10 (13.3 hours to 14.6 hours), Set 14 (38.2 hours to 41.3 hours) and Set 18 (62.8 hours to 64.9 hours) were taken at the start of the flood to higher high water during tropic tides.

accomplished by a strong flow of water up the Strait, which caused the largest cross-stream component values observed in the whole experiment. The floats on the north side of the plume turned sharply enough to make the downstream component become positive before they were removed. As in all the graphs in this series, the total speeds of the floats in the central region decrease quite smoothly, approximately linearly, with distance.

The observed velocities in Sets 11 and 15 were considered to be sufficiently different that a graph of average velocity components versus distance would not be very representative. Preliminary attempts at such a graph did indicate that, although the directions of motion in the two sets were almost at right angles, the total speeds were quite similar. Those in Set 15 did move slightly faster.

4.4 Comparison with other observations

In reading the literature on observations made in the Strait of Georgia one finds very little data taken in the area of the Fraser plume which can be readily compared with the results of the IOUBC experiment. Included in the data published by Tabata *et al* (1970), however, is a set of current meter data taken in the Fraser plume during freshet. Current velocity measurements were made from a wooden-hulled vessel, anchored 6 km from Sand Heads in the direction indicated by the Steveston Jetty. A Hydro Products Model 465 meter with remote read-out was used to make hourly measurements of the current at a number of depths on May 23-27, 1967. The seventy-five hour period included three cycles of tropic tides. The data taken at a depth of 1m were assumed to be comparable to those which would be observed by drogue tracking.

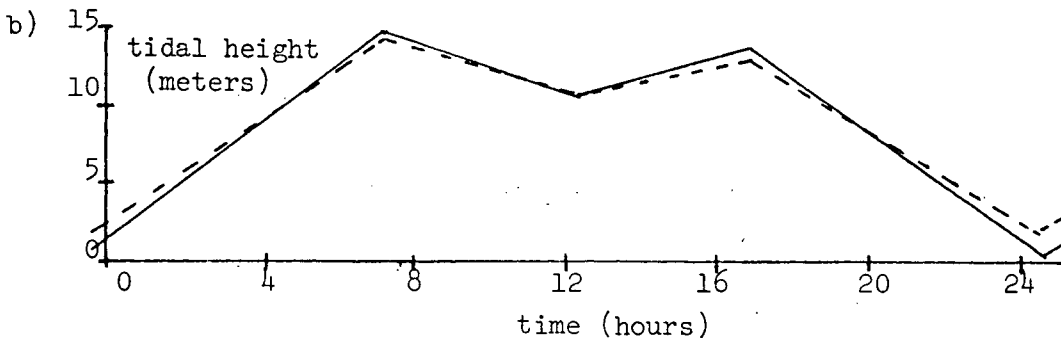
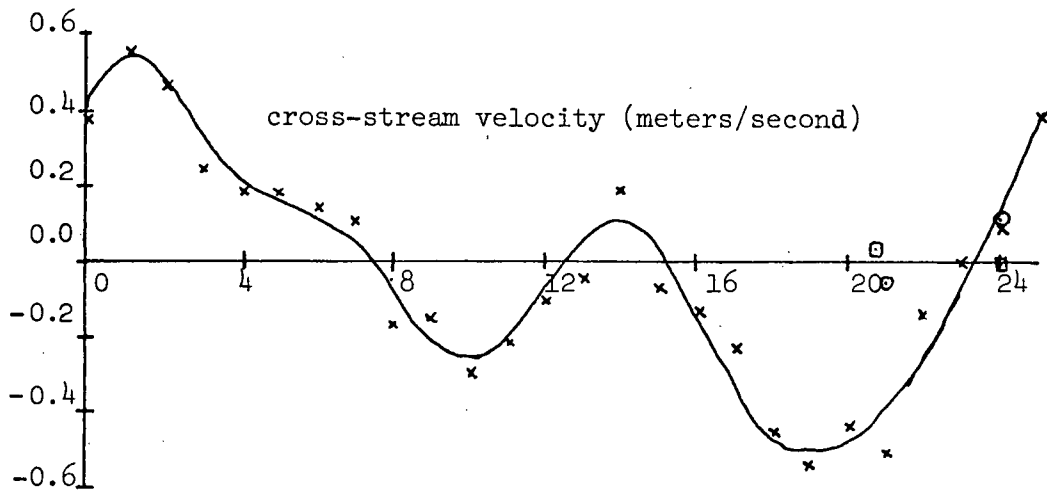
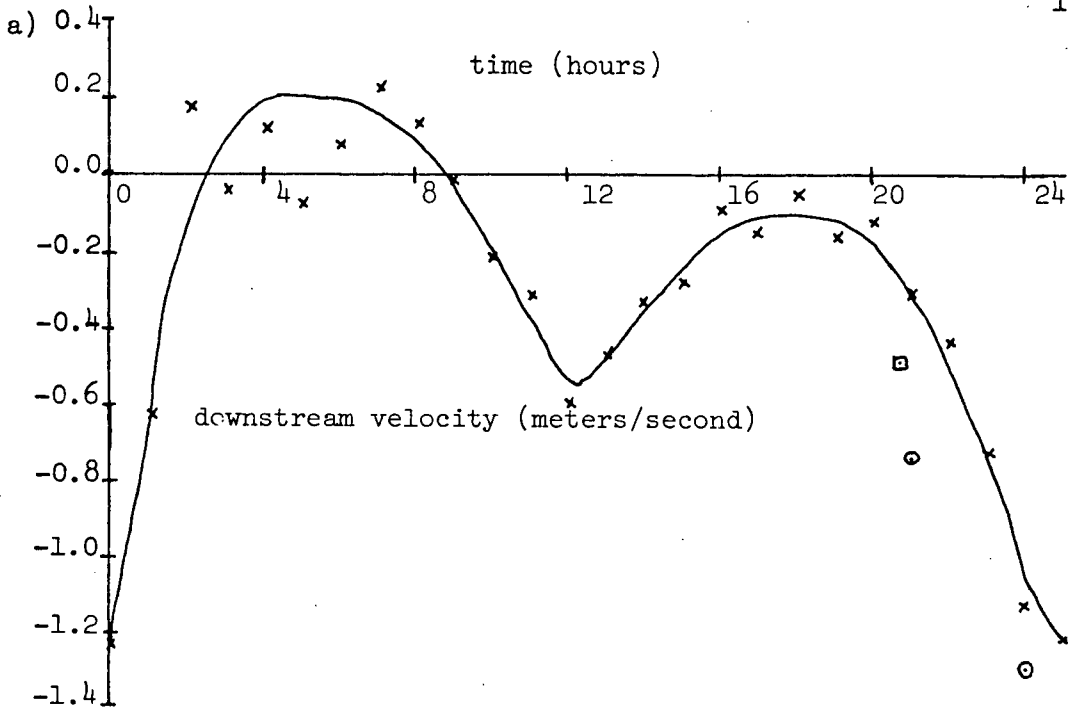
To facilitate comparison, the velocities were resolved into components parallel and perpendicular to the Steveston Jetty, and phase averaged to show variations over a single tidal cycle (Figure 4.55). The tide heights were found in Canadian Tide and Current Tables (1967). Similar tidal conditions occurred during the second week of drogoue tracking, but in that week drogues entered the half-mile square around the current meter station on only four occasions. Velocity components for each of those periods of up to an hour were averaged and plotted in Figure 4.55 at the appropriate tidal phase.

Drogues reached the area of the current meter station only on the large ebb tide. Their speeds are comparable to those measured by the current meter but they had smaller cross-stream velocity components and larger downstream ones. Differences in wind are probably responsible for the variations. The tidal amplitudes during the IOUBC experiment (dotted lines in Figure 4.55) were slightly smaller than those occurring when the current meter data were taken. The discharge from the Fraser River was slightly larger during the 1967 measurements.

4.5 Estimates of entrainment

A further calculation based on the experimental data provides an interesting comparison with the results of a study involving scale models of a river with an arrested salt wedge. While the situation in the Fraser plume is different in many respects from the model, it is interesting to note that there are apparent similarities in the mechanism of entrainment.

Figure 4.55 a, Velocity components as a function of time, phase averaged from hourly observations over three tidal cycles. The velocities were measured with a current meter at a station six kilometers from Sand Heads on May 23-27, 1967. They have been resolved into components parallel and perpendicular to the Steveston Jetty. Velocities observed during my experiment near the current meter station have been plotted at the appropriate tidal phase and marked with a circle (June 5) or a box (June 6). b, Average tide height at Tsawwassen for May 23-27, 1967 (solid line) and June 4-6, 1974) dotted line.



The fresh water discharged from the mouth of the Fraser River is no longer horizontally constrained, and forms a spreading plume with non-zero horizontal divergence. Since, in an incompressible fluid, there can be no net divergence, salt water is entrained from below to maintain the continuity of the upper layer. The continuity equation is

$$\text{div } \underline{U} = \frac{\partial u}{\partial x} + \frac{\partial v}{\partial y} + \frac{\partial w}{\partial z} = 0$$

where the velocity is $\underline{U} = (u, v, w)$. The vertical velocity w must be zero at the surface, $z = 0$. While it is quite probable that the horizontal divergence, $\text{div}_H \underline{U} = \frac{\partial u}{\partial x} + \frac{\partial v}{\partial y}$, varies with the depth, no estimate of the variation can be obtained from the experimental data. Since the surface layer is reasonably well mixed and probably quite turbulent, it is reasonable to assume that any entrained fluid is mixed throughout the layer quite quickly. It thus seems reasonable to assume that $\text{div}_H \underline{U}$ is independent of depth over the surface layer, from $z = 0$ to $z = -h$. Integrating vertically, we obtain an expression for the vertical velocity at the interface, U_m .

$$\int_0^{-h} \frac{\partial w}{\partial z} dz = \int_0^{-h} -\text{div}_H \underline{U} dz$$

$$w \Big|_0^{-h} = \text{div}_H \underline{U} \Big|_0^{-h} z$$

$$U_m = h \text{div}_H \underline{U}$$

U_m is, of course, an average value since the physical processes which

accomplish the entrainment are non-uniform. If the process is similar to the one described by Keulegan (1966), then entrainment is caused by parcels of salt water being introduced into the fresh layer at the apices of breaking internal waves.

The situation discussed by Keulegan (1966) is that of an arrested salt wedge intruding into the channel of a river which empties into a tideless sea. Although the wedge remains stationary, salt water may be entrained by the moving fresh water above if its speed exceeds a critical value. This critical speed U_c , depends on the relative densities of the two layers, ρ and $\rho - \Delta\rho$, the kinematic viscosity of the lower layer, ν_2 , gravity, and a proportionality constant, C' :

$$U_c = C' \left(\frac{\Delta\rho}{\rho} \nu_2 g \right)^{1/3}$$

where g is the acceleration due to gravity. The empirically determined value of C' is 7.3 for an arrested salt wedge.

To study salt wedges Keulegan constructed small scale models of river channels with rectangular cross sections. Based on measurements of the flow in these models, he gives an empirical formula for the entrainment velocity at the interface:

$$U_m = k' (U - U_c).$$

k' is a proportionality constant which he evaluated by measuring the amount of salt mixed into the upper layer and $U = (u^2 + v^2)^{1/2}$ is the speed of the upper layer. The measurements were done with three different

density ratios, using a model channel 5.3 cm wide and 11.2 cm deep. His value for k' is 2.12×10^{-4} .

To compare Keulegan's results with the situation in the Fraser plume, the two expressions for U_m , the vertical velocity at the interface, may be equated, giving

$$h \operatorname{div}_{\underline{H}} \underline{U} = k' (U - U_c) .$$

Evaluating U_c for the Fraser plume yields a value of approximately 3 cm/s, which is so much smaller than typical speeds found in the plume that this term may be neglected. Thus

$$k' \approx \frac{h \operatorname{div}_{\underline{H}} \underline{U}}{U} .$$

If a reasonable estimate is made for the value of h , the expression on the right may be evaluated from the composite velocity fields. The only measurements of the surface layer thickness in the IOUBC experiment were those obtained with the CSTD. Unfortunately, the depth data are not sufficiently reliable near the surface to show variations in h due to position and tidal phase. Based on the CSTD data, a uniform layer thickness of 3 m has been assumed; this assumption probably introduces no larger errors than other approximations made in doing the calculations.

$\frac{\text{Div}_H \mathbf{U}}{U}$ was evaluated for the composite velocity fields shown in Figures 4.6, 4.21, 4.22, 4.37, 4.42 and 4.46. In order to estimate values of $\frac{\partial u}{\partial x}$ and $\frac{\partial v}{\partial y}$ at grid points where u and v are known, $\frac{\Delta u}{\Delta x}$ and $\frac{\Delta v}{\Delta y}$ were calculated from the values of u and v at the points on either side of the point in question.

The results of these calculations give a scattered collection of values for k' at the various grid points, as Figure 4.56, the sample calculation based on Figure 4.6, demonstrates. The average values and standard errors of the mean for the composite velocity fields are

<u>Figure</u>	<u># points</u>	<u>k'</u>	<u>Tidal phase</u>
4.6	12	$(2.67 \pm .74) \times 10^{-4}$	End of ebb
4.21	19	$(1.26 \pm 1.25) \times 10^{-4}$	Small flood
4.22	38	$(2.47 \pm .95) \times 10^{-4}$	Small ebb
4.37	20	$(4.89 \pm .98) \times 10^{-4}$	Start of large ebb
4.42	31	$(1.76 \pm .50) \times 10^{-4}$	End of large ebb
4.46	16	$(3.40 \pm 1.02) \times 10^{-4}$	Start of large flood

The overall average of the 136 points gives an estimate of $k' = (2.62 \pm .40) \times 10^{-4}$, which is remarkably close to Keulegan's value of 2.12×10^{-4} .

Within each composite there were negative values of k' , indicating areas of convergence and downward vertical velocity. That situation did occur near the north side of the plume when it curled sharply around, and along the boundary between old and new sections of the plume. However, some apparent instances of convergence were probably caused by the data distribution and the averaging procedure. For

				.017		
				<u>+.232</u>		
				.249		
				÷.810		
				.307		
	-.309	-.243	-.120	-.110	-.060	-.130
	<u>+.273</u>	<u>+.321</u>	<u>+.403</u>	<u>+.347</u>	<u>+.280</u>	<u>+.334</u>
	-.036	.078	.283	.237	.220	.204
	÷.851	÷1.04	÷1.08	÷1.15	÷1.18	÷1.21
	-.042	.075	.263	.205	.185	.168
-.111	-.192	-.315	-.030	.291		
<u>+.232</u>	<u>+.224</u>	<u>+.244</u>	<u>+.282</u>	<u>+.278</u>		
.121	.032	-.071	.252	.569		
÷.901	÷.949	÷1.08	÷1.26	÷1.13		
.134	.034	-.066	.200	.506		

Figure 4.56 Sample calculation of Keulegan's constant k' , based on the composite velocity field Figure 4.6. Each box corresponds to a grid point and contains $\frac{\Delta u}{\Delta x}$, $\frac{\Delta v}{\Delta y}$ and the

and the horizontal divergence $\frac{\Delta u}{\Delta x} + \frac{\Delta v}{\Delta y}$ ($\text{ms}^{-1}\text{mi}^{-1}$), the horizontal speed U (ms^{-1}) and $\frac{k'}{h} = \frac{\Delta u}{\Delta x} + \frac{\Delta v}{\Delta y}$ (mi^{-1}).

U

To obtain the dimensionless constant k' , these values of k'/h were averaged, and the average was multiplied by $h =$

$$\frac{3\text{m} \times 1 \text{ mi}}{1853 \text{ m}} \quad k' = \frac{.164 \text{ mi}^{-1}}{1853 \text{ m mi}^{-1}} \times 3 \text{ m} = 2.67 \times 10^{-4}$$

example, the track of a quickly moving drogue might end, leaving only more slowly moving ones to form the average velocity in the next square.

Despite the differences between Keulegan's small scale model of an arrested saline wedge in a tideless river channel and the experimental situation of a spreading surface layer overriding a salt layer in a tidal strait, the nearness of the two estimates of k' indicates that the process of entrainment in the two cases may be quite similar. From observations of the change of salt content in the Fraser plume, de Lange Boom (1976) obtained an average value for k' of 2.4×10^{-4} which is also very close to Keulegan's result.

CHAPTER 5

SUMMARY AND CONCLUSIONS

The examination of the data collected in the drogue tracking experiment showed that tidal forces were usually the dominant factor in determining the pattern of flow in the Fraser plume. Winds (unless quite strong) and Coriolis force had lesser effects. Discharge from the river remained relatively constant during the experiment. To summarize the results, the composite velocity fields from Chapter 4 have been collected here. Brief comments will be made on their main features.

Data covering the small flood and ebb stages of the equatorial tides were collected during the days of the first week (Figure 5.1). Throughout most of these periods the winds were light enough (speeds not over 10 knots) that they had little effect on the flow (Figure 4.1).

Sets 2 and 6 (Figure 5.1a) occurred near lower low tide, when the discharge from the river was at its maximum for the week 1 tidal cycles. The small amount of cross-stream motion observed was probably caused by the Coriolis force and the beginning of the subsequent flood tide. Observations of the small flood tide comprise the first parts of Sets 4 and 7 (Figure 5.1b). Discharge from the river was held back by the rising tide, so outflow speeds decreased and the plume was pushed up the Strait. Just before the high tide, the river's pressure head became large enough to overcome the rising tide and the southern floats began to move south. The small ebb stage of the tide was observed during Set 1 and the final parts of Sets 4 and 7 (Figure 5.1c). The falling tide led to a gradual turning to the south, while the curling

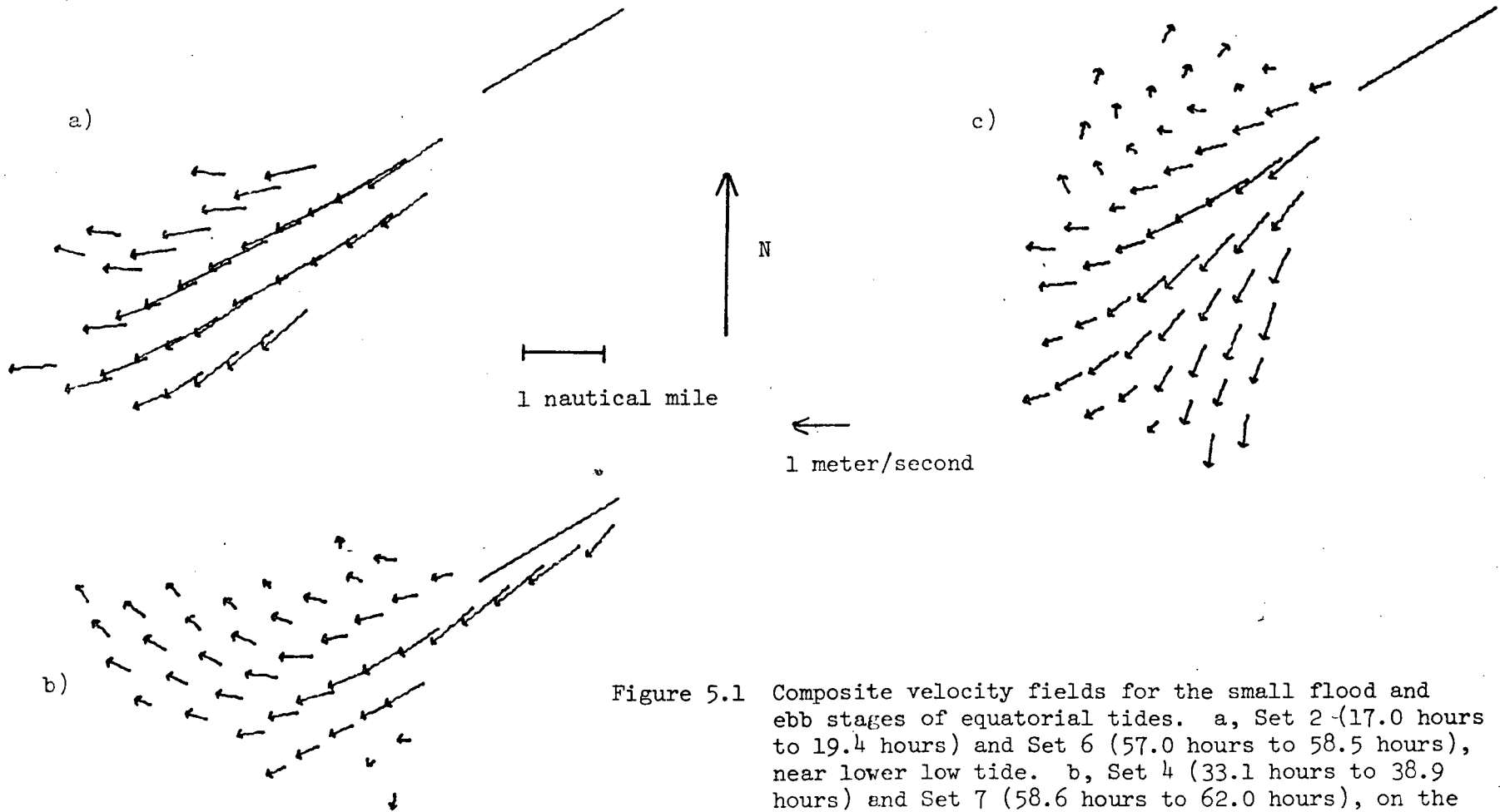


Figure 5.1 Composite velocity fields for the small flood and ebb stages of equatorial tides. a, Set 2 (17.0 hours to 19.4 hours) and Set 6 (57.0 hours to 58.5 hours), near lower low tide. b, Set 4 (33.1 hours to 38.9 hours) and Set 7 (58.6 hours to 62.0 hours), on the rise to lower high tide. c, Set 1 (11.6 hours to 16.7 hours), Set 4 (38.9 hours to 43.6 hours) and Set 7 (64.7 hours to 67.5 hours), on the ebb from lower high tide.

on the north side of the plume was a remnant of the flow from the preceding flood tide.

During the nights of the first week of the experiment observations were made of the rise to and ebb from higher high tide. Only one line of floats was tracked each night. The winds during Set 3 were strong enough (northwest 19 knots) to affect the flow considerably and to make conditions bad enough that float tracking was stopped early. During Set 5 the winds were sufficiently strong (increasing to northeast 17) to transfer some momentum to the flow, but Set 8 was unaffected by the light winds of that night. The flow has been divided into two regimes: that on the flood tide and that which occurred after the flow turned with the ebb tide.

On the flood tide the floats moved out from Sand Heads with very little turning or divergence, though their speed decreased quite markedly (Figure 5.2a). When the ebb began, the three lines of floats were at different distances from Sand Heads, so the velocity field (Figure 5.2b) shows how the strength of the ebb varied across the Strait. Of course, wind conditions for the three sets were so different that the data cannot be considered synoptic; the floats in Set 3 (nearest Sand Heads) were particularly affected by the high winds.

The large ebbs and floods of tropic tides occurred during the days of the second week of the experiment (Figure 4.32). Observations were not made of the small floods and ebbs during the nights. High winds delayed the start of operations on the first day, and winds were strong enough to affect the observed flow during Sets 14 and 15.

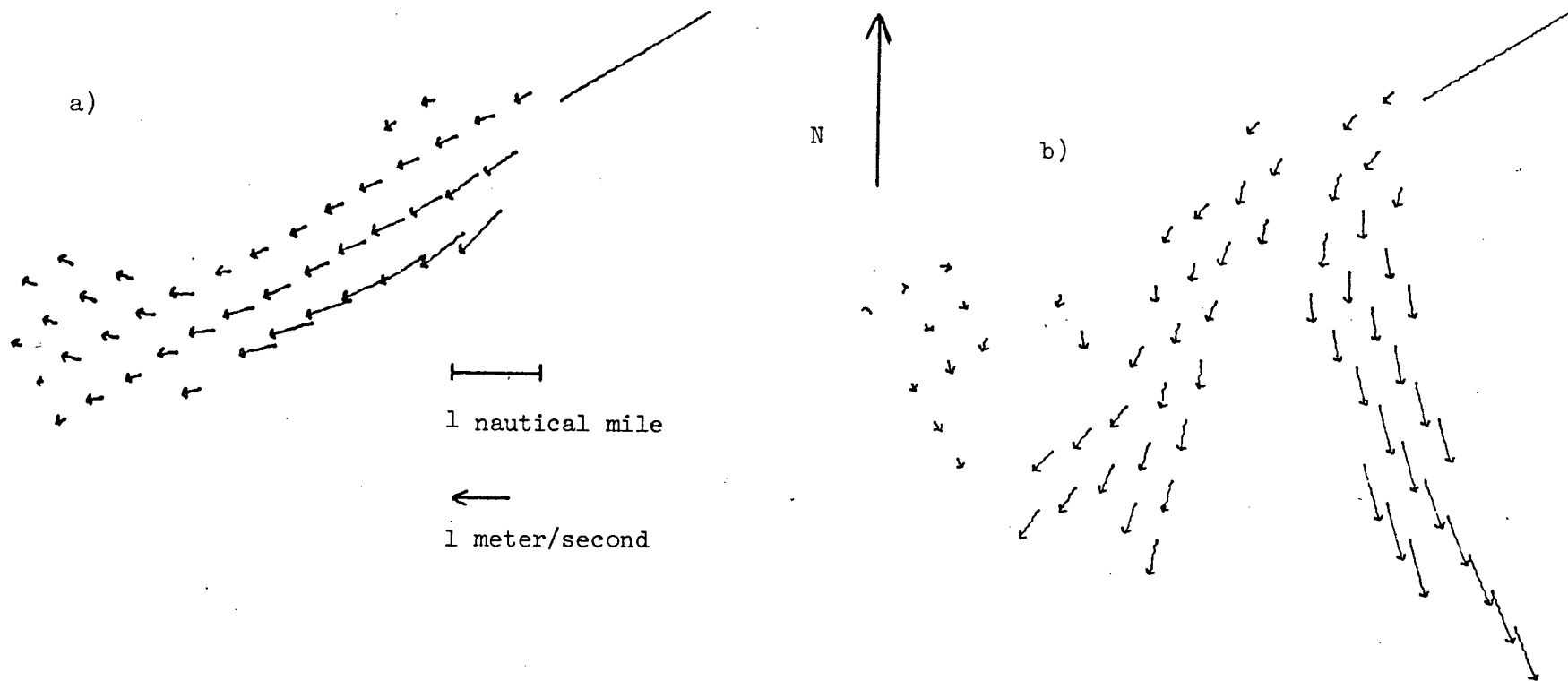


Figure 5.2 Composite velocity fields for the large flood and ebb stages of equatorial tides. a, Set 5 (45.9 hours to 49.0 hours) and Set 8 (69.7 hours to 76.0 hours), on the rise to higher high tide. b, Set 3 (22.8 hours to 27.0 hours), Set 5 (49.0 hours to 54.5 hours) and Set 8 (76.0 hours to 79.0 hours), on the ebb from higher high tide.

The composite velocity fields based on the week's observations comprise Figure 5.3.

Sets 12 and 16 (before 59.0 hours) which cover the early part of the ebb (Figure 5.3a) show some divergence and turning to the south under the influence of the ebbing tide. Speeds are relatively small; the high speed indicated near Sand Heads is due to the first float of a new line put in later on the tidal cycle. The flow near the end of the ebb (Sets 9, 13, 16 (after 59.0 hours) and 17, Figure 5.3b) exhibits the largest speeds measured during the experiment. There is little divergence in the flow, which moves almost straight out from Sand Heads. (The arrows on the south side represent floats which were moving south near the beginning of the interval.) The slight curvature to the right is consistent with the predicted effect of the Coriolis force. The measurements in the river were made just after lower low tide, so those floats were slowed near Sand Heads by the beginning of the flood tide.

The flood from lower low to higher high tide began during Sets 10, 14 and 18 (Figure 5.3c). The measurements near Sand Heads were made on the early stages of the flood, when the river's pressure head was large enough that the outflow was not slowed too much. The flooding tide did, however, turn the plume sharply up the Strait. Winds during all three sets were from the south or southwest at speeds near 10 knots. Such winds would be strong enough to add slightly to the northward turning caused by the tide. Near higher high tide fresh water collects near the river mouth, as illustrated by the very low speeds observed in

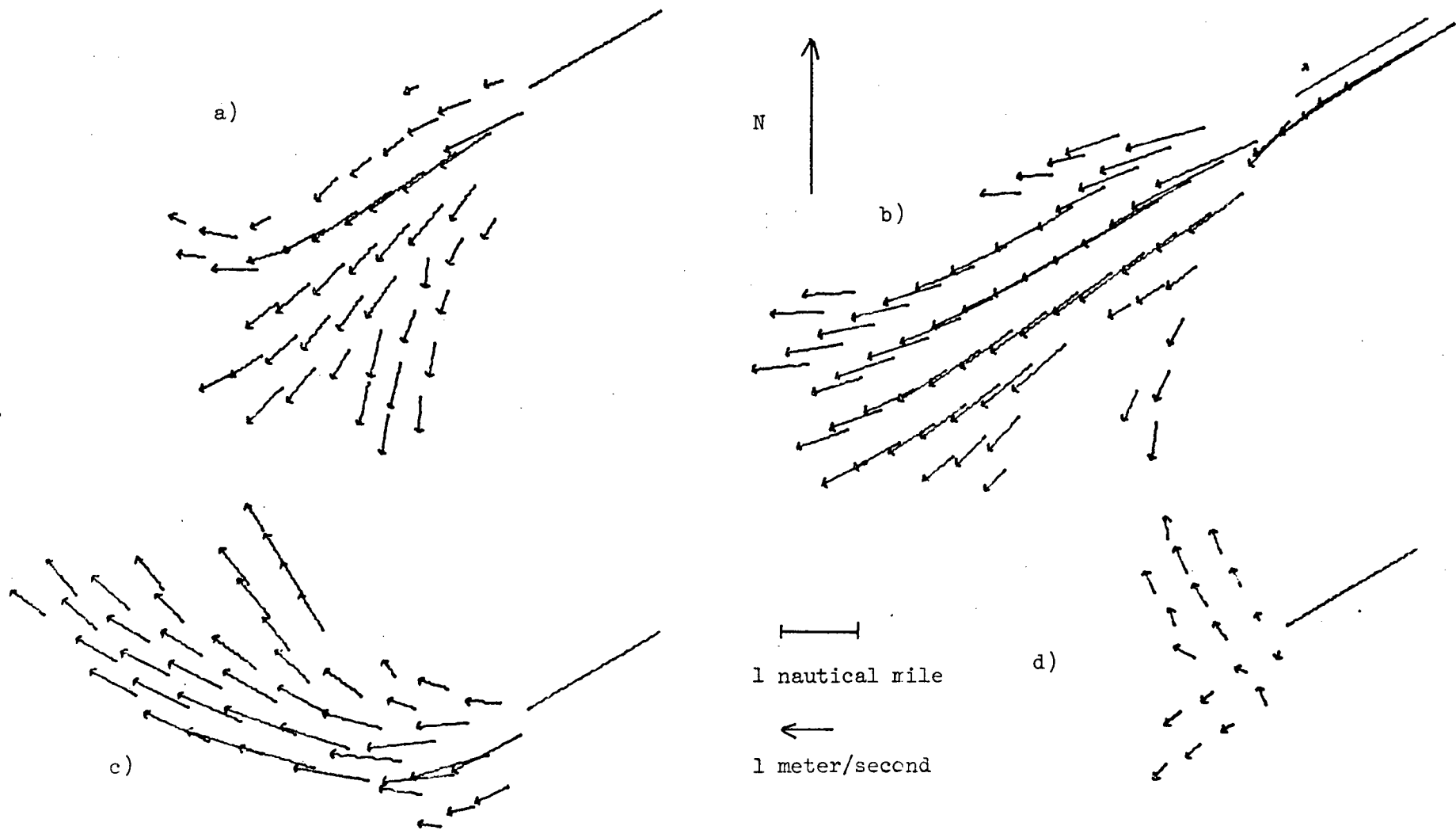


Figure 5.3 Composite velocity for the large ebb and flood stage of tropic tides. a, Set 12 (30.8 hours to 34.8 hours) and Set 16 (54.7 hours to 59.0 hours), at the start of the large ebb. b, Set 9 (12.1 hours to 13.1 hours), Set 13 (35.1 hours to 37.4 hours), Set 16 (59.0 hours to 60.8 hours) and Set 17 (59.8 hours to 62.1 hours), at the end of the large ebb. c, Set 10 (13.3 hours to 14.6 hours), Set 14 (38.2 hours to 41.3 hours) and Set 18 (62.8 hours to 64.9 hours), at the start of the large flood. d, Set 11 (15.5 hours to 20.1 hours) and Set 15 (41.3 hours to 44.2 hours), at the end of the large flood.

Sets 11 and 15 (Figure 5.3d). The wind conditions made the flow patterns of the two sets quite different. During Set 11 the east 5 wind had little effect on the flow, which moved out from Sand Heads with little turning, but the southeast 17 wind during Set 15 was the predominant force, turning the flow sharply up the Strait.

Average velocity components were plotted as a function of distance travelled from Sand Heads. Graphs corresponding to Figures 5.1a, b, c and 5.3a, b, c, were shown in Chapter 4, Section 3. Generally, the component in the direction along the jetty dominated (except for the field of Figure 5.3c). This component was strongest for the central region of the plume and showed an approximately linear decrease with distance from Sand Heads.

Examination of the horizontal divergence led to estimates of the entrainment velocity consistent with those of Keulegan's (1966) formula based on laboratory scale models and of de Lange Boom's (1976) estimate derived from salt conservation in the Fraser plume.

After an experiment has been completed, it is usually possible to suggest improvements which could be made in subsequent experiments. Some changes are relatively minor, while others involve major revisions.

Experience showed that the log sheets used to record the Mini-Fix data could have been better organized. Space should be provided for the name of the vessel as well as the names of the operators. The vessel number and the information about the type of fix (installing, removing or just checking the float) and the float number should come first. Next should be the position coordinates, followed by the time.

Even better coverage could possibly be obtained with the use of floats equipped with transmitters. Each float would send out a distinctive signal, allowing it to be identified. Such floats have been used in other experiments (e.g. the SOFAR floats which were used to follow subsurface currents in MODE, the Mid Ocean Dynamics Experiment). Obtaining or building the transmitters and receivers necessary for such an experiment would involve considerable expense, but such a system would have many advantages. The vessels would only be needed to install and remove the floats, allowing more floats to be tracked. The chance of losing floats would be greatly reduced, and the difficulty of distinguishing them from other objects which appear on a radar screen would be eliminated.

Having the information in this order would make recording, transmitting and preliminary plotting of the data easier.

During the experiment we tried to measure the velocities of the floats over short distances by taking pairs of fixes separated by only a few minutes, with intervals of twenty minutes or so between successive pairs of positions for each float. This procedure was probably not worthwhile. The method of interpolation of positions and velocities which was eventually chosen would have given good results even without the double fixes, and the time could have been better spent in following more floats.

Major changes could be suggested in the basic design of the experiment. Tracking floats with Mini-Fix does have disadvantages, since having to visit each float to measure its position severely limits the number of floats which can be handled with the available vessels. Alternative methods might allow better coverage.

For an area like the Fraser River plume, radar tracking was considered impractical because we wanted to examine more of the flow than the three-mile range of the radar set would permit. A practical alternative might be to use radar tracking near the river mouth and Mini-Fix positioning when floats moved farther out. This combination of methods would call for good organization of the vessels to ensure that floats were taken over for Mini-Fix tracking when they reached the edge of the area of radar coverage. The early stages of the data reduction would be complicated by having data from two sources to be combined. However, a significant improvement in coverage of the area might be obtained with equipment already available.

LIST OF REFERENCES

- BUCKLEY, J.R. 1977. The currents, winds and tides of northern Howe Sound. Ph.D. Thesis. University of British Columbia, Vancouver, B.C. 225 pp.
- BUCKLEY, J.R. and S. POND. 1976. Wind and the surface circulation of a fjord. *Journal of the Fisheries Research Board of Canada*, 33(10): 2265-2271.
- CANADA. Department of the Environment. Marine Sciences Directorate. Canadian Hydrographic Service. Canadian Tide and Current Tables 1974, Volume 5, Juan de Fuca and Georgia Straits.
- CANADA. Department of Mines and Technical Surveys. Marine Sciences Branch. Canadian Hydrographic Service. Canadian Tide and Current Tables 1967, Volume 5, Juan de Fuca and Georgia Straits.
- DE LANGE BOOM, B. 1976. Mathematical modelling of the chlorophyll distribution in the Fraser River plume, British Columbia. M.Sc. Thesis. University of British Columbia, Vancouver, B.C. 140 pp.
- EKMAN, V.W. 1905. On the influence of the Earth's rotation on ocean currents. *Arkiv foer Matematik, Astronomi och Fysik*. 2(11): 1.
- FRASER, C.M. and A.T. CAMERON. 1916. Variations in density and temperature in the coastal waters of British Columbia. *Contributions to Canadian Biology*, 1914-1915, pp. 133-143.
- GIOVANDO, L.F. and S. TABATA. 1970. Measurement of surface flow in the Strait of Georgia by means of free-floating current followers. Fisheries Research Board of Canada, Technical Report No. 163, 69 pp.
- HUTCHINSON, A.H. and C.C. LUCAS. 1931. Epithalassa of the Strait of Georgia. *Canadian Journal of Research*, 5: 231-284.
- KEULEGAN, G.H. 1966. The Mechanisms of an Arrested Saline Wedge. *Estuary and Coastline Hydronamics*, A.T. Ippen, Ed. McGraw-Hill, New York. pp. 546-574.
- MADDEROM, P. 1974. Curve fitting using cubic splines. University of British Columbia Computing Centre, Technical Note 17, 6 pp.
- MOREL, P. and M. DESBOIS. 1974. Mean 200-mb circulation in the southern hemisphere deduced from EOLE balloon flights. *Journal of the Atmospheric Sciences*, 31(2): 394-406.

LIST OF REFERENCES (continued)

- REINSCH, C.H. 1971. Smoothing by spline functions, II. *Numerische Mathematik*, 16: 451-454.
- TABATA, S. 1972. The movement of the Fraser River - influenced surface water in the Strait of Georgia as deduced from a series of aerial photographs. Pacific Marine Sciences Report 72-6, 69 pp.
- TABATA, S., L.F. GIOVANDO and D. DEVLIN. Current velocities in the vicinity of the Greater Vancouver Sewerage and Drainage District's Iona Island Outfall - 1968. Fisheries Research Board of Canada, Technical Report No. 263, 110 pp.
- TABATA, S., L.F. GIOVANDO, J.A. STICKLAND and J. WONG, 1970. Current velocity measurements in the Strait of Georgia - 1967. Fisheries Research Board of Canada, Technical Report No. 169, 245 pp.
- TULLY, J.P. and A.J. DODIMEAD. 1957. Properties of the water in the Strait of Georgia and influencing factors. *Journal of the Fisheries Research Board of Canada*, 14(3): 241-319.
- VACHON, W.A. 1974. Improved drifting buoy performance by scale model drogue testing. *Marine Technology Society Journal*, 8(8): 58-62.
- WALDICHUK, M. 1957. Physical oceanography of the Strait of Georgia, British Columbia. *Journal of the Fisheries Research Board of Canada*, 14(3): 321-486.
- WALDICHUK, M. 1958. Drift bottle observations in the Strait of Georgia. *Journal of the Fisheries Research Board of Canada*, 15(5): 1065-1102.